

**STABILITY ANALYSIS AND CONTROLLER  
SYNTHESIS OF SWITCHED SYSTEMS**

**YANG YUE**

*(B. Eng., Harbin Institute of Technology)*

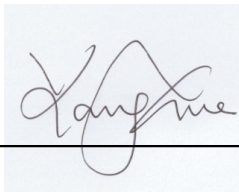
**A THESIS SUBMITTED  
FOR THE DEGREE OF DOCTOR OF PHILOSOPHY  
DEPARTMENT OF ELECTRICAL AND COMPUTER ENGINEERING  
NATIONAL UNIVERSITY OF SINGAPORE**

**2014**

## **DECLARATION**

**I hereby declare that this thesis is my original work and it has been written by me in its entirety. I have duly acknowledged all the sources of information which have been used in the thesis.**

**This thesis has also not been submitted for any degree in any university previously.**

A handwritten signature in cursive script, appearing to read 'Yang Yue', is centered on a light blue rectangular background. A solid black horizontal line is drawn across the page, passing through the bottom of the signature box.

Yang Yue

29 July 2014

## Acknowledgments

First and foremost, I will always owe sincere gratitude to my main supervisor, Prof. Xiang Cheng. From numerous discussions with him during the past four years, I have benefited immensely from his erudite knowledge, originality of thought, and emphasis on critical thinking. This thesis cannot be finished without his careful guidance, constant support and encouragement.

I would also like to express my great appreciation to my co-supervisor, Prof. Lee Tong Heng, for his insight, guidance and encouragement throughout the past four years.

I would like to thank Prof. Chen Benmei, Prof. Pang Chee Khiang, Justin and Prof. Wang Qing-Guo for their kind encouragement and constructive suggestions, which have improved the quality of my work. I shall extend my thanks to all my colleagues at the Control & Simulation Lab, for their kind assistance and friendship during my stay at National University of Singapore.

Finally, my special thanks go to my wife Yang Jing for her support, patience and understanding, and to my parents and grandparents for their love, support, and encouragement over the years.

# Contents

<b>Acknowledgments</b>	<b>I</b>
<b>Summary</b>	<b>VII</b>
<b>List of Tables</b>	<b>IX</b>
<b>List of Figures</b>	<b>X</b>
<b>1 Introduction</b>	<b>1</b>
1.1 Stability Analysis of Switched Systems . . . . .	4
1.1.1 Stability under Arbitrary Switching . . . . .	6
1.1.2 Switching Stabilization . . . . .	15
1.2 Controller Synthesis of Switched Systems . . . . .	19
1.2.1 Identification using Multiple Models . . . . .	21
1.2.2 Control using Multiple Models and Switching . . . . .	23
1.3 Objectives and Contributions . . . . .	25
1.4 Thesis Organization . . . . .	26
<b>I Stability Analysis of Switched Systems</b>	<b>28</b>
<b>2 Polar Coordinates Analysis</b>	<b>29</b>

2.1	Introduction . . . . .	29
2.2	A Single Second-order LTI System in Polar Coordinates . . . . .	31
2.3	The Switched System (2.1) with $N = 2$ in Polar Coordinates . . . . .	33
2.4	The Switched System (2.1) with $N \geq 2$ in Polar Coordinates . . . . .	37
2.5	Summary . . . . .	41
<b>3 Stability of Second-order Switched Linear Systems under Arbitrary Switching</b>		
		<b>43</b>
3.1	Introduction . . . . .	43
3.2	Statement of the Problem . . . . .	44
3.3	Worst Case Analysis for the Switched System (3.1) . . . . .	45
3.3.1	WCSS Criteria for the Switched System (3.1) with $N = 2$ . . . . .	46
3.3.2	WCSS Criteria for the Switched System (3.1) with $N \geq 2$ . . . . .	46
3.4	A Necessary and Sufficient Condition for the Stability of the Switched System (3.1) with $N \geq 2$ under Arbitrary Switching . . . . .	49
3.4.1	Proof of Theorem 3.1 . . . . .	53
3.4.2	Instability Mechanisms for the Switched System (3.1) with $N \geq 2$ under Arbitrary Switching . . . . .	62
3.4.3	Application of Theorem 3.1 . . . . .	63
3.5	Summary . . . . .	66
<b>4 Switching Stabilizability of Second-order Switched Linear Systems</b>		
		<b>67</b>
4.1	Introduction . . . . .	67
4.2	Statement of the Problem . . . . .	68
4.3	Best Case Analysis for the Switched System (4.1) of Category I . . . . .	71

4.3.1	BCSS Criteria for the Switched System (4.1) of Category I with $N = 2$ . . . . .	71
4.3.2	BCSS Criteria for the Switched System (4.1) of Category I with $N \geq 2$ . . . . .	72
4.4	A Necessary and Sufficient Condition for the Switching Stabilizability of the Switched System (4.1) of Category I with $N \geq 2$ . . . . .	74
4.4.1	Proof of Theorem 4.1 . . . . .	76
4.4.2	Stabilization Switching Laws for the Switched System (4.1) of Category I with $N \geq 2$ . . . . .	85
4.4.3	Application of Theorem 4.1 . . . . .	86
4.5	Extensions . . . . .	88
4.5.1	Extension to the Switched System (4.1) of Category II with $N \geq 2$ . . . . .	88
4.5.2	Extension to the Switched System (4.1) of Category III with $N \geq 2$ . . . . .	88
4.6	Summary . . . . .	89
<b>II Controller Synthesis of Switched Systems</b>		<b>90</b>
<b>5 Identification of Nonlinear Systems using Multiple Models</b>		<b>91</b>
5.1	Introduction . . . . .	91
5.2	Mathematical Preliminaries . . . . .	92
5.2.1	The NARMA Model . . . . .	94
5.2.2	The NARMA-L2 Model . . . . .	96
5.3	Multiple NARMA-L2 Models . . . . .	97

---

5.4	Identification of Multiple NARMA-L2 Models using Neural Networks . . . . .	100
5.5	Simulation Studies . . . . .	101
5.5.1	Nonlinear Example 1 . . . . .	102
5.5.2	Nonlinear Example 2 . . . . .	104
5.5.3	Nonlinear Example 3 . . . . .	106
5.5.4	Nonlinear Example 4 . . . . .	108
5.6	Experimental Studies . . . . .	110
5.7	Summary . . . . .	116
<b>6</b>	<b>Control of Nonlinear Systems using Multiple Models and Switching</b>	<b>117</b>
6.1	Introduction . . . . .	117
6.2	Sub-controllers Design . . . . .	118
6.3	Switching Mechanism . . . . .	120
6.4	Simulation Studies . . . . .	121
6.4.1	Nonlinear Example 1 . . . . .	122
6.4.2	Nonlinear Example 2 . . . . .	122
6.4.3	Nonlinear Example 3 . . . . .	124
6.4.4	Nonlinear Example 4 . . . . .	126
6.5	Experimental Studies . . . . .	126
6.6	Summary . . . . .	128
<b>7</b>	<b>Conclusions</b>	<b>132</b>
7.1	Main Contributions . . . . .	133
7.2	Suggestions for Future Work . . . . .	135

CONTENTS

---

<b>Bibliography</b>	<b>138</b>
<b>Publication List</b>	<b>148</b>



## Summary

Switched systems are a particular kind of hybrid systems that consist of a number of subsystems and a switching rule governing the switching among these subsystems. Due to their importance in theory and potential in application, the last two decades have witnessed numerous research activities in this field. Among the various topics, the stability analysis and controller synthesis of switched systems are studied in this thesis.

It is the existence of switching that makes the stability issues of switched systems very challenging. Due to the conservativeness of the common Lyapunov functions based methods, the worst case analysis (resp. best case analysis) approach has been widely used in establishing less conservative conditions for the stability under arbitrary switching (resp. switching stabilizability) of second-order switched linear systems in recent years. While significant progress has been made, most of the existing results are restricted to second-order switched linear systems with two subsystems. The first two main contributions of this thesis are to derive easily verifiable necessary and sufficient conditions for the stability under arbitrary switching and switching stabilizability of second-order switched linear systems with any finite number of subsystems.

On the other hand, switched systems provide a powerful approach for the identification and control of nonlinear systems with large operating range based on the divide-and-conquer strategy. In particular, the piecewise affine (PWA) models have drawn most of the attention in recent years. However, there are two major issues for the PWA model based identification and control: the “curse of

dimensionality” and the computational complexity. To resolve these two issues, a novel multiple model approach is developed for the identification and control of nonlinear systems, which is the third main contribution of this thesis. Both simulation studies and experimental results demonstrate the effectiveness of the proposed multiple model approach.

# List of Tables

3.1	Generalized regions of $k$ for Example 3.1 . . . . .	64
4.1	Generalized regions of $k$ for Example 4.1 . . . . .	87
5.1	Fit values for the test set of nonlinear system 1 with different models	103
5.2	Fit values for the test set of nonlinear system 2 with different models	105
5.3	Fit values for the test set of nonlinear system 3 with different models	108
5.4	Fit values for the test set of nonlinear system 4 with different models	110
5.5	Fit values for the modified DC motor with different models . . .	114
6.1	Variance of tracking errors for the modified DC motor with dif- ferent models . . . . .	128

# List of Figures

1.1	Switching between two stable subsystems . . . . .	5
1.2	Switching between two unstable subsystems . . . . .	5
1.3	A multi-controller switched system . . . . .	20
2.1	The phase diagrams of second-order LTI systems in polar coordi- nates . . . . .	32
2.2	The variation of $h_1$ under switching . . . . .	34
2.3	Two symmetric conic sectors for a region of $k$ . . . . .	37
2.4	Different types of regions . . . . .	41
2.5	Different types of boundaries . . . . .	41
3.1	Invariance property of $\gamma_{wc}$ . . . . .	52
3.2	Case 3.1: All the boundaries are of Type (a) . . . . .	53
3.3	Case 3.2: At least one boundary is of Type (b) and none of the boundaries is of Type (c) . . . . .	55
3.4	Case 3.3: At least one boundary is of Type (c) and none of the boundaries is of Type (b) . . . . .	57
3.5	Case 3.4: At least one boundary is of Type (b) and at least one boundary is of Type (c) . . . . .	60

3.6	Two instability mechanisms for the switched system (3.1) with $N \geq 2$ under arbitrary switching . . . . .	63
3.7	The worst case trajectory of Example 3.1 . . . . .	65
4.1	Case 4.1: All the boundaries are of Type (a) . . . . .	77
4.2	Case 4.2: At least one boundary is of Type (b) and none of the boundaries is of Type (c) . . . . .	78
4.3	Case 4.3: At least one boundary is of Type (c) and none of the boundaries is of Type (b) . . . . .	80
4.4	Case 4.4: At least one boundary is of Type (b) and at least one boundary is of Type (c) . . . . .	83
4.5	Two stabilization mechanisms for the switched system (4.1) of Category I with $N \geq 2$ . . . . .	85
4.6	The best case trajectory of Example 4.1 . . . . .	87
5.1	Identification results for the test set of nonlinear system 1 with different models. Solid: Real output, dashed: Estimation output	103
5.2	Identification results for the test set of nonlinear system 2 with different models. Solid: Real output, dashed: Estimation output	105
5.3	Identification results for the test set of nonlinear system 3 with different models. Solid: Real output, dashed: Estimated output .	107
5.4	Identification results for the test set of nonlinear system 4 with different models. Solid: Real output, dashed: Estimated output .	110
5.5	Original hardware setup . . . . .	111
5.6	Schematics diagram of the original setup . . . . .	111

## LIST OF FIGURES

---

5.7	Working diagram for the identification process of the modified DC motor . . . . .	113
5.8	Identification errors for the training set of the modified DC motor with different models . . . . .	114
5.9	Identification results for the test set of the modified DC motor with different models . . . . .	115
6.1	Control results of nonlinear system 1 with different models. Solid: Reference, dashed: System output . . . . .	123
6.2	Control results of nonlinear system 2 with different models. Solid: Reference, dashed: System output . . . . .	124
6.3	Control results of nonlinear system 3 with different models. Solid: Reference, dashed: System output . . . . .	125
6.4	Control results of nonlinear system 4 with different models. Solid: Reference, dashed: System output . . . . .	127
6.5	Working diagram for the control procedure of the modified DC motor . . . . .	127
6.6	Control results of the modified DC motor for reference signal 1 with different models . . . . .	129
6.7	Control results of the modified DC motor for reference signal 2 with different models . . . . .	130
6.8	Control results of the modified DC motor for reference signal 3 with different models . . . . .	131

# Chapter 1

## Introduction

It is well known that the traditional control theory has focused either on continuous or on discrete behavior. However, many real-world dynamical systems display interaction between continuous and discrete dynamics, such as an automobile with a manual gearbox [1], a furnace with on-off behavior [2], and a genetic regulatory network consisting of a set of interacting genes [3], etc. Such systems are called *hybrid systems*.

Hybrid systems have attracted the attention of people from different communities due to their intrinsic interdisciplinary nature. People specializing in computer science concentrate on studying the discrete behavior of hybrid systems by assuming a relatively simple form for the continuous dynamics. Many researchers in systems and control theory, on the other hand, tend to regard hybrid systems as continuous systems with switching and place a greater emphasis on properties of the continuous state. It is the latter point of view that prevails in this dissertation.

Therefore, we are interested in continuous-time systems with discrete switch-

ing events, which are referred to as *switched systems*. More specifically, switched systems are a special kind of hybrid systems that consist of a finite number of subsystems and a switching rule governing the switching among these subsystems. One convenient way to classify switched systems is based on the dynamics of their subsystems. For example, continuous-time or discrete-time, linear or nonlinear, etc.

Mathematically, a continuous-time switched system can be described by a collection of indexed differential equations of the form

$$\dot{x}(t) = f_{\sigma}(x(t), u(t)) \quad (1.1)$$

where the state  $x \in \mathbb{R}^n$ , the control input  $u \in \mathbb{R}^m$ , and  $\sigma : \mathbb{R}^+ \rightarrow \mathcal{I}_N = \{1, 2, \dots, N\}$  is a piecewise constant function, called a switching signal.  $\mathbb{R}^+$  denotes the set of nonnegative real numbers. By requesting a switching signal to be piecewise constant, we mean that the switching signal has a finite number of discontinuities on any finite interval of  $\mathbb{R}^+$ , which corresponds to the no-chattering requirement for continuous-time switched systems.

Similarly, a discrete-time switched system can be represented as a collection of indexed difference equations of the form

$$x(k+1) = f_{\sigma}(x(k), u(k)) \quad (1.2)$$

where the switching signal  $\sigma : \mathbb{Z}^+ \rightarrow \mathcal{I}_N$  is a discrete-time sequence and  $\mathbb{Z}^+$  stands for the set of nonnegative integers. Note that the piecewise constant requirement for the switching signal is not an issue for the discrete-time case.



In general, the switching signal at time  $t$  may depend not only on the time instant  $t$ , but also on the current state  $x(t)$  and/or previous active mode. Accordingly, the switching logic can be classified as *time-dependent* (switching depends on time  $t$  only), *state-dependent* (switching depends on state  $x(t)$  as well), and with or without memory (switching also depends on the history of active modes) [4, 5]. Of course, the combinations of several types of switching are also possible.

In particular, if all the subsystems are linear time-invariant (LTI) and autonomous, we obtain the *autonomous switched linear systems*, which have attracted most of the attention in the literature [6, 7, 8], given by

$$\dot{x}(t) = A_\sigma x(t) \tag{1.3}$$

$$x(k+1) = A_\sigma x(k) \tag{1.4}$$

where  $A_i \in \mathbb{R}^{n \times n}$  ( $i \in \mathcal{I}_N$ ) is the matrix for the  $i^{\text{th}}$  LTI subsystem  $\Sigma_{A_i}$  :  $\dot{x}(t) = A_i x(t)$  and the origin is an equilibrium point (maybe unstable) of the system. The set of the state matrices for all the subsystems is denoted by  $\mathcal{A} = \{A_1, A_2, \dots, A_N\}$ .

The study of switched systems is motivated by two main reasons. First, many real-world systems can be modeled by switched systems, such as power systems, biological systems and communication networks, etc. Second, there exists a large class of nonlinear systems that can be stabilized by switching control schemes, but cannot be stabilized by any continuous static state feedback control law [9]. Due to their importance in theory and great potential in application, the last two decades have witnessed numerous studies on their controllability [10, 11, 12, 13],

observability [14, 15], stability [4, 16, 17, 18, 5] and controller design [19, 20, 21].

In this dissertation, we limit the scope of our study to the stability analysis and controller synthesis of switched systems, for which a brief review of the recent results is presented in this chapter.

## 1.1 Stability Analysis of Switched Systems

The stability is a fundamental issue for any control system. A control strategy can find wide applications in industry only when its stability properties are well understood. For the stability issues of switched systems, there are several interesting phenomena. For example, even when all the subsystems are asymptotically stable, the switched systems may have divergent trajectories for certain switching signals [17, 22]. Consider the trajectories of two second-order asymptotically stable subsystems, which are sketched in Fig. 1.1. It is shown that the switched system can be made unstable by a certain switching signal. On the other hand, even when all the subsystems are unstable, it may still be possible to stabilize the switched system by an appropriately designed switching signal [17, 22]. This fact is illustrated in Fig. 1.2.

As these examples suggest, the stability of switched systems depends not only on the dynamics of each subsystem, but also on the properties of the switching signals. Therefore, there are mainly two types of problems considering the stability analysis of switched systems. One is the stability under given switching signals, while the other one is the stabilization for a given collection of subsystems.

For the stability under given switching signals, there are mainly two types of

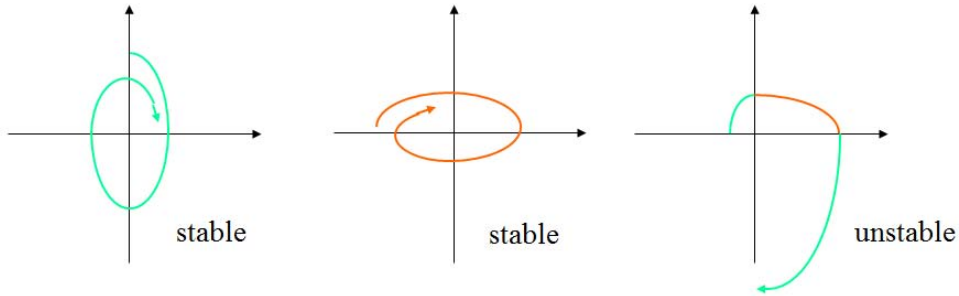


Figure 1.1: Switching between two stable subsystems

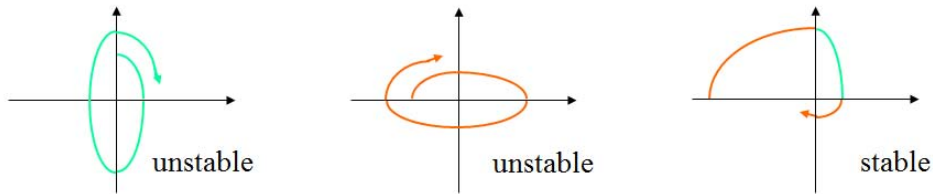


Figure 1.2: Switching between two unstable subsystems

switching signals that have been addressed in the literature, which are arbitrary switching signals and restricted switching signals. The former case is mainly investigated by constructing a common Lyapunov function for all the subsystems [4]. For the latter case, the restrictions on switching signals may be either time domain restrictions (e.g., dwell-time and average dwell-time switching signals) [23] or state-space restrictions (e.g., abstractions from partitions of the state-space) [24]. It is well known that the multiple Lyapunov function approach is more efficient in offering greater freedom for demonstrating the stability of switched systems under restricted switching [25].

As for the stabilization of switched systems, there are mainly two problems. The first one is to design feedback controllers for each subsystem to make the closed-loop system stable under a specific switching signal, which is referred

to as the feedback stabilization problem of switched systems. Several types of switching signals have been studied in the literature, such as arbitrary switching [26, 27], slow switching [28] and restricted switching induced by partitions of the state-space [29, 30]. On the other hand, another problem of interest is to design stabilizing switching signals for a collection of subsystems, which is referred to as the switching stabilization problem of switched systems.

In this dissertation, we focus on the stability under arbitrary switching and the switching stabilization of switched linear systems.

### **1.1.1 Stability under Arbitrary Switching**

One common question asked for a switched system is its stability conditions when there is no restriction on the switching signals, which is known as the stability under arbitrary switching and is of great practical importance. For example, when multiple controllers are designed for a plant to satisfy certain performance requirements, it is important to guarantee that the switching among these controllers does not cause instability. Obviously, it is not an issue if the closed-loop switched system is stable under arbitrary switching. For this problem, it is necessary to require that all the subsystems are asymptotically stable. Otherwise, the trajectory of the switched system can blow up by keeping the switching signal on the unstable subsystem all the time. However, this condition is not sufficient for the stability under arbitrary switching. Therefore, some additional conditions on the subsystems' state matrices need to be determined.

## Common Lyapunov Functions

Lyapunov theory plays a vital role in the stability analysis of dynamical systems [31, 32]. The key idea is to establish the stability of a dynamical system by demonstrating the existence of a positive valued, norm-like function that decreases along all trajectories of the system as time evolves. This is the basis for most of the recent studies on the stability of switched linear systems.

If a candidate Lyapunov function  $V(x)$  decreases along all trajectories of a switched linear system under arbitrary switching, it must be true for all constant switching signals  $\sigma = i$  ( $i \in \mathcal{I}_N$ ). Therefore, such function  $V(x)$  is a common Lyapunov function for each subsystem of the switched linear system. It was well established [33, 34] that a switched system is uniformly exponentially stable under arbitrary switching if a common Lyapunov function exists for all its subsystems. We now discuss different types of common Lyapunov functions for switched linear systems in the literature.

**Common Quadratic Lyapunov Functions** The existence of a common quadratic Lyapunov function (CQLF) [35] for all its subsystems assures the quadratic stability of a switched linear system. Quadratic stability is a special class of exponential stability, which implies asymptotic stability. More specifically, if there exists a positive definite matrix  $P \succ 0$  satisfying

$$PA_i + A_i^T P \prec 0, \quad i \in \mathcal{I}_N, \quad (1.5)$$

then all the subsystems admit a CQLF of the form

$$V(x) = x^T P x, \quad (1.6)$$

and the continuous-time autonomous switched system (1.3) is asymptotically stable under arbitrary switching.

*Remark 1.1.* The geometric meaning of the existence of a CQLF is that, in the domain of linearly transformed coordinates, the squared magnitudes of the states of all the subsystems decay exponentially.

It is noted that the condition (1.5) is a linear matrix inequality (LMI) and can be solved using standard convex optimization tools [36]. While LMIs provide an effective way to verify the existence of a CQLF among a family of LTI subsystems, they offer little insight into the relationship between the existence of a CQLF and the dynamics of switched linear systems. Moreover, LMI-based methods may become inefficient when the number of subsystems is very large. Therefore, it is of great interest to determine algebraic conditions on the subsystems' state matrices for the existence of a CQLF.

A simple condition to guarantee the existence of a CQLF among a group of LTI subsystems is that their state matrices commute pairwise.

**Theorem 1.1.** [37] *A sufficient condition for the Hurwitz matrices  $A_1, A_2, \dots, A_N$  in  $\mathbb{R}^{n \times n}$  to have a CQLF is that they commute pairwise. Given a symmetric positive definite matrix  $P_0$ , let  $P_1, P_2, \dots, P_N$  be the unique symmetric positive definite matrices that satisfy the Lyapunov equations*

$$A_i^T P_i + P_i A_i = -P_{i-1}, \quad i = 1, 2, \dots, N, \quad (1.7)$$

then the function  $V(x) = x^T P_N x$  is a CQLF for all the subsystems.

However, the above condition is too restrictive to be satisfied for switched linear systems in general. Therefore, more general conditions need to be found.

By considering a second-order switched linear system with two subsystems, Shorten and Narendra [38, 39] derived a necessary and sufficient condition for the existence of a CQLF based on the stability of the matrix pencil. Given two matrices  $A_1$  and  $A_2$ , the matrix pencil  $\gamma_\alpha(A_1, A_2)$  is defined as the one-parameter family of matrices  $\gamma_\alpha(A_1, A_2) = \alpha A_1 + (1 - \alpha)A_2$ ,  $\alpha \in [0, 1]$ . The matrix pencil  $\gamma_\alpha(A_1, A_2)$  is said to be Hurwitz if all its eigenvalues are in the open left half plane for all  $0 \leq \alpha \leq 1$ .

**Theorem 1.2.** [38, 39] *Let  $A_1, A_2$  be two Hurwitz matrices in  $\mathbb{R}^{2 \times 2}$ . The following conditions are equivalent:*

- 1) *there exists a CQLF for the switched linear system with  $A_1, A_2$  as two subsystems;*
- 2) *the matrix pencil  $\gamma_\alpha(A_1, A_2)$  and  $\gamma_\alpha(A_1, A_2^{-1})$  are both Hurwitz;*
- 3) *the matrices  $A_1 A_2$  and  $A_1 A_2^{-1}$  do not have any negative real eigenvalues.*

Theorem 1.2 provides an algebraic condition to verify the existence of a CQLF based on the subsystems' state matrices. However, it turns out to be difficult to generalize this condition to higher-order switched linear systems.

In [40, 41], necessary and sufficient algebraic conditions were derived for the non-existence of a CQLF for third-order switched linear systems with a pair of subsystems. However, those conditions are not easy to be verified. For a pair of  $n$ th-order LTI systems, a necessary condition for the existence of a CQLF was derived in [42, 43] as follows.

**Theorem 1.3.** [42, 43] *Let  $A_1, A_2$  be two Hurwitz matrices in  $\mathbb{R}^{n \times n}$ . A necessary condition for the existence of a CQLF is that the matrix products  $A_1[\alpha A_1 + (1 - \alpha)A_2]$  and  $A_1[\alpha A_1 + (1 - \alpha)A_2]^{-1}$  do not have any negative real eigenvalues for all  $0 \leq \alpha \leq 1$ .*

As a special case, consider a switched linear system with two LTI subsystems whose state matrices have rank one difference. A necessary and sufficient condition for the existence of a CQLF was obtained in [44].

**Theorem 1.4.** [44] *Let  $A_1, A_2$  be two Hurwitz matrices in  $\mathbb{R}^{n \times n}$  with  $\text{rank}(A_2 - A_1) = 1$ . A necessary and sufficient condition for the existence of a CQLF is that the matrix product  $A_1 A_2$  does not have any negative real eigenvalues. Equivalently, the matrix  $A_1 + \gamma A_2$  is non-singular for all  $\gamma \in [0, +\infty)$ .*

An independent proof for this condition was presented in [45] based on convex analysis and the theory of moments.

So far, our discussion on the existence of a CQLF has been restricted to switched linear systems with two subsystems. However, in general, switched systems may have more than two modes. Obviously, a necessary condition for the existence of a CQLF for a switched linear system with more than two subsystems is that each pair of its subsystems admits a CQLF. Actually, the existence of a CQLF pairwise may also imply the existence of a CQLF for the switched system in certain special cases, e.g., second-order switched positive linear systems [46]. However, this is not true for general switched systems. The existence of a CQLF for a finite number of second-order LTI systems was studied in [39] with the following result.



**Theorem 1.5.** [39] *Let  $A_1, A_2, \dots, A_N$  be Hurwitz matrices in  $\mathbb{R}^{2 \times 2}$  with  $a_{21i} \neq 0$  for all  $i \in \mathcal{I}_N$ . A necessary and sufficient condition for the existence of a CQLF is that a CQLF exists for every 3-tuple of systems  $\{A_i, A_j, A_k\}$ ,  $i \neq j \neq k$  for all  $i, j, k \in \mathcal{I}_N$ .*

Meanwhile, an equivalent necessary and sufficient condition for the existence of a CQLF among a finite number of second-order LTI systems, which is simple in computational complexity, was also proposed in [47] based on the topological structure.

Alternatively, a sufficient condition for the existence of a CQLF among a finite number of LTI systems was derived based on the solvability of the Lie algebra generated by the subsystems' state matrices.

**Theorem 1.6.** [22] *If all matrices  $A_i$ ,  $i \in \mathcal{I}_N$  are Hurwitz and the Lie algebra  $\{A_i, i \in \mathcal{I}_{NLA}\}$  is solvable, then there exists a CQLF.*

This condition was extended to the local stability of switched nonlinear systems based on Lyapunov's first method in [48]. See [49] for an overview of the Lie-algebraic global stability criteria for nonlinear switched systems. However, the Lie algebraic conditions are only sufficient for the existence of a CQLF and are not easy to be verified.

In addition to the above elegant results, some special cases were also studied. One special case is when all the subsystems are symmetric [50], i.e.,  $A_i^T = A_i$  for all  $i \in \mathcal{I}_N$ . Stability of  $A_i$  implies  $A_i^T + A_i \prec 0$ , which means that  $V(x) = x^T x$  is a CQLF for the switched linear system. Similarly, if the subsystems' state matrices are normal, i.e.,  $A_i A_i^T = A_i^T A_i$  for all  $i \in \mathcal{I}_N$ ,  $V(x) = x^T x$  is also a CQLF for the switched linear system [51].

On the other hand, if the Hurwitz matrices  $A_1, A_2, \dots, A_N$  are all in upper triangular form, then it was shown in [52] and [53] that the collection of systems  $\Sigma_{A_i}$  always admits a CQLF and the matrix  $P$  that defines the CQLF can be chosen to be diagonal.

While numerous elegant results have been obtained for the existence of a CQLF for switched linear systems, the problem of finding necessary and sufficient conditions for the existence of a CQLF for general higher-order switched linear systems is still open. Moreover, the existence of a CQLF is only sufficient for the asymptotical stability of switched systems under arbitrary switching [6]. Therefore, it is of great interest to investigate other types of common Lyapunov functions.

**Converse Lyapunov Theorems** Considering the globally uniformly asymptotically stable and locally uniformly exponentially stable continuous-time switched systems under arbitrary switching, a converse Lyapunov theorem was derived in [34].

**Theorem 1.7.** *[34] If the switched system is globally uniformly asymptotically stable and in addition uniformly exponentially stable, the family of subsystems has a common Lyapunov function.*

This condition was extended to switched nonlinear systems that are globally uniformly asymptotically stable with respect to a compact forward invariant set in [54]. These converse Lyapunov theorems suggest the study of non-quadratic Lyapunov functions.

Based on the equivalence between the asymptotic stability of switched systems under arbitrary switching and the robust stability of polytopic uncertain

linear time-variant systems, some well-known converse Lyapunov theorems have been introduced.

**Theorem 1.8.** [33] *The switched linear system  $\dot{x}(t) = A_\sigma x(t)$  is uniformly exponentially stable for arbitrary switching signal if and only if there exists a strictly convex, homogeneous (of second order), Lyapunov function  $V(x)$  of a quasi-quadratic form*

$$V(x) = x^T L(x)x, \quad (1.8)$$

such that

$$\max_{z \in Ax} \frac{\partial V(x)}{\partial z} \leq -\gamma \|x\|^2, \quad \gamma > 0, \quad (1.9)$$

where  $L(x) \in \mathbb{R}^{n \times n}$ ,  $L(x)^T = L(x) = L(cx)$  for all nonzero  $c \in \mathbb{R}$  and  $x \in \mathbb{R}^n$ .

Moreover,  $\|x\|$  is the Euclidean norm of vector  $x$ .

**Polyhedral Lyapunov Functions** Furthermore, we can focus on polyhedral Lyapunov functions (also known as piecewise linear Lyapunov functions) [55] as the following result pointed out.

**Theorem 1.9.** [33, 55] *If a switched linear system is asymptotically stable under arbitrary switching, then there exists a polyhedral Lyapunov function, which is monotonically decreasing along the switched system's trajectories.*

Several numerical algorithms have been developed for automated construction of a common polyhedral Lyapunov function in the literature. In [56], the Lyapunov function construction problem was converted to the design of a balanced polyhedron satisfying some invariance properties. An alternative approach was proposed in [33, 57], where linear programming based methods were developed for deriving stability conditions. Recently, a numerical approach, called

ray-gridding [58], was suggested to calculate polyhedral Lyapunov functions based on uniform partitions of the state-space in terms of ray directions. However, it has been found that the construction of such piecewise Lyapunov functions is, in general, not simple.

### **Worst Case Analysis**

It is noted that the stability of switched linear systems under arbitrary switching is closely related to the absolute stability and robust stability of differential or difference inclusions. Therefore, the results in these fields can be used to study the stability of switched systems under arbitrary switching. An interesting line of research in the absolute stability literature is to characterize the “most unstable” trajectory of a differential or difference inclusion through variational principles [59]. The basic idea is simple: if the “most unstable” trajectory is stable, then the whole system should be stable as well. By characterizing the “most unstable” nonlinearity using variational calculus, Pyatnitskiy and Rapoport [60] derived a necessary and sufficient condition for the absolute stability of second-order and third-order systems. Unfortunately, this condition is difficult to be verified since it requires the solution of a nonlinear equation with three unknowns. By introducing the concept of generalized first integrals, Margaliot and his co-workers [61, 62] reduced the number of unknowns of the nonlinear equation from three to one, and derived a verifiable necessary and sufficient condition for the absolute stability of second-order systems, which was extended to third-order systems in [63, 64]. However, these conditions are ad hoc, and offer little insight into the actual stability mechanism of switched systems.

Recently, for second-order switched linear systems with two subsystems  $\Sigma_{A_1}$

and  $\Sigma_{A_2}$ , where the eigenvalues of  $A_1$  and  $A_2$  have strictly negative real part (diagonalizable), a necessary and sufficient condition for the stability under arbitrary switching was proposed in [65] by studying the locus in which the two vector fields  $A_1x$  and  $A_2x$  are collinear. This condition was extended to the non-diagonalizable case in [66]. By combining the results of [65] and [66], a compact necessary and sufficient condition was derived for the stability of second-order switched linear systems with two subsystems under arbitrary switching in [67]. On the other hand, by denoting the switching signal that drives the switched system to the “most unstable” trajectory as the worst case switching signal (WCSS) and deriving detailed WCSS criteria in polar coordinates, an easily verifiable necessary and sufficient condition for the stability of second-order switched linear systems with two subsystems under arbitrary switching was derived in [68, 69].

However, it should be noted that all these results are restricted to second-order switched linear systems with two subsystems. To the best of the author’s knowledge, to derive easily verifiable necessary and sufficient conditions for the stability of second-order switched linear systems with more than two subsystems under arbitrary switching has been an open problem, which is to be investigated in this thesis.

### 1.1.2 Switching Stabilization

In addition to the stability under arbitrary switching, another problem of interest is the switching stabilization of switched systems, which is to determine stabilizing switching rules for a given collection of subsystems. For this problem, it is necessary to require that all the subsystems are unstable. Otherwise, the trajectory of the switched system will converge to the origin by keeping

the switching signal on the stable subsystem all the time. However, this condition is not sufficient for the switching stabilizability. Therefore, some additional conditions on the subsystems' state matrices need to be determined.

### Quadratic Switching Stabilization

Early efforts in this field have focused on quadratic stabilization for certain classes of switched systems. A switched system is called quadratically stabilizable when there exist switching signals that stabilize the switched system along a quadratic Lyapunov function  $V(x) = x^T P x$ .

For continuous-time switched linear systems with two unstable subsystems, it was shown in [70, 71, 72] that the existence of a stable convex combination of the two subsystems' state matrices is necessary and sufficient for the quadratic stabilizability of the switched systems. Specifically,

**Theorem 1.10.** [70, 71, 72] *A switched system that contains two LTI subsystems,  $\dot{x}(t) = A_i x(t)$ ,  $i = 1, 2$ , is quadratically stabilizable if and only if the matrix pencil  $\gamma_\alpha(A_1, A_2)$  contains a stable matrix.*

In [73], a “min-projection” strategy was proposed to generalize the quadratic stabilizing law to switched linear systems with more than two unstable subsystems.

**Theorem 1.11.** [73] *For the switched linear system  $\dot{x}(t) = A_\sigma x(t)$ ,  $\sigma \in \mathcal{I}_N$ , if there exist constants  $\alpha_i \in [0, 1]$ , and  $\sum_{i \in \mathcal{I}_N} \alpha_i = 1$  such that*

$$A_\alpha = \sum_{i \in \mathcal{I}_N} \alpha_i A_i, \tag{1.10}$$

is stable, then the min-projection strategy

$$\sigma(t) = \arg \min_{i \in \mathcal{I}_N} x(t)^T P A_i x(t), \quad (1.11)$$

quadratically stabilizes the switched system.

However, the existence of a stable convex combination matrix is only sufficient for the quadratic stabilization of switched linear systems with more than two modes. In other words, there exist certain switched linear systems that are quadratically stabilizable without having a stable convex combination matrix.

For general switched linear systems, a necessary and sufficient quadratic stabilizability condition was derived in [74].

**Theorem 1.12.** [74] *The switched linear system  $\dot{x}(t) = A_\sigma x(t)$ ,  $\sigma \in \mathcal{I}_N$  is quadratically stabilizable if and only if there exists a positive definite real symmetric matrix  $P = P^T \succ 0$  such that the set of matrices  $\{A_i P + P A_i^T\}$  is strictly complete, i.e., for any  $x \in \mathbb{R}^n / \{0\}$ , there exists  $i \in \mathcal{I}_N$  such that  $x^T (A_i P + P A_i^T) x < 0$ . In addition, a stabilizing switching signal can be selected as  $\sigma(t) = \min_i \{x(t)^T (A_i P + P A_i^T) x(t)\}$ .*

Obviously, the existence of a convex combination of state matrices,  $A_\alpha$ , automatically satisfies the above strict completeness conditions due to convexity, while the inverse is not true in general. Unfortunately, to check the strict completeness of a set of matrices is NP hard [74].

It is to be noted that all these conditions are conservative in the sense that there exist a class of switched systems that can be asymptotically stabilized without having a CQLF [15]. In order to derive less conservative results, some

recent efforts tried to construct stabilizing switching signals based on multiple Lyapunov functions, especially piecewise quadratic Lyapunov functions [17]. In particular, a stabilizing switching law was proposed in [75] by employing piecewise quadratic Lyapunov functions for switched linear systems with two subsystems. Pettersson [76] studied the exponential stabilization of switched linear systems based on piecewise quadratic Lyapunov functions and formulated the switching stabilization problem as a bilinear matrix inequality (BMI) problem. In [77], a probabilistic algorithm was proposed for the synthesis of a stabilizing law for switched linear systems along with a piecewise quadratic Lyapunov function. Recently, exponentially stabilizing switching signals were designed based on solving extended linear-quadratic regulator (LQR) optimal problems [78]. However, these conditions are still sufficient only for the existence of stabilizing switching laws for a given collection of unstable LTI subsystems.

### **Best Case Analysis**

In order to derive less conservative conditions for switching stabilizability, several researchers attempted to find the “most stable” switching signal, the stability under which is equivalent to the switching stabilizability of the switched systems. By vector field analysis and geometric characteristics in two-dimensional state-space, several switching stabilizability conditions for second-order switched linear systems were proposed in the literature.

In particular, Xu and Antsaklis [79] proposed several necessary and sufficient conditions for asymptotic stabilization of second-order switched linear systems with two unstable subsystems  $\Sigma_{A_1}$  and  $\Sigma_{A_2}$  in the following cases: (1) both  $A_1$  and  $A_2$  have complex eigenvalues with positive real part; (2) both  $A_1$  and  $A_2$



have real eigenvalues of opposite signs; (3) both  $A_1$  and  $A_2$  have real positive eigenvalues. In addition, the switching stabilizability of second-order switched linear systems consisting of two subsystems with unstable foci was discussed in [80]. In [81], the constraint on one of the subsystems was released. However, these stabilizability conditions are not general since not all the possible combinations of subsystem dynamics were considered. Recently, detailed criteria to determine the “most stable” switching signal, which was called the best case switching signal (BCSS), was derived in polar coordinates in [82]. With these criteria, easily verifiable necessary and sufficient conditions for the switching stabilizability of generic second-order switched linear systems with two subsystems were also derived in [82].

Similar to the stability under arbitrary switching problem mentioned earlier, all these results are only applicable to second-order switched linear systems with two subsystems. It has been also an open problem to derive easily verifiable necessary and sufficient conditions for the switching stabilizability of second-order switched linear systems with more than two subsystems, which is to be studied in this dissertation.

## 1.2 Controller Synthesis of Switched Systems

It is well known that numerous techniques were developed to control simple systems in an efficient manner during the period 1932-1960. In particular, using both frequency domain methods as well as time domain methods based on pole-zero configurations of the relevant transfer functions, various design methods were developed for the control of linear systems described by difference or

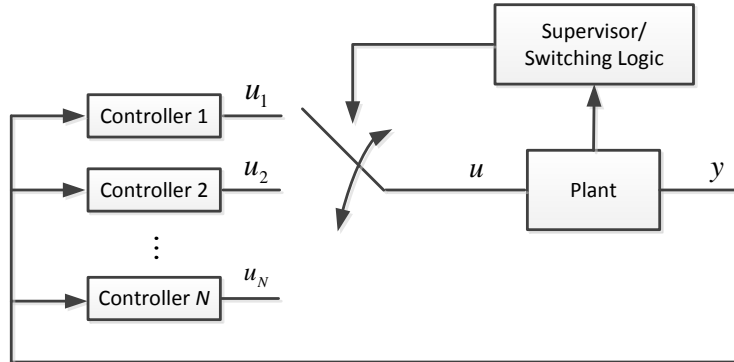


Figure 1.3: A multi-controller switched system

differential equations with known parameters.

While the linear control methods have been used extensively in the industry to design controllers for innumerable systems and have been found to be extremely robust and reliable, they rely on the key assumption that the systems are linear or at least linear within a small operating range. However, most real-world systems are inherently nonlinear and are supposed to work over a wide operating range. As such, we cannot expect a satisfactory performance with a linear controller.

Switched systems, in this case, provide a switching control method for nonlinear systems based on the divide-and-conquer strategy. The basic idea is to divide the whole operating range of a nonlinear system into several sub-regions, identify a local submodel with a simple structure within each sub-region, and design a corresponding sub-controller based on the local submodel. Switching among the family of sub-controllers can be implemented by incorporating logic-based decisions into the control law. This yields a multi-controller switched system, as shown in Fig. 1.3.

In fact, the use of multiple models and switching is not new in control the-

ory. The gain scheduling theory originated during the late 1960s, which utilizes a divide-and-conquer type of design procedure and decomposes the nonlinear control design task into a number of linear sub-problems, is one of the most popular approaches to nonlinear control design and has been widely and successfully applied in fields ranging from aerospace to process control. For example, Stein *et al.* [83] and Kallstrom *et al.* [84] used the gain scheduling approach in the control of F-8 aircraft and tankers, in 1977 and 1979 respectively. See [85, 86] for an overview of the gain scheduling approach. In the 1990s, Morse [87, 88] proposed the supervisory control of families of linear set-point controllers, in which multiple fixed models and optimization were used. Narendra and Balakrishnan [89] proposed the idea of using multiple adaptive models and switching to improve the performance of an adaptive system while assuring stability. This framework was extended to the combination of a number of fixed models and a reinitialized adaptive model in [90], and to the discrete-time case in [91]. The idea of using multiple models to deal with rapidly time-varying systems was also initiated by Narendra *et al.* in [92].

In this thesis, we focus on the identification and control of discrete-time nonlinear systems using multiple models and switching. The primary reason to consider discrete-time systems is that most complex nonlinear systems with large operating range are controlled by computers that are discrete in nature.

### 1.2.1 Identification using Multiple Models

In order to identify nonlinear systems using multiple models, an accurate multiple model architecture is necessary. Intuitively, the simplest case is when all the submodels are linear/affine, which are called the piecewise linear/affine

models [93, 94].

Piecewise affine (PWA) models are obtained by partitioning the state-input domain (or the regressor domain, for systems in input-output form) into a finite number of non-overlapping convex polyhedral, and by considering linear/affine subsystems in each region [93]. PWA systems have drawn most of the attention in recent years since they are equivalent to several classes of hybrid systems [95, 96], and thus can be used to obtain hybrid models from data. More importantly, the universal approximation properties of PWA maps [97, 98] make PWA models attractive for the identification of nonlinear systems.

Identification of PWA models is a challenging problem that involves the estimation of both the parameters of the affine submodels and the coefficients of the hyperplanes defining the partition of the state-input domain (or the regressor domain). The main difficulty is that the identification problem is coupled with a data classification problem, wherein each data point needs to be associated with the most suitable submodel. Concerning the partitioning, there are two scenarios: (1) the partition is fixed a priori; (2) the partition is estimated along with the submodels.

In the first scenario, data classification is simple, and estimation of the submodels can be carried out using standard linear identification techniques. However, due to the linearity requirement on the submodels, it is not easy to fix the partition a priori in practice. In most times, we have to deal with the second scenario, where the regions must be shaped to the clusters of data, and the strict relation among data classification, parameter estimation and region estimation makes the identification problem very challenging. Although complicated, sev-

eral techniques have been proposed for the identification of PWA models in the past decade [99, 100, 101, 102, 103, 104]. For an overview of the PWA identification techniques, see [105, 106]. Recently, the identification of PWA models was formulated as an optimization problem [107, 108]. In particular, the parameters of the affine submodels were first estimated through a least-square-based identification method using multiple models, and the partition of the regressor space was then estimated using standard pattern recognition techniques.

While PWA models provide an attractive model structure for the identification of nonlinear systems, the number of submodels and the need for data grow exponentially as the dimension of the regressor space increases, which is referred to as the “curse of dimensionality” problem in the literature. The main reason for this problem is that all dimensions of the regressor space are engaged in the partitioning. Therefore, the PWA models are impracticable for high-dimensional nonlinear systems and it is of great practical importance to develop a novel multiple model architecture for the identification of nonlinear systems to resolve this problem.

### **1.2.2 Control using Multiple Models and Switching**

With an accurate multiple model structure, we can control nonlinear systems using a switching controller. In general, there are two steps for the switching controller design. First, we need to design sub-controllers based on each submodel. By far, the most popular control methodology for switched systems is the multiple model predictive control (MMPC) [109, 110, 111, 112, 113, 114, 115, 116, 117]. Different from the conventional model predictive control based on a single model, where the control signal is computed by minimizing a cost function that penalizes

the future output error and the variation in control signal, the switching among different local submodels and their corresponding sub-controllers also need to be taken into consideration. By viewing the activation and deactivation of the sub-controllers as a discrete state of one or zero, some researchers proposed to include this discrete state in the cost function, and solve a mixed-integer linear/quadratic problem [19, 112]. However, it is challenging to implement these controllers due to the complexity of the mixed-integer programming. In this case, the optimization problem was recast as multi-parametric mixed-integer programming in [109, 118], where the optimal control signal was first obtained as an explicit function of the states by off-line calculation and recalculated via a simple function evaluation in real-time implementation. However, this method is not suitable for general tracking purpose. Most recently, the sub-controllers design problem based on PWA models was transformed into several quadratic optimization problems with complex nonlinear constraints in [107]. However, the computational load is still too high to be used in real-time applications.

After having all the sub-controllers, the second step is to determine the switching mechanism among them. In [87, 88], the “supervisor” determines the best sub-controller to be used at a particular instant by evaluating certain norm-squared output estimation errors of the local submodels. Moreover, [119] evaluated the best sub-controller to be activated by comparing the “virtual” closed-loop performance. In addition, it is also possible to weight the output of each sub-controller based on some fuzzy or Bayesian rules and sum them up as the final control signal [114]. In [107], the switching mechanism was determined by evaluating the cost functions for all the sub-controllers and choosing the one

with the smallest cost value at every time instant.

### 1.3 Objectives and Contributions

As discussed in the previous two sections, despite the extensive work in the field of stability analysis and controller synthesis of switched systems, there are still some challenges that have not been studied thoroughly. The principle aim of this thesis is to extend the stability and stabilizability conditions for second-order switched linear systems with two subsystems to the general case, and develop a novel multiple model approach for the identification and control of nonlinear systems. The main contributions of this thesis are as follows.

**1) An easily verifiable necessary and sufficient condition for the stability of second-order switched linear systems with any finite number of subsystems under arbitrary switching.** While several stability conditions have been derived for second-order switched linear systems under arbitrary switching based on the worst case analysis [65, 66, 67, 68, 69], most of them are only applicable to two-mode switched systems. However, in general, switched systems may have more than two modes. Motivated by this limitation, this thesis extends the worst case switching signal (WCSS) criteria for second-order switched linear systems with two subsystems to the general case with any finite number of subsystems, and derives an easily verifiable necessary and sufficient condition for the stability of second-order switched linear systems with any finite number of subsystems under arbitrary switching.

**2) Easily verifiable necessary and sufficient conditions for the switching stabilizability of second-order switched linear systems with any fi-**

**nite number of subsystems.** Similarly, while the best case analysis approach has been used to derive necessary and sufficient conditions for the switching stabilizability of second-order switched linear systems [79, 80, 81, 82], most of the results are restricted to systems with two modes. However, we may have higher degree of freedom in designing stabilizing switching laws with more subsystems. Motivated by this limitation, this thesis extends the best case switching signal (BCSS) criteria for second-order switched linear systems with two subsystems to the general case with any finite number of subsystems, and derives several easily verifiable necessary and sufficient conditions for the switching stabilizability of second-order switched linear systems with any finite number of subsystems.

**3) A novel multiple model approach for the identification and control of nonlinear systems.** While PWA models have drawn most of the attention in the identification and control of nonlinear systems [99, 101, 103, 107], there are two major issues for the PWA model based identification and control: the curse of dimensionality and the computational complexity. To resolve these two issues, a novel multiple model approach, which includes a multiple model architecture and a switching control algorithm, is proposed for the identification and control of nonlinear systems in this dissertation.

## 1.4 Thesis Organization

The rest of the thesis consists of two parts and is organized as follows.

The first part, which includes three chapters (Chapters 2, 3, and 4), focuses on the stability analysis of second-order switched linear systems. Chapter 2 presents some mathematical preliminaries for the stability analysis of second-



order switched linear systems in polar coordinates. In Chapter 3, an easily verifiable necessary and sufficient condition for the stability of second-order switched linear systems with a finite number of subsystems under arbitrary switching is derived by extending the WCSS criteria for the two-mode case to the general case. Chapter 4, on the other hand, extends the BCSS criteria for the two-mode case to the general case and derives several easily verifiable necessary and sufficient conditions for the switching stabilizability of second-order switched linear systems with a finite number of subsystems.

The second part, which consists of two chapters (Chapters 5 and 6), develops a novel multiple model approach for the identification and control of nonlinear systems. In particular, Chapter 5 derives a multiple model architecture, which circumvents the curse of dimensionality problem, to identify nonlinear systems. A theoretical upper bound for the estimation error is also obtained based on the Taylor's theorem. With the identified multiple model architecture, Chapter 6 then designs a computationally effective switching control algorithm for nonlinear systems using the weighted one-step-ahead predictive control method and constrained optimization techniques. Both simulation studies and experimental results demonstrate the effectiveness of the multiple model architecture and switching control algorithm.

Finally, Chapter 7 concludes the dissertation with a summary of the main contributions and possible future research directions.

Part I

**Stability Analysis of Switched  
Systems**

## Chapter 2

# Polar Coordinates Analysis

### 2.1 Introduction

As mentioned in Chapter 1, most of the stability (resp. stabilizability) results based on the worst (resp. best) case analysis are restricted to second-order switched linear systems with two subsystems. However, in general, switched systems may have more than two modes. Moreover, we may have higher degree of freedom in designing stabilizing switching laws with more subsystems. Therefore, it is of vital importance to extend the existing results to general second-order switched linear systems with any finite number of subsystems.

This chapter provides some mathematical preliminaries for the extensions by analyzing second-order switched linear systems in polar coordinates ( $r - \theta$  coordinates). First, the analysis of second-order switched linear systems with two subsystems in polar coordinates is extended to the general case with any finite number of subsystems by considering all the subsystems pairwise. Then, the polar coordinates space can be partitioned into several regions, in the interior of which all the subsystems are classified into two groups based on the direction

of trajectories for each subsystem in the interior of the corresponding region. With a similar criterion, we can also have two groups of subsystems on each boundary.

Mathematically, this chapter considers the following continuous-time second-order switched linear system with  $N$  ( $N \geq 2$ ) subsystems of the form

$$\dot{x}(t) = A_{\sigma}x(t) \quad (2.1)$$

with

$$A_i = \begin{bmatrix} a_{11i} & a_{12i} \\ a_{21i} & a_{22i} \end{bmatrix} \quad (2.2)$$

where  $x(t) \in \mathbb{R}^2$  is the state and  $\sigma : \mathbb{R}^+ \rightarrow \mathcal{I}_N = \{1, 2, \dots, N\}$  is the switching signal that determines the active mode of the system among  $N$  possible modes in  $\mathcal{A} = \{A_1, A_2, \dots, A_N\}$ .

As mentioned in Chapter 1, all the subsystems are asymptotically stable in studying the stability under arbitrary switching, while all the subsystems are unstable in the switching stabilization problem. To simplify the analysis, three special cases are excluded by the following assumptions. These three cases will be discussed separately in Section 3.2 and Section 4.2 for the stability under arbitrary switching and the switching stabilizability.

**Assumption 2.1.**  $A_i \neq cA_j$ , where  $c \in \mathbb{R}$ ,  $c > 0$ ,  $i, j \in \mathcal{I}_N$ , and  $i \neq j$ .

**Assumption 2.2.**  $A_i \neq c \begin{bmatrix} 1 & 0 \\ 0 & 1 \end{bmatrix}$ , where  $c \in \mathbb{R}$ ,  $c \neq 0$ , and  $i \in \mathcal{I}_N$ .

**Assumption 2.3.** There does not exist a common real eigenvector for all  $A_i \in \mathcal{A}$ .

## 2.2 A Single Second-order LTI System in Polar Coordinates

Consider a single second-order LTI system of the form

$$\dot{x} = Ax = \begin{bmatrix} a_{11} & a_{12} \\ a_{21} & a_{22} \end{bmatrix} x \quad (2.3)$$

where  $x = [x_1, x_2]^T$ .

Define  $x_1 = r \cos \theta$  and  $x_2 = r \sin \theta$ , it follows that

$$\frac{dr}{dt} = r[a_{11} \cos^2 \theta + a_{22} \sin^2 \theta + (a_{12} + a_{21}) \sin \theta \cos \theta], \quad (2.4)$$

$$\frac{d\theta}{dt} = a_{21} \cos^2 \theta - a_{12} \sin^2 \theta + (a_{22} - a_{11}) \sin \theta \cos \theta. \quad (2.5)$$

It is noted that the real vectors satisfying  $\frac{d\theta}{dt} = 0$  correspond to the real eigenvectors of  $A$ . The solution of system (2.3) on a real eigenvector is  $r(t) = r_0 e^{\lambda_A t}$ ,  $\theta(t) = \theta_0$ , where  $(r_0, \theta_0)$  is the the initial state and  $\lambda_A$  is the corresponding eigenvalue of the real eigenvector.

When  $\frac{d\theta}{dt} \neq 0$ , we have

$$\frac{dr}{d\theta} = r \frac{a_{11} \cos^2 \theta + a_{22} \sin^2 \theta + (a_{12} + a_{21}) \sin \theta \cos \theta}{a_{21} \cos^2 \theta - a_{12} \sin^2 \theta + (a_{22} - a_{11}) \sin \theta \cos \theta}. \quad (2.6)$$

Denote

$$f(\theta) = \frac{a_{11} \cos^2 \theta + a_{22} \sin^2 \theta + (a_{12} + a_{21}) \sin \theta \cos \theta}{a_{21} \cos^2 \theta - a_{12} \sin^2 \theta + (a_{22} - a_{11}) \sin \theta \cos \theta}, \quad (2.7)$$

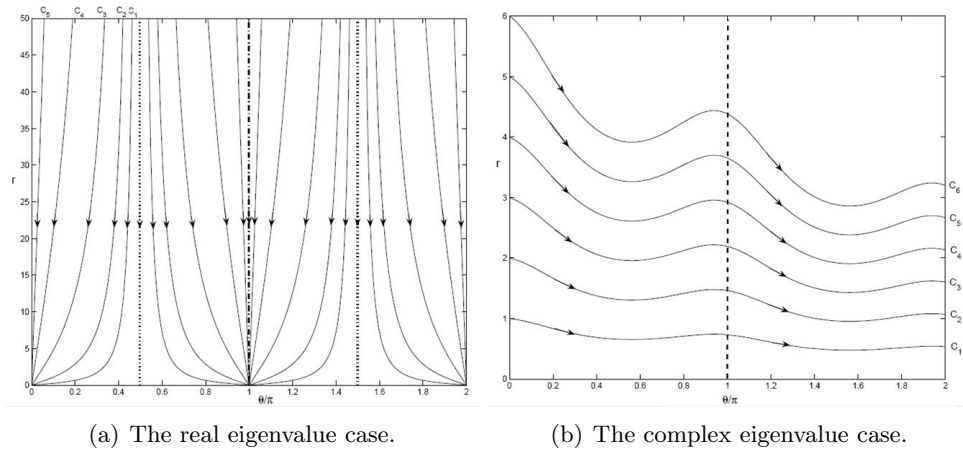


Figure 2.1: The phase diagrams of second-order LTI systems in polar coordinates

we have

$$\frac{1}{r}dr = f(\theta)d\theta. \quad (2.8)$$

**Lemma 2.1** ([69]). *The trajectories of the second-order LTI system (2.3) in  $r$ - $\theta$  coordinates, except the ones along the real eigenvectors, can be expressed as*

$$r(t) = Cg(\theta(t)) = Ce^{\int_{\theta^*}^{\theta(t)} f(\tau)d\tau} \quad (2.9)$$

where  $C$ , the constant of integration, is a positive constant depending on the initial state  $(r_0, \theta_0)$  and  $\theta^*$ . Note that  $\theta^*$  can be chosen as any value except the angle of any real eigenvector of matrix  $A$ .

Typical phase trajectories of second-order LTI systems in polar coordinates are shown in Fig. 2.1.

*Remark 2.1.* It is noted that the constant of integration  $C$  only depends on the initial state and  $\theta^*$ . It remains invariant for the whole trajectory of the LTI system (2.3). Geometrically, a larger  $C$  indicates an outer layer trajectory, as shown in Fig. 2.1, where  $C_1 < C_2 < C_3 < \dots < C_6$ .

*Remark 2.2.* It follows from (2.9) that

$$\frac{r(\theta + \pi)}{r(\theta)} = \frac{C e^{\int_{\theta^*}^{\theta + \pi} f(\tau) d\tau}}{C e^{\int_{\theta^*}^{\theta} f(\tau) d\tau}} = e^{\int_{\theta}^{\theta + \pi} f(\tau) d\tau} \quad (2.10)$$

which is a constant since  $f(\theta)$  is a periodic function with a period of  $\pi$ . Therefore, it is sufficient to analyze the stability of system (2.3) in an interval of  $\theta \in [-\frac{\pi}{2}, \frac{\pi}{2}]$ .

## 2.3 The Switched System (2.1) with $N = 2$ in Polar Coordinates

Consider the switched system (2.1) with  $N = 2$ . From Lemma 2.1, the solutions of the two subsystems are  $r_1(t) = C_1 g_1(\theta(t))$  and  $r_2(t) = C_2 g_2(\theta(t))$  respectively. By combining them together, we can have a piecewise solution for the switched system (2.1) with  $N = 2$  of the form

$$r(t) = \begin{cases} C_1(t) g_1(\theta(t)) & \sigma(t) = 1 \\ C_2(t) g_2(\theta(t)) & \sigma(t) = 2 \end{cases} \quad (2.11)$$

where  $C_1(t)$  and  $C_2(t)$  are invariant during the period when the states move along their own phase trajectories, which means

$$\left. \frac{dC_1(t)}{dt} \right|_{\sigma=1} = 0, \quad \left. \frac{dC_2(t)}{dt} \right|_{\sigma=2} = 0. \quad (2.12)$$

Then, a compact solution for the switched system (2.1) with  $N = 2$ , except the ones along the eigenvectors, can be obtained as

$$r(t) = h_1(\theta(t)) g_1(\theta(t)), \quad (2.13)$$

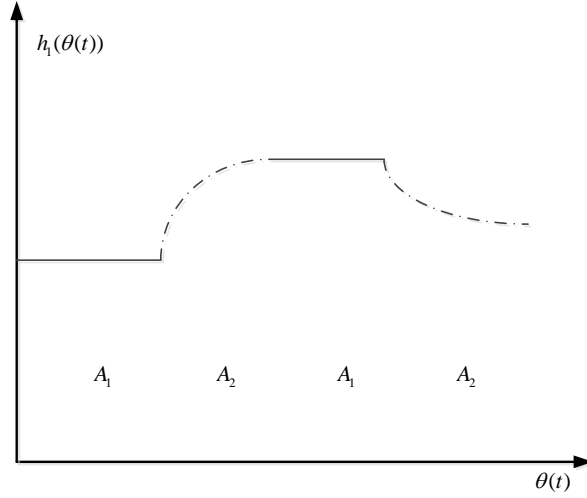


Figure 2.2: The variation of  $h_1$  under switching

where

$$h_1(\theta(t)) = \begin{cases} C_1(t) & \sigma(t) = 1 \\ C_2(t) \frac{g_2(\theta(t))}{g_1(\theta(t))} & \sigma(t) = 2 \end{cases} \quad (2.14)$$

or similarly

$$r(t) = h_2(\theta(t))g_2(\theta(t)), \quad (2.15)$$

where

$$h_2(\theta(t)) = \begin{cases} C_1(t) \frac{g_1(\theta(t))}{g_2(\theta(t))} & \sigma(t) = 1 \\ C_2(t) & \sigma(t) = 2 \end{cases}. \quad (2.16)$$

Equations (2.13) indicates that even when the actual trajectory follows  $\Sigma_{A_2}$ , it can still be described by the same form as that of the solution of  $\Sigma_{A_1}$  with a varying  $h_1$ . Therefore, the variation of  $h_1$  can be used to describe the behavior of the switched system (2.1) with  $N = 2$ , as shown in Fig. 2.2.

For convenience, we denote

$$H_{12}(\theta(t)) = \left. \frac{dh_1(\theta(t))}{dt} \right|_{\sigma=2}, \quad H_{21}(\theta(t)) = \left. \frac{dh_2(\theta(t))}{dt} \right|_{\sigma=1}. \quad (2.17)$$



*Remark 2.3.* Geometrically, a positive  $H_{12}(\theta)$ , or equivalently an increase of  $h_1(\theta)$  when  $\Sigma_{A_2}$  is active, means that the vector field of  $\Sigma_{A_2}$  points outwards relative to  $\Sigma_{A_1}$ . In fact, the signs of  $H_{12}(\theta(t))$  and  $H_{21}(\theta(t))$  are indicators to determine which subsystem is more “unstable” for every  $\theta$ .

In addition, we also need to know how  $\theta$  varies with time  $t$ , which is determined by the signs of  $Q_1(\theta(t))$  and  $Q_2(\theta(t))$  defined as

$$Q_1(\theta(t)) = \left. \frac{d\theta}{dt} \right|_{\sigma=1}, \quad Q_2(\theta(t)) = \left. \frac{d\theta}{dt} \right|_{\sigma=2}. \quad (2.18)$$

*Remark 2.4.* The geometrical meaning of the sign of  $Q_i(\theta)$  ( $i \in \{1, 2\}$ ) is the direction of trajectories for  $\Sigma_{A_i}$  in the  $x - y$  coordinates. A positive  $Q_i(\theta)$  implies counterclockwise trajectories of  $\Sigma_{A_i}$ , and vice versa.

After defining  $H_{12}(\theta)$ ,  $H_{21}(\theta)$ ,  $Q_1(\theta)$  and  $Q_2(\theta)$  for the switched system (2.1) with  $N = 2$ , we can have the following equalities by straightforward algebraic manipulations.

$$Q_1(\theta + \pi) = Q_1(\theta) \quad (2.19)$$

$$Q_2(\theta + \pi) = Q_2(\theta) \quad (2.20)$$

$$\text{sgn}(H_{12}(\theta + \pi)) = \text{sgn}(H_{12}(\theta)) \quad (2.21)$$

$$\text{sgn}(H_{21}(\theta + \pi)) = \text{sgn}(H_{21}(\theta)) \quad (2.22)$$

where  $\text{sgn}(\cdot)$  is the signum function.

*Remark 2.5.* It was proved in [69] that the WCSS (resp. BCSS) for the switched system (2.1) with  $N = 2$  is only determined by the signs of  $H_{12}(\theta)$ ,  $H_{21}(\theta)$ ,  $Q_1(\theta)$  and  $Q_2(\theta)$ . Based on equations (2.19)-(2.22), it is sufficient to study the

WCSS (resp. BCSS) of the switched system (2.1) with  $N = 2$  in an interval of  $\theta \in [-\frac{\pi}{2}, \frac{\pi}{2})$ .

Since the interval of interest is  $\theta \in [-\frac{\pi}{2}, \frac{\pi}{2})$ , all the functions of  $\theta$  can be transformed to the functions of  $k$  by denoting  $k = \tan \theta$  (the special case when  $\theta = -\frac{\pi}{2}$  can be considered as a boundary separately). Straightforward algebraic manipulations yield

$$\operatorname{sgn}(H_{12}(k)) = \operatorname{sgn}\left(\frac{N_{12}(k)}{D_1(k)}\right) \quad (2.23)$$

$$\operatorname{sgn}(H_{21}(k)) = -\operatorname{sgn}\left(\frac{N_{12}(k)}{D_2(k)}\right) \quad (2.24)$$

$$\operatorname{sgn}(Q_1(k)) = -\operatorname{sgn}(D_1(k)) \quad (2.25)$$

$$\operatorname{sgn}(Q_2(k)) = -\operatorname{sgn}(D_2(k)) \quad (2.26)$$

where

$$D_1(k) = a_{121}k^2 + (a_{111} - a_{221})k - a_{211} \quad (2.27)$$

$$D_2(k) = a_{122}k^2 + (a_{112} - a_{222})k - a_{212} \quad (2.28)$$

and

$$\begin{aligned} N_{12}(k) = & (a_{121}a_{222} - a_{221}a_{122})k^2 + (a_{121}a_{212} + a_{111}a_{222} \\ & - a_{211}a_{122} - a_{221}a_{112})k + a_{111}a_{212} - a_{211}a_{112}. \end{aligned} \quad (2.29)$$

**Definition 2.1.** A region of  $k$  is a continuous interval of  $k$  where the signs of  $H_{12}(k)$ ,  $H_{21}(k)$ ,  $Q_1(k)$  and  $Q_2(k)$  are constants for all  $k$  in that interval.

*Remark 2.6.* A region of  $k$  corresponds to two symmetric conic sectors (without boundaries) in the  $x - y$  coordinates, as shown in Fig. 2.3.

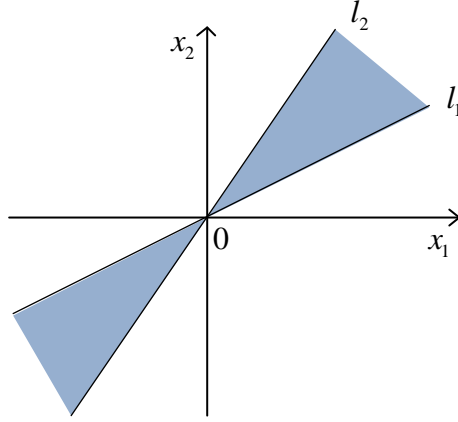


Figure 2.3: Two symmetric conic sectors for a region of  $k$

*Remark 2.7.* The boundaries for the regions of  $k$ , if exists, are lines whose slopes satisfy  $D_1(k) = 0$  (real eigenvectors of  $A_1$ ),  $D_2(k) = 0$  (real eigenvectors of  $A_2$ ), or  $N_{12}(k) = 0$  (lines where the trajectories of the two subsystems are tangent to each other).

## 2.4 The Switched System (2.1) with $N \geq 2$ in Polar Coordinates

Based on the analysis of the switched system (2.1) with  $N = 2$  in polar coordinates, we can analyze the switched system (2.1) with  $N \geq 2$  in polar coordinates by considering every two subsystems pairwise. For any two subsystems  $\Sigma_{A_i}$  and  $\Sigma_{A_j}$  ( $i, j \in \mathcal{I}_N$ ,  $i < j$ ), we can define the following four terms according to equations (2.17) and (2.18).

$$Q_i(\theta(t)) = \left. \frac{d\theta}{dt} \right|_{\sigma=i}, \quad Q_j(\theta(t)) = \left. \frac{d\theta}{dt} \right|_{\sigma=j} \quad (2.30)$$

$$H_{ij}(\theta(t)) = \left. \frac{dh_i(\theta(t))}{dt} \right|_{\sigma=j}, \quad H_{ji}(\theta(t)) = \left. \frac{dh_j(\theta(t))}{dt} \right|_{\sigma=i} \quad (2.31)$$

where

$$h_i(\theta(t)) = \begin{cases} C_i(t) & \sigma(t) = i \\ C_j(t) \frac{g_j(\theta(t))}{g_i(\theta(t))} & \sigma(t) = j \end{cases} \quad (2.32)$$

and

$$h_j(\theta(t)) = \begin{cases} C_j(t) & \sigma(t) = j \\ C_i(t) \frac{g_i(\theta(t))}{g_j(\theta(t))} & \sigma(t) = i. \end{cases} \quad (2.33)$$

It is noted that equations (2.19)-(2.22) are still true for every two subsystems  $\Sigma_{A_i}$  and  $\Sigma_{A_j}$  of the switched system (2.1) with  $N \geq 2$ , which means

$$Q_i(\theta + \pi) = Q_i(\theta) \quad (2.34)$$

$$Q_j(\theta + \pi) = Q_j(\theta) \quad (2.35)$$

$$\text{sgn}(H_{ij}(\theta + \pi)) = \text{sgn}(H_{ij}(\theta)) \quad (2.36)$$

$$\text{sgn}(H_{ji}(\theta + \pi)) = \text{sgn}(H_{ji}(\theta)) \quad (2.37)$$

Similarly, we can have the generalization of equations (2.23)-(2.26) with the form of

$$\text{sgn}(H_{ij}(k)) = \text{sgn}\left(\frac{N_{ij}(k)}{D_i(k)}\right) \quad (2.38)$$

$$\text{sgn}(H_{ji}(k)) = -\text{sgn}\left(\frac{N_{ij}(k)}{D_j(k)}\right) \quad (2.39)$$

$$\text{sgn}(Q_i(k)) = -\text{sgn}(D_i(k)) \quad (2.40)$$

$$\text{sgn}(Q_j(k)) = -\text{sgn}(D_j(k)) \quad (2.41)$$

where

$$D_i(k) = a_{12i}k^2 + (a_{11i} - a_{22i})k - a_{21i} \quad (2.42)$$

$$D_j(k) = a_{12j}k^2 + (a_{11j} - a_{22j})k - a_{21j} \quad (2.43)$$

and

$$\begin{aligned} N_{ij}(k) = & (a_{12i}a_{22j} - a_{22i}a_{12j})k^2 + (a_{12i}a_{21j} + a_{11i}a_{22j} \\ & - a_{21i}a_{12j} - a_{22i}a_{11j})k + a_{11i}a_{21j} - a_{21i}a_{11j}. \end{aligned} \quad (2.44)$$

**Definition 2.2.** A generalized region of  $k$ , is a continuous interval of  $k$  in the interior of which the signs of  $H_{ij}(k)$ ,  $H_{ji}(k)$ ,  $Q_i(k)$  and  $Q_j(k)$  are constants for any  $i, j \in \mathcal{I}_N$ , and  $i < j$ .

*Remark 2.8.* A generalized region of  $k$  also corresponds to two symmetric conic sectors (without boundaries) in the  $x - y$  coordinates.

*Remark 2.9.* Based on Remark 2.7, the boundaries for the generalized regions of  $k$  include lines whose slopes are real roots of  $D_i(k) = 0$  ( $i \in \mathcal{I}_N$ ) and lines whose slopes are real roots of  $N_{ij}(k) = 0$  ( $i, j \in \mathcal{I}_N$ , and  $i < j$ ).

*Remark 2.10.* According to equations (2.38)-(2.41), the signs of  $H_{ij}(k)$  and  $H_{ji}(k)$  are opposite if  $Q_i(k)$  and  $Q_j(k)$  have the same sign in the interior of a generalized region of  $k$ .

According to Definition 2.2, the direction of trajectories for any subsystem in the interior of a generalized region of  $k$  keeps invariant. Therefore, all the subsystems in  $\mathcal{A}$  can be classified into two groups in a generalized region of  $k$  based on the direction of trajectories for each subsystem: the clockwise subsystems

tems group  $\mathcal{A}_{rc}$  and the counterclockwise subsystems group  $\mathcal{A}_{rcc}$  in the interior of that region. Then, we have three types of generalized regions of  $k$  as follows.

- Type (a) Region:  $\mathcal{A}_{rc} \neq \emptyset$ , and  $\mathcal{A}_{rcc} \neq \emptyset$
- Type (b) Region:  $\mathcal{A}_{rc} = \emptyset$ , and  $\mathcal{A}_{rcc} \neq \emptyset$
- Type (c) Region:  $\mathcal{A}_{rc} \neq \emptyset$ , and  $\mathcal{A}_{rcc} = \emptyset$

Similarly, on any boundary, all the subsystems in  $\mathcal{A}$  except the ones with eigenvectors on this boundary can also be classified into two groups based on the direction of trajectories for each subsystem on that boundary. They are the clockwise subsystems group  $\mathcal{A}_{bc}$  and the counterclockwise subsystems group  $\mathcal{A}_{bcc}$  on that boundary. Similarly, we have three types of boundaries as follows.

- Type (a) Boundary:  $\mathcal{A}_{bc} \neq \emptyset$ , and  $\mathcal{A}_{bcc} \neq \emptyset$
- Type (b) Boundary:  $\mathcal{A}_{bc} = \emptyset$ , and  $\mathcal{A}_{bcc} \neq \emptyset$
- Type (c) Boundary:  $\mathcal{A}_{bc} \neq \emptyset$ , and  $\mathcal{A}_{bcc} = \emptyset$

Different types of regions and boundaries can be described by the diagrams in Figs. 2.4 and 2.5, where the vertical dashed lines represent the boundaries of regions. In Fig. 2.4, a dashed (resp. solid) horizontal line with arrows in a generalized region of  $k$  means that the clockwise (resp. counterclockwise) subsystems group  $\mathcal{A}_{rc}$  (resp.  $\mathcal{A}_{rcc}$ ) in the interior of that region is nonempty. In Fig. 2.5, a solid circle with an arrow pointing to the left (resp. right) on a boundary means that the clockwise (resp. counterclockwise) subsystems group  $\mathcal{A}_{bc}$  ( $\mathcal{A}_{bcc}$ ) on that boundary is nonempty.

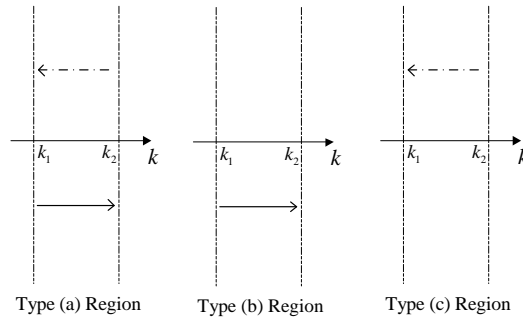


Figure 2.4: Different types of regions

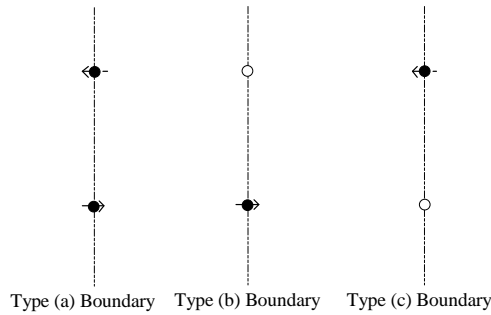


Figure 2.5: Different types of boundaries

From Fig. 2.4 and Fig. 2.5, it is obvious that the two boundaries of a Type (b) (resp. Type (c)) Region are both Type (b) (resp. Type (c)) Boundaries. However, the two boundaries of a Type (a) Region can be of any type.

## 2.5 Summary

In this chapter, the polar coordinates analysis for second-order switched linear systems with two subsystems was extended to the general case with any finite number of subsystems by considering all the subsystems pairwise. After partitioning the polar coordinates space into several regions, all the subsystems were classified into two groups in the interior of a region or on a boundary based on the direction of trajectories for each subsystem in the interior of the corre-

sponding region or on the corresponding boundary. The contents in this chapter provide important basis for the stability analysis of second-order switched linear systems with a finite number of subsystems in the next two chapters.



## Chapter 3

# Stability of Second-order Switched Linear Systems under Arbitrary Switching

### 3.1 Introduction

Based on the results in Chapter 2, this chapter aims to extend the worst case switching signal (WCSS) criteria for second-order switched linear systems with two subsystems in [69] to the general case with any finite number of subsystems and derive an easily verifiable necessary and sufficient condition for the stability under arbitrary switching. The key idea is to compare the subsystems for each group in the interior of a region pairwise, and determine the most “unstable” subsystem for the corresponding group. Based on this idea, the worst case analysis among all the subsystems in the interior of a region can be reduced to the worst case analysis between the two most “unstable” subsystems in the

interior of that region.

The contents of this chapter are organized as follows. Section 3.2 presents a unified statement of the problem. In Section 3.3, the WCSS criteria for second-order switched linear systems with two subsystems are extended to the general case with a finite number of subsystems. An easily verifiable necessary and sufficient condition for the stability of second-order switched linear systems with any finite number of subsystems under arbitrary switching is proposed in Section 3.4. Finally, in Section 3.5, a summary is given.

## 3.2 Statement of the Problem

Motivated by the limitations of the existing results outlined in Chapter 1, our aim is to derive an easily verifiable necessary and sufficient condition for the stability of second-order switched linear system with any finite number of subsystems under arbitrary switching. In particular, we consider the continuous-time second-order switched linear system with  $N$  ( $N \geq 2$ ) asymptotically stable subsystems under arbitrary switching signal of the form

$$\dot{x}(t) = A_{\sigma}x(t) \tag{3.1}$$

with

$$A_i = \begin{bmatrix} a_{11i} & a_{12i} \\ a_{21i} & a_{22i} \end{bmatrix} \tag{3.2}$$

where  $x(t) \in \mathbb{R}^2$  is the state, and  $\sigma : \mathbb{R}^+ \rightarrow \mathcal{I}_N = \{1, 2, \dots, N\}$  is the arbitrary switching signal that determines the active mode of the system among  $N$  possible modes in  $\mathcal{A} = \{A_1, A_2, \dots, A_N\}$ .

Recall the three assumptions made in Section 2.1 and rewrite them for the switched system (3.1) in the following form.

**Assumption 3.1.**  $A_i \neq cA_j$ , where  $c \in \mathbb{R}$ ,  $c > 0$ ,  $i, j \in \mathcal{I}_N$  and  $i \neq j$ .

When Assumption 3.1 is violated, the trajectories of  $\Sigma_{A_i}$  and  $\Sigma_{A_j}$  are identical for the same initial state. Therefore, only one of them needs to be considered in the worst case analysis.

**Assumption 3.2.**  $A_i \neq c \begin{bmatrix} 1 & 0 \\ 0 & 1 \end{bmatrix}$ , where  $c \in \mathbb{R}$ ,  $c < 0$ , and  $i \in \mathcal{I}_N$ .

When Assumption 3.2 is violated, any switching to  $A_i$  can only make the trajectories of the switched system (3.1) become more “stable” ( $\theta$  keeps invariant and  $r$  becomes smaller). In this case, there is no need to take  $A_i$  into account in the worst case analysis.

**Assumption 3.3.** There does not exist a common real eigenvector for all  $A_i \in \mathcal{A}$ .

When Assumption 3.3 is violated, all matrices in  $\mathcal{A}$  are simultaneously similar to upper triangular matrices, and thus they admit a CQLF [120]. In this case, the switched system (3.1) is always asymptotically stable under arbitrary switching.

### 3.3 Worst Case Analysis for the Switched System

#### (3.1)

In this section, we generalize the WCSS criteria for the switched system (3.1) with  $N = 2$  in [69] to the general case when  $N \geq 2$ .

### 3.3.1 WCSS Criteria for the Switched System (3.1) with $N = 2$

**Lemma 3.1.** [69] *For the switched system (3.1) with  $N = 2$ , we have*

1) *The switched system is not asymptotically stable under arbitrary switching if there exists a region of  $k$  where both  $H_{12}$  and  $H_{21}$  are positive;*

2) *In regions where  $H_{12} > 0$ ,  $H_{21} < 0$ , the switching signal staying on  $\Sigma_{A_2}$  is the local WCSS;*

3) *In regions where  $H_{12} < 0$ ,  $H_{21} > 0$ , the switching signal staying on  $\Sigma_{A_1}$  is the local WCSS.*

**Lemma 3.2.** *For the switched system (3.1) with  $N = 2$ , the local WCSS cannot have any switch between the two subsystems in regions where both  $H_{12}(k)$  and  $H_{21}(k)$  are negative.*

This lemma can be easily proved based on the definition of  $H_{12}$  and  $H_{21}$ .

### 3.3.2 WCSS Criteria for the Switched System (3.1) with $N \geq 2$

#### WCSS criteria in the interior of generalized regions of $k$

According to Remark 2.10 and Lemma 3.1, we can determine the more “unstable” subsystem for any two subsystems belonging to the same group in a generalized region of  $k$ . For all the subsystems in  $\mathcal{A}_{rc}$  (resp.  $\mathcal{A}_{rcc}$ ), by comparing pairwise, the most “unstable” clockwise (resp. counterclockwise) subsystem in the interior of that region can then be determined.

**Definition 3.1.** In the interior of a generalized region of  $k$ , the most “unstable” clockwise (resp. counterclockwise) subsystem is called the worst clockwise (resp. counterclockwise) subsystem in that region.

*Remark 3.1.* According to Lemma 3.1, the worst clockwise (resp. counterclockwise) subsystem in the interior of a generalized region of  $k$  is  $\Sigma_{A_p}$  (resp.  $\Sigma_{A_q}$ ) whose  $H_{ip}$  ( $H_{jq}$ ) terms are all positive with  $A_i \in \mathcal{A}_{rc}$ ,  $i \neq p$  (resp.  $A_j \in \mathcal{A}_{rcc}$ ,  $j \neq q$ ).

**Lemma 3.3.** *The local WCSS in a generalized region of  $k$  only relates to the worst clockwise subsystem and the worst counterclockwise subsystem in that region.*

*Proof.* First, let us assume the local WCSS in a generalized region of  $k$  relates to a third subsystem. Then, a switching signal that is more “unstable” can always be constructed by replacing the portion on this third subsystem with  $A_p$  (clockwise part) or  $A_q$  (counterclockwise part), which contradicts to the definition of the WCSS.  $\square$

From Lemma 3.3, we know that the local WCSS in the interior of a Type (b) (resp. Type (c)) Region is the switching signal staying on the worst counterclockwise (resp. clockwise) subsystem in that region. For a Type (a) Region, we have the following two lemmas.

**Lemma 3.4.** *The switched system (3.1) with  $N \geq 2$  is not asymptotically stable under arbitrary switching if there exists a Type (a) Region where both  $H_{pq}(k)$  and  $H_{qp}(k)$  are positive.*

**Lemma 3.5.** *In the interior of a Type (a) Region where both  $H_{pq}(k)$  and  $H_{qp}(k)$  are negative, the local WCSS for the switched system (3.1) with  $N \geq 2$  cannot have any switch between  $A_p$  and  $A_q$ .*

These two lemmas can be easily proved based on Lemmas 3.1-3.3.

**Definition 3.2.** In the worst case analysis, a Type (a) Region where both  $H_{pq}$  and  $H_{qp}$  are positive (resp. negative) is called an unstable (resp. a stable) Type (a) Region.

### WCSS criteria on boundaries of generalized regions of $k$

It is obvious that the WCSS on the eigenvector of a stable subsystem cannot be the switching signal staying on this subsystem. Therefore, the subsystems on their corresponding eigenvectors can be ignored in the worst case analysis, and the worst case trajectory of the switched system (3.1) with  $N \geq 2$  cannot stay on any boundary of the regions. According to the properties of linear systems, the time spent on any boundary is zero. Therefore, we only need to study whether the direction of the worst case trajectory will change after reaching a boundary. For a Type (b) Boundary or a Type (c) Boundary, there is no doubt since only one direction is possible. For a Type (a) Boundary, we have

**Lemma 3.6.** *If there does not exist any unstable Type (a) Region, the direction of the worst case trajectory for the switched system (3.1) with  $N \geq 2$  will keep invariant after reaching a Type (a) Boundary.*

*Proof.* It is obvious that the two adjacent regions sharing a Type (a) Boundary are both stable Type (a) Regions. Let's assume that the worst case trajectory for the switched system (3.1) with  $N \geq 2$  changes direction after reaching a Type (a) Boundary. Then, the switching signal would have infinite number of discontinuities on a finite interval of time, which contradicts to the no-chattering requirement for continuous-time switched systems.  $\square$

### 3.4 A Necessary and Sufficient Condition for the Stability of the Switched System (3.1) with $N \geq 2$ under Arbitrary Switching

Before proceeding, several notations and lemmas need to be given. For every subsystem  $\Sigma_{A_i}$ , we can define the following two regions

$$E_{ic} = \{\theta | Q_i(\theta) \leq 0\} \quad (3.3)$$

$$E_{icc} = \{\theta | Q_i(\theta) \geq 0\} \quad (3.4)$$

where  $E_{ic}$  (resp.  $E_{icc}$ ) represents the regions in the interior of which subsystem  $\Sigma_{A_i}$  travels clockwise (resp. counterclockwise). Denote  $E_{ic}^o$  (resp.  $E_{icc}^o$ ) as the interior of  $E_{ic}$  (resp.  $E_{icc}$ ), we have the following lemma.

**Lemma 3.7.**  $\bigcup_{i=1}^N E_{ic}^o = \mathbb{R}^2$  if and only if there is no Type (b) Boundary in the polar coordinates space.  $\bigcup_{i=1}^N E_{icc}^o = \mathbb{R}^2$  if and only if there is no Type (c) Boundary in the polar coordinates space.

*Proof.* Without loss of generality, only the first part of this lemma is proved.

The second part follows the similar line and is thus omitted.

**Sufficiency:** If there is no Type (b) Boundary in the polar coordinates space, all the boundaries are of Type (a) or Type (c). In this case, there cannot exist any Type (b) Region and therefore  $\bigcup_{i=1}^N E_{ic}^o = \mathbb{R}^2$ .

**Necessity:** Let's assume that there exists a Type (b) Boundary in the polar coordinates space. Then, there does not exist a subsystem whose trajectory direction is clockwise on this boundary and therefore  $\bigcup_{i=1}^N E_{ic}^o \neq \mathbb{R}^2$ .  $\square$

If  $\bigcup_{i=1}^N E_{ic}^o = \mathbb{R}^2$  (resp.  $\bigcup_{i=1}^N E_{icc}^o = \mathbb{R}^2$ ), the trajectory of the switched system (3.1) with  $N \geq 2$  under the switching signal staying on the corresponding worst clockwise (resp. counterclockwise) subsystem in each region will be a clockwise (resp. counterclockwise) spiral around the origin for any non-zero initial state  $x(t_0)$  in the  $x - y$  coordinates. To determine the convergence or divergence of such trajectories, we can define the worst clockwise ratio  $\gamma_{wc}(x(t_0))$  (resp. the worst counterclockwise ratio  $\gamma_{wcc}(x(t_0))$ ) between the magnitudes of the state after one full clockwise (resp. counterclockwise) circle and the non-zero initial state  $x(t_0)$  in the  $x - y$  coordinates with the form of

$$\gamma_{wc}(x(t_0)) = \frac{\|\Phi_{wc}(x(t_0))x(t_0)\|}{\|x(t_0)\|} \quad (3.5)$$

$$\gamma_{wcc}(x(t_0)) = \frac{\|\Phi_{wcc}(x(t_0))x(t_0)\|}{\|x(t_0)\|} \quad (3.6)$$

where  $\Phi_{wc}(x(t_0))$  (resp.  $\Phi_{wcc}(x(t_0))$ ) represents the state transition matrix for a full clockwise (resp. counterclockwise) spiral under the switching signal staying on the corresponding worst clockwise (resp. counterclockwise) subsystem in each region for the initial state  $x(t_0)$ .

Due to the symmetric property of the WCSS, we only need to consider half plane. Denote the worst clockwise (resp. counterclockwise) subsystems from the ray that  $x(t_0)$  falls on as  $A_1, A_2, \dots, A_m$  in clockwise (resp. counterclockwise) direction before reaching the opposite ray where  $-x(t_0)$  falls on. According to the isochronism property of linear systems, the time  $T_i$  spend in the  $i^{\text{th}}$  subsystem



is a constant and can be calculated by

$$T_i = \int_{\theta_i}^{\theta_{i+1}} \frac{1}{Q_i(\theta)} d\theta \quad (3.7)$$

where  $\theta_i$  and  $\theta_{i+1}$  are the angles of the two boundaries for the region in the interior of which  $A_i$  is the worst clockwise (resp. counterclockwise) subsystem.

Then, we have

$$\Phi_{wc}(x(t_0)) = (\exp(A_m T_m) \cdots \exp(A_2 T_2) \exp(A_1 T_1))^2 \quad (3.8)$$

$$\Phi_{wcc}(x(t_0)) = (\exp(A_m T_m) \cdots \exp(A_2 T_2) \exp(A_1 T_1))^2 \quad (3.9)$$

**Lemma 3.8.**  $\gamma_{wc}(x(t_0))$  and  $\gamma_{wcc}(x(t_0))$  are invariant for any initial state  $x(t_0)$ .

*Proof.* Without loss of generality, we only give the proof for the invariance of  $\gamma_{wc}$ . The proof for the invariance of  $\gamma_{wcc}$  follows the similar line and is thus omitted.

First, we need to show that  $\gamma_{wc}$  is invariant for different initial states on the same ray. Based on equation (3.8), it is obvious that  $\Phi_{wc}(x(t_0))$  is a constant matrix for all initial states on ray  $l_1$ , as shown in Fig. 3.1. After finishing a full clockwise spiral around the origin under the switching signal staying on the corresponding worst clockwise subsystem in each region, the state becomes  $x(t_f) = \Phi_{wc}(x(t_0))x(t_0)$ . Since  $x(t_f)$  and  $x(t_0)$  are on the same ray, there exists a positive constant  $\lambda$  such that  $x(t_f) = \lambda x(t_0)$ . Thus,  $x(t_0)$  is an eigenvector of the matrix  $\Phi_{wc}(x(t_0))$ , and  $\lambda$  is the corresponding eigenvalue. Then, we have

$$\gamma_{wc}(x(t_0)) = \frac{\|x(t_f)\|}{\|x(t_0)\|} = \frac{\|\Phi_{wc}(x(t_0))x(t_0)\|}{\|x(t_0)\|} = \frac{\|\lambda x(t_0)\|}{\|x(t_0)\|} = \lambda. \quad (3.10)$$

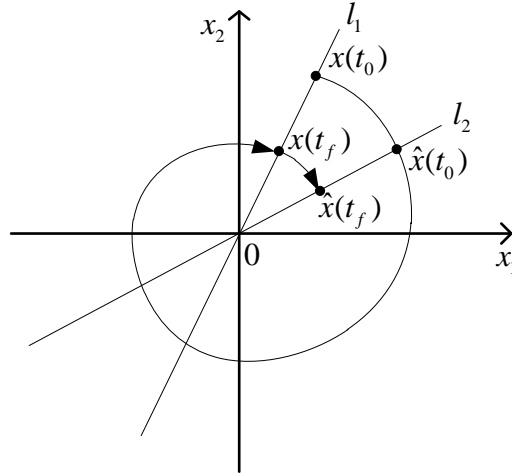


Figure 3.1: Invariance property of  $\gamma_{wc}$

Then, consider another initial state on another ray  $l_2$ . Since  $\gamma_{wc}$  is invariant for any initial state on the same ray, we can choose  $\hat{x}(t_0)$  as the intersection of  $l_2$  and the previous trajectory. Denote the transition matrix for the clockwise rotation from  $l_1$  to  $l_2$  under the switching signal staying on the corresponding worst clockwise subsystem in each region as  $\Phi_1$ , and we have  $\hat{x}(t_0) = \Phi_1 x(t_0)$ . After finishing a full clockwise spiral from  $\hat{x}(t_0)$  under the switching signal staying the corresponding worst clockwise subsystem in each region, the state becomes  $\hat{x}(t_f)$ . According to the symmetry property of the WCSS, we know  $\hat{x}(t_f) = \Phi_1 x(t_f) = \Phi_1 \Phi_{wc}(x(t_0))x(t_0)$ . Therefore,

$$\gamma_{wc}(\hat{x}(t_0)) = \frac{\|\hat{x}(t_f)\|}{\|\hat{x}(t_0)\|} = \frac{\|\Phi_1 \Phi_{wc}(x(t_0))x(t_0)\|}{\|\Phi_1 x(t_0)\|} = \frac{\|\lambda \Phi_1 x(t_0)\|}{\|\Phi_1 x(t_0)\|} = \lambda. \quad (3.11)$$

Overall,  $\gamma_{wc}$  is a constant for any initial state. The proof is done.  $\square$

Next, we give the principal result of this chapter.

**Theorem 3.1.** *The switched system (3.1) with  $N \geq 2$  is asymptotically stable*

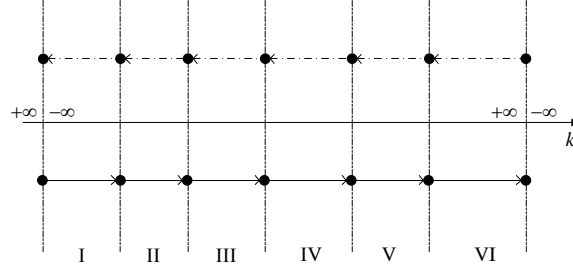


Figure 3.2: Case 3.1: All the boundaries are of Type (a)

under arbitrary switching subject to Assumptions 3.1-3.3 if and only if all of the following three conditions are satisfied.

- 1) There does not exist any unstable Type (a) Region;
- 2) If  $\bigcup_{i=1}^N E_{ic}^o = \mathbb{R}^2$ , then  $\gamma_{wc} < 1$ ;
- 3) If  $\bigcup_{i=1}^N E_{icc}^o = \mathbb{R}^2$ , then  $\gamma_{wcc} < 1$ .

### 3.4.1 Proof of Theorem 3.1

#### Proof of Sufficiency

If the first condition is satisfied, all the Type (a) Regions are stable Type (a) Regions. In addition, Lemmas 3.5 and 3.6 indicate that the worst case trajectory never changes direction. According to different types of boundaries, we have the following four cases.

**Case 3.1.** All the boundaries are of Type (a), as shown in Fig. 3.2. In this case, all the regions are Type (a) Regions. Based on Lemma 3.7, we have  $\bigcup_{i=1}^N E_{ic}^o = \mathbb{R}^2$  and  $\bigcup_{i=1}^N E_{icc}^o = \mathbb{R}^2$ . Moreover, the satisfaction of the latter two conditions indicates that  $\gamma_{wc} < 1$  and  $\gamma_{wcc} < 1$ .

For any initial state, the global WCSS for this case is either the switching signal staying on the corresponding worst clockwise subsystem in each region or

the switching signal staying on the corresponding worst counterclockwise subsystem in each region. It is obvious that the trajectories under these two switching signals are spiralling around the origin, and the stability of the switched system under these two switching signals only depends on the values of  $\gamma_{wc}$  and  $\gamma_{wcc}$ . Since both  $\gamma_{wc}$  and  $\gamma_{wcc}$  are smaller than one, the trajectories under these two switching signals will contract after one full circle (clockwise or counterclockwise) and converge to the origin finally for any initial state.

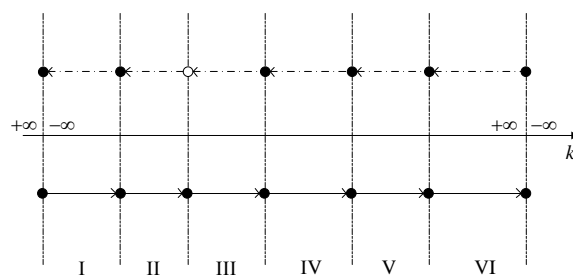
Therefore, the switched system (3.1) with  $N \geq 2$  belonging to Case 3.1 is asymptotically stable under arbitrary switching if all of the three conditions are satisfied.

**Case 3.2.** At least one boundary is of Type (b) and none of the boundaries is of Type (c). Based on Lemma 3.7, we have  $\bigcup_{i=1}^N E_{ic}^o \neq \mathbb{R}^2$  and  $\bigcup_{i=1}^N E_{icc}^o = \mathbb{R}^2$ , which means that the second condition is already satisfied. Besides, the satisfaction of the third condition indicates that  $\gamma_{wcc} < 1$ .

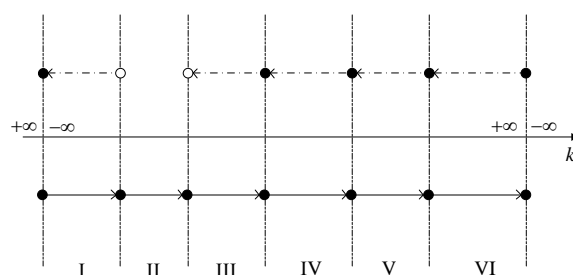
(a) All the regions are Type (a) Regions. Without loss of generality, we only consider the scenario with one Type (b) Boundary, as can be seen from Fig. 3.3(a). Note that the Type (b) Boundary is the eigenvector for the worst clockwise subsystems in Regions II and III.

If the initial state is on the Type (b) Boundary, the global WCSS is the switching signal staying on the corresponding worst counterclockwise subsystem in each region. Similar to Case 3.1, the switched system is asymptotically stable under this switching signal since  $\gamma_{wcc} < 1$ .

If the initial state is in the interior of any Type (a) Region or on any Type (a) Boundary, there are two possibilities for the global WCSS. The first one is the



(a)



(b)

Figure 3.3: Case 3.2: At least one boundary is of Type (b) and none of the boundaries is of Type (c)

switching signal staying on the corresponding worst counterclockwise subsystem in each region, under which the switched system is asymptotically stable since  $\gamma_{wcc} < 1$ . The other possibility is the switching signal staying on the corresponding worst clockwise subsystem in each region. Since the Type (b) Boundary is the eigenvector for the worst clockwise subsystem in Region III, the trajectory under this switching signal will converge to the origin in Region III and the switched system is asymptotically stable under this switching signal.

**(b)** There exists at least one Type (b) Region. Without loss of generality, we only consider the scenario with one Type (b) Region, as can be seen from Fig. 3.3(b). Note that the two boundaries of the Type (b) Region are both Type (b) Boundaries and they are eigenvectors for the worst clockwise subsystems in Region I and Region III respectively.

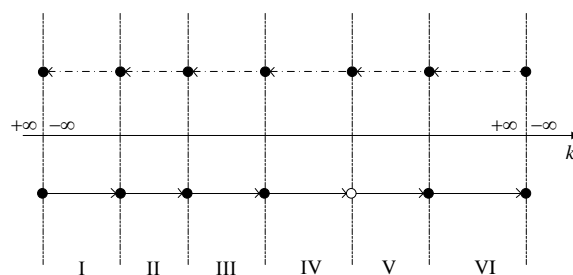
If the initial state is in the interior of the Type (b) Region or on any Type (b) Boundary, the global WCSS is the switching signal staying on the corresponding worst counterclockwise subsystem in each region. Similar to Case 3.1, the switched system is asymptotically stable under this switching signal since  $\gamma_{wcc} < 1$ .

If the initial state is in the interior of any Type (a) Region or on any Type (a) Boundary, there are two possibilities for the global WCSS. The first one is the switching signal staying on the corresponding worst counterclockwise subsystem in each region, under which the switched system is asymptotically stable since  $\gamma_{wcc} < 1$ . The other possibility is the switching signal staying on the corresponding worst clockwise subsystem in each region. Since the two Type (b) Boundaries are eigenvectors for the worst clockwise subsystems in Region I and Region III respectively, the trajectory under this switching signal will converge to the origin in Region III and the switched system is asymptotically stable under this switching signal.

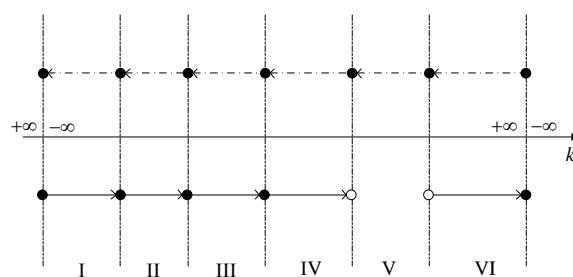
Therefore, the switched system (3.1) with  $N \geq 2$  belonging to Case 3.2 is asymptotically stable under arbitrary switching if all of the three conditions are satisfied.

**Case 3.3.** At least one boundary is of Type (c) and none of the boundaries is of Type (b). Based on Lemma 3.7, we have  $\bigcup_{i=1}^N E_{ic}^o = \mathbb{R}^2$  and  $\bigcup_{i=1}^N E_{icc}^o \neq \mathbb{R}^2$ , which means the third condition is already satisfied. Besides, the satisfaction of the second condition indicates that  $\gamma_{wc} < 1$ .

(a) All the regions are Type (a) Regions. Without loss of generality, we only consider the scenario with one Type (c) Boundary, as can be seen from



(a)



(b)

Figure 3.4: Case 3.3: At least one boundary is of Type (c) and none of the boundaries is of Type (b)

Fig. 3.4(a). Note that the Type (c) Boundary is the eigenvector for the worst counterclockwise subsystems in Regions IV and V.

If the initial state is on the Type (c) Boundary, the global WCSS is the switching signal staying on the corresponding worst clockwise subsystem in each region. Similar to Case 3.1, the switched system is asymptotically stable under this switching signal since  $\gamma_{wc} < 1$ .

If the initial state is in the interior of any Type (a) Region or on any Type (a) Boundary, there are two possibilities for the global WCSS. The first one is the switching signal staying on the corresponding worst clockwise subsystem in each region, under which the switched system is asymptotically stable since  $\gamma_{wc} < 1$ . The other possibility is the switching signal staying on the corresponding worst counterclockwise subsystem in each region. Since the Type (c) Boundary is the

eigenvector for the worst counterclockwise subsystem in Region IV, the trajectory under this switching signal will converge to the origin in Region IV and the switched system is asymptotically stable under this switching signal.

**(b)** There exists at least one Type (c) Region. Without loss of generality, we only consider the scenario with one Type (c) Region, as can be seen from Fig. 3.4(b). Note that the two boundaries of the Type (c) Region are both Type (c) Boundaries and they are eigenvectors for the worst counterclockwise subsystems in Region IV and Region VI respectively.

If the initial state is in the interior of the Type (c) Region or on any Type (c) Boundary, the global WCSS is the switching signal staying on the corresponding worst clockwise subsystem in each region. Similar to Case 3.1, the switched system is asymptotically stable under this switching signal since  $\gamma_{wc} < 1$ .

If the initial state is in the interior of any Type (a) Region or on any Type (a) Boundary, there are two possibilities for the global WCSS. The first one is the switching signal staying on the corresponding worst clockwise subsystem in each region, under which the switched system is asymptotically stable since  $\gamma_{wc} < 1$ . The other possibility is the switching signal staying on the corresponding worst counterclockwise subsystem in each region. Since the two Type (c) Boundaries are the eigenvectors for the worst counterclockwise subsystems in Region IV and Region VI respectively, the trajectory under this switching signal will converge to the origin in Region IV and the switched system is asymptotically stable under this switching signal.

Therefore, the switched system (3.1) with  $N \geq 2$  belonging to Case 3.3 is asymptotically stable under arbitrary switching if all of the three conditions are



satisfied.

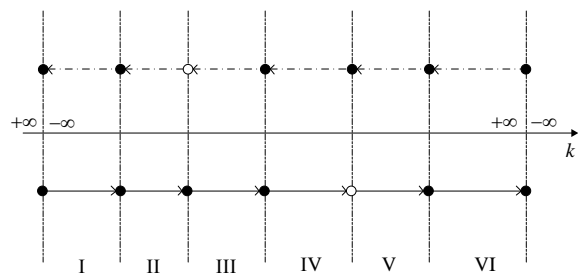
**Case 3.4.** At least one boundary is of Type (b) and at least one boundary is of Type (c). According to Lemma 3.7, we have  $\bigcup_{i=1}^N E_{ic}^o \neq \mathbb{R}^2$  and  $\bigcup_{i=1}^N E_{icc}^o \neq \mathbb{R}^2$ , which means the latter two conditions are already satisfied.

(a) All the regions are Type (a) Regions. Without loss of generality, we only consider the scenario with one Type (b) Boundary and one Type (c) Boundary, as can be seen from Fig. 3.5(a). Note that the Type (b) Boundary is the eigenvector for the worst clockwise subsystems in Regions II and III, and the Type (c) Boundary is the eigenvector for the worst counterclockwise subsystems in Regions IV and V.

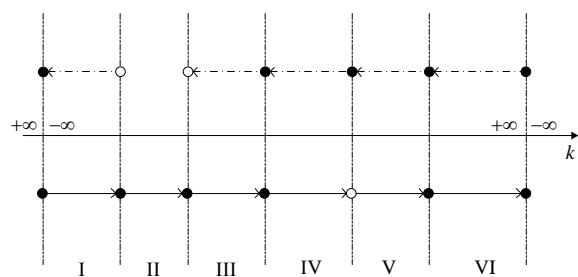
If the initial state is on the Type (b) Boundary, the global WCSS is the switching signal staying on the corresponding worst counterclockwise subsystem in each region. In Region IV, the trajectory under this switching signal will converge to the origin and the switched system is asymptotically stable under this switching signal.

If the initial state is on the Type (c) Boundary, the global WCSS is the switching signal staying on the corresponding worst clockwise subsystem in each region. In Region III, the trajectory under this switching signal will converge to the origin and the switched system is asymptotically stable under this switching signal.

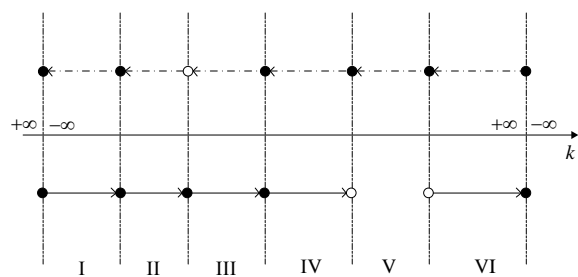
If the initial state is in the interior of any Type (a) Region or on any Type (a) Boundary, there are two possibilities for the global WCSS. Similar to the above two situations, the trajectories under both these two switching signals will converge to the origin and the switched system is asymptotically stable



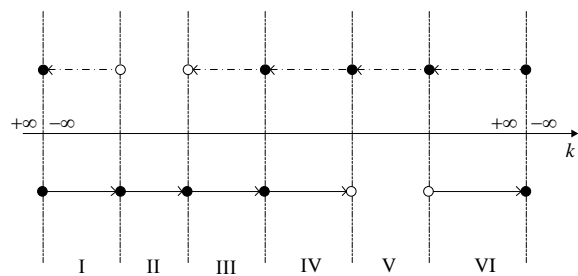
(a)



(b)



(c)



(d)

Figure 3.5: Case 3.4: At least one boundary is of Type (b) and at least one boundary is of Type (c)

under both these two switching signals.

**(b)** There exists at least one Type (b) Region and no Type (c) Region.

Without loss of generality, we only consider the scenario with one Type (b) Region and one Type (c) Boundary, as can be seen from Fig. 3.5(b).

Similar to Case 3.4(a), the switched system in this subcase is asymptotically stable under the global WCSS for any initial state.

**(c)** There exists at least one Type (c) Region and no Type (b) Region.

Without loss of generality, we only consider the scenario with one Type (c) Region and one Type (b) Boundary, as can be seen from Fig. 3.5(c).

Similar to Case 3.4(a), the switched system in this subcase is asymptotically stable under the global WCSS for any initial state.

**(d)** There exists at least one Type (b) Region and at least one Type (c) Region. Without loss of generality, we only consider the scenario with one Type (b) Region and one Type (c) Region, as can be seen from Fig. 3.5(d).

Based on Case 3.4(b) and Case 3.4(c), the switched system in this subcase is asymptotically stable under the global WCSS for any initial state.

Therefore, the switched system (3.1) with  $N \geq 2$  belonging to Case 3.4 is asymptotically stable under arbitrary switching if all of the three conditions are satisfied.

Overall, the switched system (3.1) with  $N \geq 2$  is asymptotically stable under arbitrary switching if all of the three conditions are satisfied and thus the proof of sufficiency is complete.

### **Proof of Necessity**

In order to prove the necessity of Theorem 3.1, we need to show that the switched system (3.1) with  $N \geq 2$  is not asymptotically stable under arbitrary switching if any one of the three conditions is violated.

If the first condition is violated, the switched system (3.1) with  $N \geq 2$  is not asymptotically stable under arbitrary switching according to Lemma 3.4.

If the second condition is violated, the switched system (3.1) with  $N \geq 2$  is not asymptotically stable under the switching signal staying on the corresponding worst clockwise subsystem in each region for any initial state.

If the third condition is violated, the switched system (3.1) with  $N \geq 2$  is not asymptotically stable under the switching signal staying on the corresponding worst counterclockwise subsystem in each region for any initial state.

Overall, if any one of the three conditions is violated, the switched system (3.1) with  $N \geq 2$  is not asymptotically stable under arbitrary switching and thus the proof of necessity is done.

### **3.4.2 Instability Mechanisms for the Switched System (3.1) with $N \geq 2$ under Arbitrary Switching**

Based on Theorem 3.1, there are two types of instability mechanisms for the switched system (3.1) with  $N \geq 2$ .

1) Unstable chattering: If the first condition is violated, the trajectory of the switched system will diverge to infinity by switching between the worst clockwise subsystem  $A_p$  and the worst counterclockwise subsystem  $A_q$  in the interior of the region where both  $H_{pq}$  and  $H_{qp}$  are positive, as shown in Fig. 3.6(a);

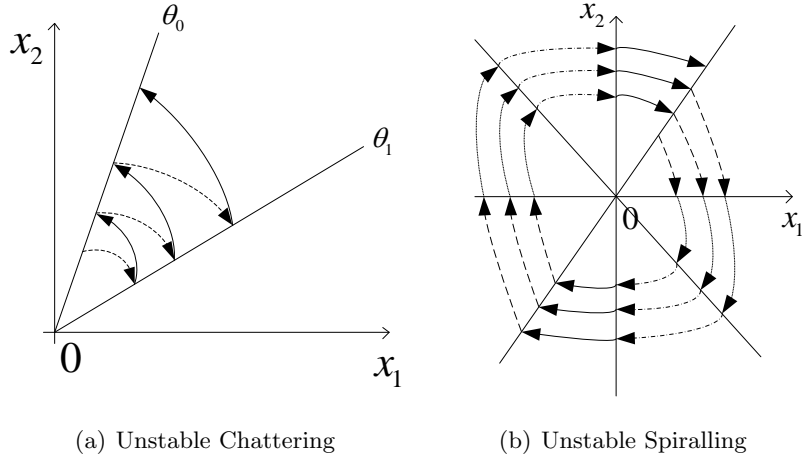


Figure 3.6: Two instability mechanisms for the switched system (3.1) with  $N \geq 2$  under arbitrary switching

2) Unstable spiralling: If the second (resp. third) condition is violated, the trajectory of the switched system will diverge to infinity by following the switching signal staying on the corresponding worst clockwise (resp. counterclockwise) subsystem in each region for any initial state, as shown in Fig. 3.6(b).

The above two instability mechanisms are similar to the ones in [69] for the two-mode case.

### 3.4.3 Application of Theorem 3.1

**Example 3.1.** Consider a switched linear system with three stable second-order LTI subsystems of the form

$$A_1 = \begin{bmatrix} 0 & 5 \\ -30 & -1 \end{bmatrix}, \quad A_2 = \begin{bmatrix} 0 & 5 \\ -26 & -1 \end{bmatrix}, \quad A_3 = \begin{bmatrix} -6 & 27 \\ -150 & -1 \end{bmatrix}. \quad (3.12)$$

It was shown in [39] that there does not exist a CQLF among these three subsystems. We will check whether the switched system is stable under arbitrary switching.

Table 3.1: Generalized regions of  $k$  for Example 3.1

$k$	$H_{12}$	$H_{21}$	$H_{13}$	$H_{31}$	$H_{23}$	$H_{32}$	WCS
$(-\infty, -4.3398)$	-	+	+	-	+	-	$A_3$
$(-4.3398, -1.7048)$	-	+	-	+	+	-	$A_1$
$(-1.7048, 0)$	-	+	-	+	-	+	$A_1$
$(0, 1.8853)$	+	-	-	+	-	+	$A_2$
$(1.88536, 4.1594)$	+	-	+	-	-	+	$A_2$
$(4.1594, \infty)$	+	-	+	-	+	-	$A_3$

Based on equations (2.42)-(2.44),  $D_i(k)$ ,  $D_j(k)$  and  $N_{ij}(k)$  for  $i, j \in \{1, 2, 3\}$ ,  $i < j$  can be calculated. With all the real roots of  $D_i(k) = 0$ ,  $D_j(k) = 0$  and  $N_{ij}(k) = 0$ , the polar coordinates space can then be partitioned into six generalized regions of  $k$ , as listed in Table 3.1. Moreover, it is noted that all the boundaries are Type (c) Boundaries and all the regions are Type (c) Regions. According to Lemma 3.7, we have  $\bigcup_{i=1}^3 E_{icc}^o = \emptyset$  and  $\bigcup_{i=1}^3 E_{ic} = \mathbb{R}^2$ . Therefore, the first condition and the third condition in Theorem 3.1 are already satisfied.

Based on equations (2.38)-(2.39), the signs of  $H_{ij}$  and  $H_{ji}$  in each region are determined and listed in Table 3.1. According to Remark 3.1, the worst clockwise subsystems (WCS) for each region can also be determined and listed in Table 3.1. From Table 3.1, we know that only three  $T_i$  need to be calculated. According to equation (3.7), we have  $T_1 = 0.08892\text{s}$ ,  $T_2 = 0.01594\text{s}$ ,  $T_3 = 0.09093\text{s}$ . Choose an initial state  $x(t_0) = [1, 0]^T$ , we have

$$\gamma_{wc} = \frac{\|e^{A_2 T_2} e^{A_3 T_3} e^{A_1 T_1} e^{A_2 T_2} e^{A_3 T_3} e^{A_1 T_1} x(t_0)\|}{\|x(t_0)\|} = 0.9575 < 1 \quad (3.13)$$

which means that the second condition in Theorem 3.1 is also satisfied. Therefore, the switched system (3.12) is asymptotically stable under arbitrary switching. The worst case trajectory is shown in Fig. 3.7.

*Remark 3.2.* Although there does not exist a CQLF for the switched system

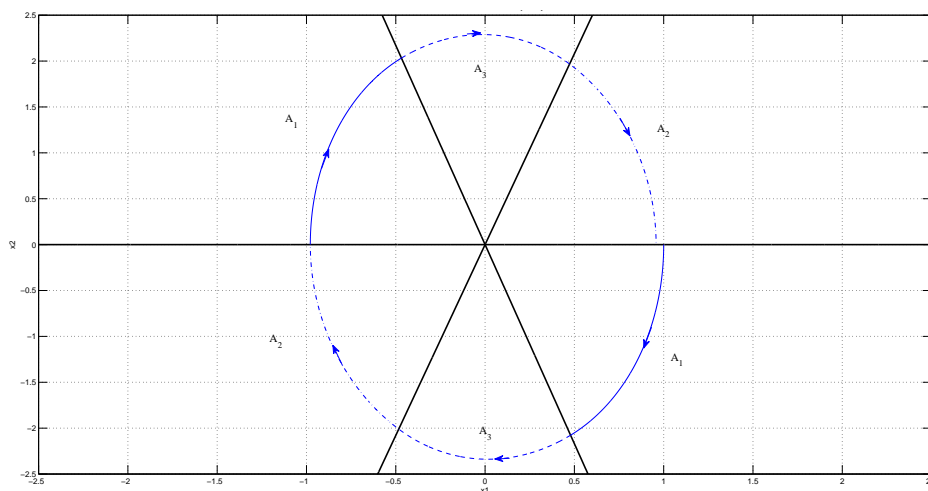


Figure 3.7: The worst case trajectory of Example 3.1

(3.12), it is still asymptotically stable under arbitrary switching. This example shows the advantage of the proposed condition in Theorem 3.1 over the CQLF conditions.

*Remark 3.3.* In [121], the  $(2, 2)$  entry of  $A_1$ ,  $a_{221}$ , was treated as a variable, and it was shown that the three subsystems will share a CQLF if  $a_{221} < -1.31225$ . On the other hand, based on the CQLF existence condition in [39], we know that every two subsystems will share a CQLF if  $a_{221} < -0.7152$ . However, according to our condition, the switched system is still asymptotically stable even when  $a_{122} = -0.5$ . Therefore, it seems that the condition for the existence of a CQLF pairwise is more restrictive than the stability condition for the switched system under arbitrary switching. Hence, from this observation, we propose the conjecture that a second-order switched linear system is always asymptotically stable under arbitrary switching when each pair of subsystems have a CQLF. No counterexample has been found yet through extensive simulation studies. However, the rigorous mathematical proof is lacking at this moment.

### 3.5 Summary

Based on the results in Chapter 2, this chapter extended the worst case switching signal (WCSS) criteria for second-order switched linear systems with two modes in [69] to the general case and derived an easily verifiable necessary and sufficient condition for the stability of second-order switched linear systems with any finite number of subsystems under arbitrary switching.



## Chapter 4

# Switching Stabilizability of Second-order Switched Linear Systems

### 4.1 Introduction

Based on the results in Chapter 2, this chapter aims to extend the best case switching signal (BCSS) criteria for second-order switched linear systems with two subsystems in [82] to the general case with any finite number of subsystems and derive easily verifiable necessary and sufficient conditions for the switching stabilizability. Similar to the previous chapter, the key idea is to compare the subsystems for each group in the interior of a region pairwise, and determine the most “stable” subsystem for the corresponding group. Then, the best case analysis among all the subsystems in the interior of a region can be reduced to the best case analysis between the two most “stable” subsystems in the interior

of that region.

The contents of this chapter are organized as follows. Section 4.2 presents a unified statement of the problem, where the second-order switched linear systems are classified into three categories. The BCSS criteria for switched systems belonging to the first category are derived in Section 4.3. In Section 4.4, an easily verifiable necessary and sufficient condition for the switching stabilizability is proposed for second-order switched linear systems with any finite number of subsystems belonging to the first category. This condition is extended to switched systems belonging to the other two categories in Section 4.5. Finally, in Section 4.6, a summary is given.

## 4.2 Statement of the Problem

Motivated by the limitations of the existing results outlined in Chapter 1, our aim is to derive easily verifiable necessary and sufficient conditions for the switching stabilizability of second-order switched linear system with any finite number of subsystems. In particular, we consider the continuous-time second-order switched linear system with  $N$  ( $N \geq 2$ ) unstable subsystems of the form

$$\dot{x}(t) = A_{\sigma(t)}x(t) \tag{4.1}$$

with

$$A_i = \begin{bmatrix} a_{11i} & a_{12i} \\ a_{21i} & a_{22i} \end{bmatrix} \tag{4.2}$$

where  $x(t) \in \mathbb{R}^2$  is the state, and  $\sigma : \mathbb{R}^+ \rightarrow \mathcal{I}_N = \{1, 2, \dots, N\}$  is the switching signal that determines the active mode of the system among  $N$  possible modes

in  $\mathcal{A} = \{A_1, A_2, \dots, A_N\}$ .

It is noted that an unstable second-order LTI system  $\Sigma_{A_i}$  with two eigenvalues  $\lambda_{i1}$  and  $\lambda_{i2}$  can be classified into three types according to its eigenvalue structure.

Type 1: Both  $\lambda_{i1}$  and  $\lambda_{i2}$  have positive real part;

Type 2: Both  $\lambda_{i1}$  and  $\lambda_{i2}$  have non-negative real part and at least one of them has zero real part;

Type 3: One of  $\lambda_{i1}$  and  $\lambda_{i2}$  is negative (the other one can be zero or positive).

Then, the switched system (4.1) can be classified into three categories as follows.

- Category I: All the subsystems are of Type 1;
- Category II: At least one of the subsystems is of Type 2 and none of the subsystems is of Type 3;
- Category III: At least one of the subsystems is of Type 3.

For clarity, two types of asymptotic stabilizability are defined as follow.

**Definition 4.1.** The switched system (4.1) is said to be *globally asymptotically stabilizable* (GAS), if for any initial state, there exists a switching signal under which the trajectory will asymptotically converge to zero.

**Definition 4.2.** The switched system (4.1) is said to be *regionally asymptotically stabilizable* (RAS), if there exists at least one region (non-empty, open set) such that for any initial state in that region, there exists a switching signal under which the trajectory will asymptotically converge to zero.

*Remark 4.1.* Although the global asymptotic stabilizability is our preference in designing stabilizing switching laws, there exists a class of switched systems that

may not be GAS, but still can be stabilized if the system trajectories can be driven into certain regions. In fact, for these switched systems, it is possible to force the system trajectories into such regions for most of the initial states.

Recall the three assumptions made in Section 2.1 and rewrite them for the switched system (4.1) in the following form.

**Assumption 4.1.**  $A_i \neq cA_j$ , where  $c \in \mathbb{R}$ ,  $c > 0$ ,  $i, j \in \mathcal{I}_N$  and  $i \neq j$ .

When Assumption 4.1 is violated, the trajectories of  $\Sigma_{A_i}$  and  $\Sigma_{A_j}$  are identical for the same initial state. Therefore, only one of them needs to be considered in the best case analysis.

**Assumption 4.2.**  $A_i \neq c \begin{bmatrix} 1 & 0 \\ 0 & 1 \end{bmatrix}$ , where  $c \in \mathbb{R}$ ,  $c > 0$ , and  $i \in \mathcal{I}_N$ .

When Assumption 4.2 is violated, any switching to  $A_i$  can only make the trajectories of the switched system (4.1) become more “unstable” ( $\theta$  keeps invariant and  $r$  becomes bigger). In this case, there is no need to take  $A_i$  into account in the best case analysis.

**Assumption 4.3.** There does not exist a common real eigenvector for all  $A_i \in \mathcal{A}$ .

When Assumption 4.3 is violated, all the matrices in  $\mathcal{A}$  are simultaneously lower-triangularizable. According to Appendix A in [82], the switched system (4.1) is RAS if and only if at least one of the (1,1) entries of the lower-triangular matrices is negative.

### 4.3 Best Case Analysis for the Switched System (4.1) of Category I

In this section, we generalize the BCSS criteria for the switched system (4.1) of Category I with  $N = 2$  in [82] to the general case when  $N \geq 2$ .

#### 4.3.1 BCSS Criteria for the Switched System (4.1) of Category I with $N = 2$

**Lemma 4.1** ([82]). *For the switched system (4.1) of Category I with  $N = 2$ , we have*

1) *The switched system is RAS if there exists a region of  $k$  where both  $H_{12}(k)$  and  $H_{21}(k)$  are negative;*

2) *In regions where  $H_{12}(k) > 0$  and  $H_{21}(k) < 0$ , the switching signal staying on  $\Sigma_{A_1}$  is the local BCSS;*

3) *In regions where  $H_{12}(k) < 0$  and  $H_{21}(k) > 0$ , the switching signal staying on  $\Sigma_{A_2}$  is the local BCSS.*

**Lemma 4.2.** *In regions where both  $H_{12}(k)$  and  $H_{21}(k)$  are positive, the local BCSS cannot have any switch between the two subsystems.*

Similar to Lemma 3.2, this lemma can be easily proved based on the definition of  $H_{12}$  and  $H_{21}$ .

### 4.3.2 BCSS Criteria for the Switched System (4.1) of Category I with $N \geq 2$

#### BCSS criteria in the interior of generalized regions of $k$

According to Remark 2.10 and Lemma 4.1, we can determine the more “stable” subsystem for any two subsystems in the interior of a generalized region of  $k$ . For all the subsystems in  $\mathcal{A}_{rc}$  (resp.  $\mathcal{A}_{rcc}$ ), by comparing pairwise, the most “stable” clockwise (resp. counterclockwise) subsystem in the interior of that region can then be determined.

**Definition 4.3.** In the interior of a generalized region of  $k$ , the most “stable” clockwise (resp. counterclockwise) subsystem is called the best clockwise (resp. counterclockwise) subsystem in that region.

*Remark 4.2.* According to Lemma 4.1, the best clockwise (resp. counterclockwise) subsystem in the interior of a generalized region of  $k$  is  $\Sigma_{A_v}$  (resp.  $\Sigma_{A_w}$ ) whose  $H_{iv}$  ( $H_{jw}$ ) terms are all negative with  $A_i \in \mathcal{A}_{rc}$ ,  $i \neq v$  (resp.  $A_j \in \mathcal{A}_{rcc}$ ,  $j \neq w$ ).

**Lemma 4.3.** *The local BCSS in a generalized region of  $k$  only relates to the best clockwise subsystem and the best counterclockwise subsystem in that region.*

The proof of this lemma follows the similar line as that of Lemma 3.3.

From Lemma 4.3, we know that the local BCSS in the interior of a Type (b) (resp. Type (c)) Region is the switching signal staying on the best counterclockwise (resp. clockwise) subsystem in this region. For a Type (a) Region, we have the following two lemmas.

**Lemma 4.4.** *The switched system (4.1) of Category I with  $N \geq 2$  is RAS if there exists a Type (a) Region where both  $H_{vw}(k)$  and  $H_{wv}(k)$  are negative.*

**Lemma 4.5.** *In the interior of a Type (a) Region where both  $H_{vw}(k)$  and  $H_{wv}(k)$  are positive, the local BCSS for the switched system (4.1) of Category I with  $N \geq 2$  cannot have any switch between  $A_v$  and  $A_w$ .*

These two lemmas can be easily proved based on Lemmas 4.1-4.3.

**Definition 4.4.** In the best case analysis, a Type (a) Region where both  $H_{vw}$  and  $H_{wv}$  are negative (resp. positive) is called a stabilizable (resp. an unstabilizable) Type (a) Region.

#### BCSS criteria on boundaries of generalized regions of $k$

It is obvious that the BCSS on the eigenvector of a Type 1 subsystem cannot be the switching signal staying on this subsystem. Therefore, subsystems on their corresponding eigenvectors can be ignored in the best case analysis, and the best case trajectory of the switched system (4.1) of Category I with  $N \geq 2$  cannot stay on any boundary of the regions. According to the properties of linear subsystems, the time spent on any boundary is zero. Therefore, we only need to study whether the direction of the best case trajectory will change after reaching a boundary. For a Type (b) Boundary or a Type (c) Boundary, there is no doubt since only one possible direction exists. For a Type (a) Boundary, we have

**Lemma 4.6.** *If there does not exist any stabilizable Type (a) Region, the direction of the best case trajectory for the switched system (4.1) of Category I with  $N \geq 2$  will keep invariant after reaching a Type (a) Boundary.*

The proof of this lemma follows the similar line as that of Lemma 3.6.

#### 4.4 A Necessary and Sufficient Condition for the Switching Stabilizability of the Switched System (4.1) of Category I with $N \geq 2$

Similar to the worst case analysis, several useful equations are listed below.

$$E_{ic} = \{\theta | Q_i(\theta) \leq 0\} \quad (4.3)$$

$$E_{icc} = \{\theta | Q_i(\theta) \geq 0\} \quad (4.4)$$

**Lemma 4.7.**  $\bigcup_{i=1}^N E_{ic}^o = \mathbb{R}^2$  if and only if there is no Type (b) Boundary in the polar coordinates space.  $\bigcup_{i=1}^N E_{icc}^o = \mathbb{R}^2$  if and only if there is no Type (c) Boundary in the polar coordinates space.

If  $\bigcup_{i=1}^N E_{ic}^o = \mathbb{R}^2$  (resp.  $\bigcup_{i=1}^N E_{icc}^o = \mathbb{R}^2$ ), the trajectory of the switched system (4.1) belonging to Category I with  $N \geq 2$  under the switching signal staying on the corresponding best clockwise (resp. counterclockwise) subsystem in each region would be a clockwise (resp. counterclockwise) spiral around the origin for any non-zero initial state  $x(t_0)$  in the  $x - y$  coordinates. To determine the convergence or divergence of such trajectories, we can define the best clockwise ratio  $\gamma_{bc}$  (resp. the best counterclockwise ratio  $\gamma_{bcc}$ ) between the magnitudes of the state after one full clockwise (resp. counterclockwise) circle and the non-zero



initial state  $x(t_0)$  in the  $x - y$  coordinates with the form of

$$\gamma_{bc}(x(t_0)) = \frac{\|\Phi_{bc}(x(t_0))x(t_0)\|}{\|x(t_0)\|} \quad (4.5)$$

$$\gamma_{bcc}(x(t_0)) = \frac{\|\Phi_{bcc}(x(t_0))x(t_0)\|}{\|x(t_0)\|} \quad (4.6)$$

where  $\Phi_{bc}(x(t_0))$  (resp.  $\Phi_{bcc}(x(t_0))$ ) represents the state transition matrix for a full clockwise (resp. counterclockwise) spiral under the switching signal staying on the corresponding best clockwise (resp. counterclockwise) subsystem in each region for the initial state  $x(t_0)$ .

Due to the symmetric property of the BCSS, we only need to consider half plane. Denote the best clockwise (resp. counterclockwise) subsystems from the ray that  $x(t_0)$  falls on as  $A_1, A_2, \dots, A_m$  in clockwise (resp. counterclockwise) direction before reaching the opposite ray where  $-x(t_0)$  falls on. According to the isochronism property of linear systems, the time  $T_i$  spend in the  $i^{\text{th}}$  region is a constant and can be calculated by

$$T_i = \int_{\theta_i}^{\theta_{i+1}} \frac{1}{Q_i(\theta)} d\theta \quad (4.7)$$

where  $\theta_i$  and  $\theta_{i+1}$  are the angles of the two boundaries for the region in the interior of which  $A_i$  is the best clockwise (resp. counterclockwise) subsystem.

Then, we have

$$\Phi_{bc}(x(t_0)) = (\exp(A_m T_m) \cdots \exp(A_2 T_2) \exp(A_1 T_1))^2 \quad (4.8)$$

$$\Phi_{bcc}(x(t_0)) = (\exp(A_m T_m) \cdots \exp(A_2 T_2) \exp(A_1 T_1))^2 \quad (4.9)$$

**Lemma 4.8.**  $\gamma_{bc}(x(t_0))$  and  $\gamma_{bcc}(x(t_0))$  are invariant for any initial state  $x(t_0)$ .

The proof of this lemma follows the similar line as that of Lemma 3.8 and thus is omitted.

Then, we have the principle result of this chapter as follows.

**Theorem 4.1.** *The switched system (4.1) of Category I with  $N \geq 2$  is RAS subject to Assumptions 4.1-4.3 if and only if at least one of the following three conditions is satisfied.*

- 1) *There exists a stabilizable Type (a) Region;*
- 2)  $\bigcup_{i=1}^N E_{ic}^o = \mathbb{R}^2$ , and  $\gamma_{bc} < 1$ ;
- 3)  $\bigcup_{i=1}^N E_{icc}^o = \mathbb{R}^2$ , and  $\gamma_{bcc} < 1$ .

#### 4.4.1 Proof of Theorem 4.1

##### Proof of Necessity

Let's assume that none of the three conditions is satisfied. Then, all the Type (a) Regions are unstabilizable Type (a) Regions. In addition, Lemma 4.5 and Lemma 4.6 indicate that the best case trajectory never changes direction. According to different types of boundaries, we have the following four cases.

**Case 4.1.** All the boundaries are of Type (a), as shown in Fig. 4.1. In this case, all the regions are Type (a) Regions. Based on Lemma 4.7, we have  $\bigcup_{i=1}^N E_{ic}^o = \mathbb{R}^2$  and  $\bigcup_{i=1}^N E_{icc}^o = \mathbb{R}^2$ . Moreover, the violation of the latter two conditions means that  $\gamma_{bc} \geq 1$  and  $\gamma_{bcc} \geq 1$ .

The global BCSS for this case is either the switching signal staying on the corresponding best clockwise subsystem in each region or the switching signal staying on the corresponding best counterclockwise subsystem in each region.

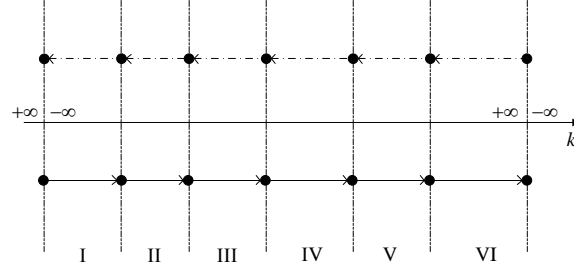


Figure 4.1: Case 4.1: All the boundaries are of Type (a)

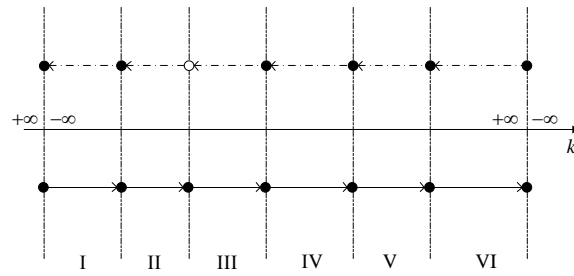
It is obvious that the trajectories under these two switching signals are spiralling around the origin and the stability of the switched system under these two switching signals only depends on the values of  $\gamma_{bc}$  and  $\gamma_{bcc}$ . Since neither  $\gamma_{bc}$  or  $\gamma_{bcc}$  is smaller than one, the trajectories under these two switching signals will never contract after one full circle (clockwise or counterclockwise) and thus will not converge to zero finally for any initial state.

Therefore, the switched system (4.1) of Category I with  $N \geq 2$  that belongs to Case 4.1 is not RAS if all of the three conditions are violated.

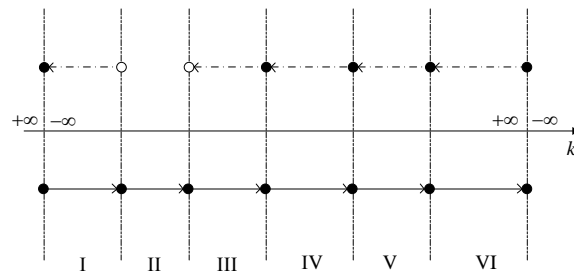
**Case 4.2.** At least one boundary is of Type (b) and none of the boundaries is of Type (c). Based on Lemma 4.7, we have  $\bigcup_{i=1}^N E_{ic}^o \neq \mathbb{R}^2$  and  $\bigcup_{i=1}^N E_{icc}^o = \mathbb{R}^2$ , which means that the second condition is already violated. Besides, the violation of the third condition indicates that  $\gamma_{bcc} \geq 1$ .

(a) All the regions are Type (a) Regions. Without loss of generality, we only consider the scenario with one Type (b) Boundary, as can be seen from Fig. 4.2(a). Note that the Type (b) Boundary is the eigenvector for the best clockwise subsystems in Regions II and III.

If the initial state is on the Type (b) Boundary, the global BCSS is the switching signal staying on the corresponding best counterclockwise subsystem in each region. Similar to Case 4.1, the switched system is not asymptotically



(a)



(b)

Figure 4.2: Case 4.2: At least one boundary is of Type (b) and none of the boundaries is of Type (c)

stabilizable since  $\gamma_{bcc} \geq 1$ .

If the initial state is in the interior of any Type (a) Region or on any Type (a) Boundary, there are two possibilities for the global BCSS. The first one is the switching signal staying on the corresponding best counterclockwise subsystem in each region, which cannot stabilize the switched system since  $\gamma_{bcc} \geq 1$ . The other possibility is the switching signal staying on the corresponding best clockwise subsystem in each region. Since this Type (b) Boundary is the eigenvector for the best clockwise subsystem in Region III, the trajectory under this switching signal will diverge to infinity in Region III and the switched system cannot be asymptotically stabilized by this switching signal.

(b) There exists at least one Type (b) Region. Without loss of generality, we only consider the scenario with one Type (b) Region, as can be seen from

Fig. 4.2(b). Note that the two boundaries of the Type (b) Region are both Type (b) Boundaries and they are eigenvectors for the best clockwise subsystems in Region I and Region III respectively.

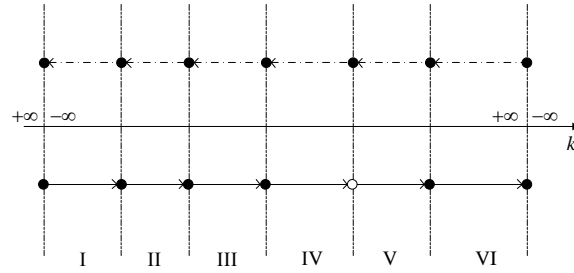
If the initial state is in the interior of the Type (b) Region or on any Type (b) Boundary, the global BCSS is the switching signal staying on the corresponding best counterclockwise subsystem in each region. Similar to Case 4.1, the switched system is not asymptotically stabilizable since  $\gamma_{bcc} \geq 1$ .

If the initial state is in the interior of any Type (a) Region or on any Type (a) Boundary, there are two possibilities for the global BCSS. The first one is the switching signal staying on the corresponding best counterclockwise subsystem in each region, which cannot stabilize the switched system since  $\gamma_{bcc} \geq 1$ . The other possibility is the switching signal staying on the corresponding best clockwise subsystem in each region. Since the two Type (b) Boundaries are the eigenvectors for the best clockwise subsystems in Region I and Region III respectively, the trajectory under this switching signal will diverge to infinity in Region III and the switched system cannot be asymptotically stabilized by this switching signal.

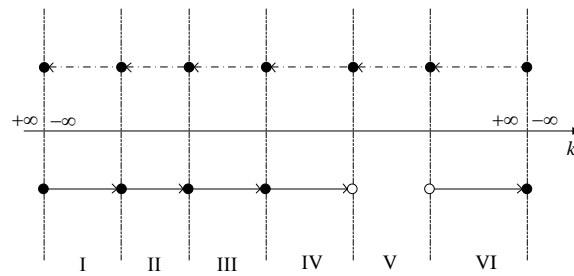
Therefore, the switched system (4.1) of Category I with  $N \geq 2$  that belongs to Case 4.2 is not RAS if all of the three conditions are violated.

**Case 4.3.** At least one boundary is of Type (c) and none of the boundaries is of Type (b). Based on Lemma 4.7, we have  $\bigcup_{i=1}^N E_{ic}^o = \mathbb{R}^2$  and  $\bigcup_{i=1}^N E_{icc}^o \neq \mathbb{R}^2$ , which means the third condition is already violated. Besides, the violation of the second condition indicates that  $\gamma_{bc} \geq 1$ .

(a) All the regions are Type (a) Regions. Without loss of generality, we only consider the scenario with one Type (c) Boundary, as can be seen from



(a)



(b)

Figure 4.3: Case 4.3: At least one boundary is of Type (c) and none of the boundaries is of Type (b)

Fig. 4.3(a). Note that the Type (c) Boundary is the eigenvector for the best counterclockwise subsystems in Regions IV and V.

If the initial state is on the Type (c) Boundary, the global BCSS is the switching signal staying on the corresponding best clockwise subsystem in each region. Similar to Case 4.1, the switched system is not asymptotically stabilizable since  $\gamma_{bc} \geq 1$ .

If the initial state is in the interior of any Type (a) Region or on any Type (a) Boundary, there are two possibilities for the global BCSS. The first one is the switching signal staying on the corresponding best clockwise subsystem in each region, under which the switched system is not asymptotically stabilizable since  $\gamma_{bc} \geq 1$ . The other possibility is the switching signal staying on the corresponding best counterclockwise subsystem in each region. Since this Type (c) Boundary

is the eigenvector for the best counterclockwise subsystem in Region IV, the trajectory under this switching signal will diverge to infinity in Region IV and the switched system cannot be asymptotically stabilized by this switching signal.

(b) There exists at least one Type (c) Region. Without loss of generality, we only consider the scenario with one Type (c) Region, as can be seen from Fig. 4.3(b). Note that the two boundaries of the Type (c) Region are both Type (c) Boundaries and they are eigenvectors for the best counterclockwise subsystems in Region IV and Region VI respectively.

If the initial state is in the interior of the Type (c) Region or on any Type (c) Boundary, the global BCSS is the switching signal staying on the corresponding best clockwise subsystem in each region. Similar to Case 4.1, the switched system is not asymptotically stabilizable since  $\gamma_{bc} \geq 1$ .

If the initial state is in the interior of any Type (a) Region or on any Type (a) Boundary, there are two possibilities for the global BCSS. The first one is the switching signal staying on the corresponding best clockwise subsystem in each region, under which the switched system is not asymptotically stabilizable since  $\gamma_{bc} \geq 1$ . The other possibility is the switching signal staying on the corresponding best counterclockwise subsystem in each region. Since the two Type (c) Boundaries are the eigenvectors for the best counterclockwise subsystems in Region IV and Region VI respectively, the trajectory under this switching signal will diverge to infinity in Region IV and the switched system cannot be asymptotically stabilized by this switching signal.

Therefore, the switched system (4.1) of Category I with  $N \geq 2$  that belongs to Case 4.3 is not RAS if all of the three conditions are violated.

**Case 4.4.** At least one boundary is of Type (b) and at least one boundary is of Type (c). According to Lemma 4.7, we have  $\bigcup_{i=1}^N E_{ic}^o \neq \mathbb{R}^2$  and  $\bigcup_{i=1}^N E_{icc}^o \neq \mathbb{R}^2$ , which means that the latter two conditions are violated.

(a) All the regions are Type (a) Regions. Without loss of generality, we only consider the scenario with one Type (b) Boundary and one Type (c) Boundary, as can be seen from Fig. 4.4(a). Note that the Type (b) Boundary is the eigenvector for the best clockwise subsystems in Regions II and III, and the Type (c) Boundary is the eigenvector for the best counterclockwise subsystems in Regions IV and V.

If the initial state is on the Type (b) Boundary, the global BCSS is the switching signal staying on the corresponding best counterclockwise subsystem in each region. In Region IV, the trajectory under this switching signal will diverge to infinity and the switched system is not asymptotically stabilizable.

If the initial state is on the Type (c) Boundary, the global BCSS is the switching signal staying on the corresponding best clockwise subsystem in each region. In Region III, the trajectory under this switching signal will diverge to infinity and the switched system is not asymptotically stabilizable.

If the the initial state is in the interior of any Type (a) Region or on any Type (a) Boundary, there are two possibilities for the global BCSS. Similar to the above two situations, the trajectories under both these two switching signals will diverge to infinity and the switched system is not asymptotically stabilizable.

(b) There exists at least one Type (b) Region and no Type (c) Region. Without loss of generality, we only consider the scenario with one Type (b) Region and one Type (c) Boundary, as can be seen from Fig. 4.4(b).



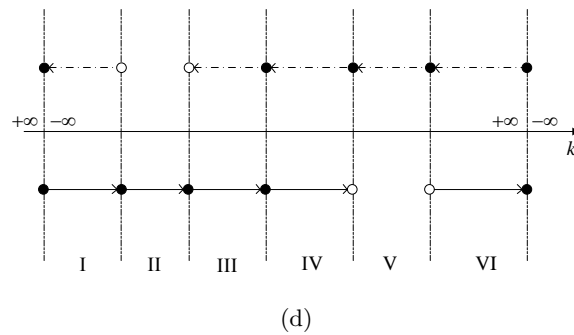
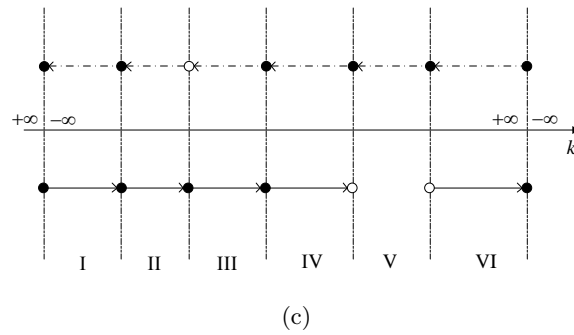
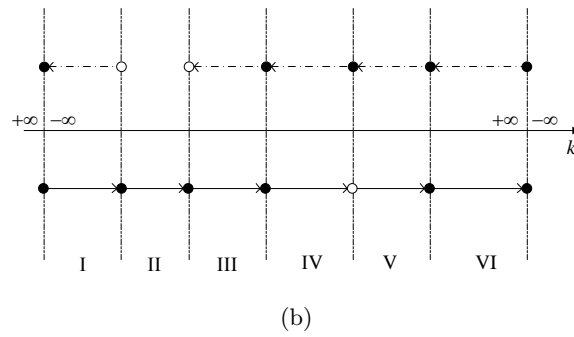
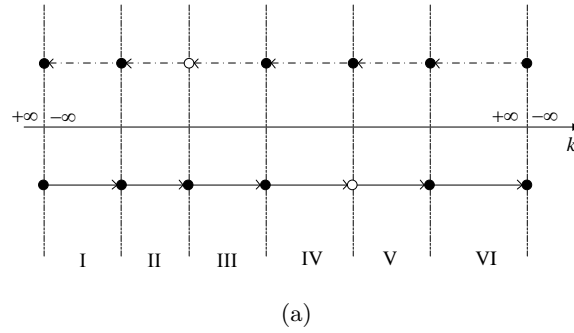


Figure 4.4: Case 4.4: At least one boundary is of Type (b) and at least one boundary is of Type (c)

Similar to Case 4.4(a), the switched system in this subcase cannot be asymptotically stabilized by the global BCSS for any initial state.

(c) There exists at least one Type (c) Region and no Type (b) Region. Without loss of generality, we only consider the scenario with one Type (c) Region and one Type (b) Boundary, as can be seen from Fig. 4.4(c).

Similar to Case 4.4(a), the switched system in this subcase cannot be asymptotically stabilized by the global BCSS for any initial state.

(d) There exists at least one Type (b) Region and at least one Type (c) Region. Without loss of generality, we only consider the scenario with one Type (b) Region and one Type (c) Region, as can be seen from Fig. 4.4(d).

Based on Case 4.4(b) and Case 4.4(c), the switched system in this subcase cannot be asymptotically stabilized by the global BCSS for any initial state.

Therefore, the switched system (4.1) of Category I with  $N \geq 2$  that belongs to Case 4.4 is not RAS if all of the three conditions are violated.

Overall, if all of the three conditions are violated, the switched system (4.1) of Category I with  $N \geq 2$  is not RAS and thus the proof of necessity is complete.

### **Proof of Sufficiency**

If the first condition is satisfied, the switched system (4.1) of Category I with  $N \geq 2$  is RAS according to Lemma 4.4. In addition, the global stabilizability of the switched system in this case depends on whether the system trajectories can be driven into the stabilizable Type (a) Region for any initial state.

If the second condition is satisfied, the switched system (4.1) of Category I with  $N \geq 2$  is GAS by the switching signal staying on the corresponding best clockwise subsystem in each region for any initial state.

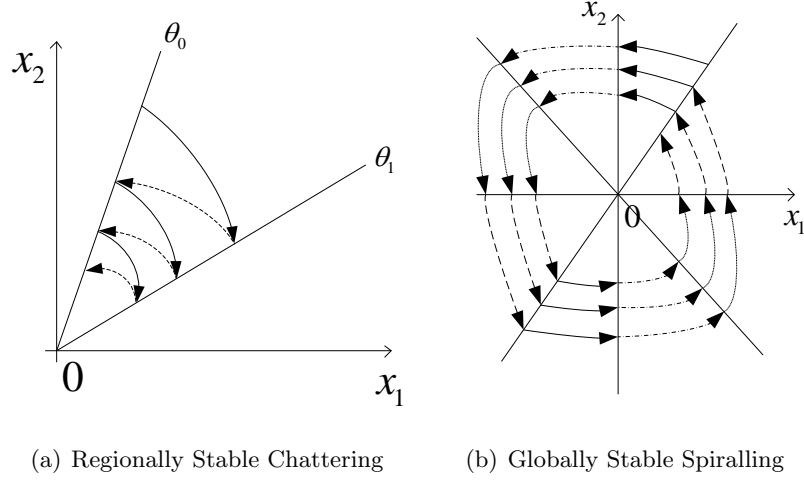


Figure 4.5: Two stabilization mechanisms for the switched system (4.1) of Category I with  $N \geq 2$

If the third condition is satisfied, the switched system (4.1) of Category I with  $N \geq 2$  is GAS by the switching signal staying on the corresponding best counterclockwise subsystem in each region for any initial state.

Overall, if any one of the three conditions is satisfied, the switched system (4.1) of Category I with  $N \geq 2$  is RAS and thus the proof of sufficiency is done.

#### 4.4.2 Stabilization Switching Laws for the Switched System (4.1) of Category I with $N \geq 2$

Based on Theorem 4.1, there are two stabilization switching laws for the switched system (4.1) of Category I with  $N \geq 2$ .

1) Regional Stabilization Switching Law: If there exists a stabilizable Type (a) Region and the system trajectories can be driven into this region, switch between the best clockwise subsystem and the best counterclockwise subsystem in this region upon intersecting the boundary of this region so as to keep the trajectory inside this region, as shown in Fig. 4.5(a);

2) Global Stabilization Switching Law: If  $\bigcup_{i=1}^N E_{ic}^o = \mathbb{R}^2$  and  $\gamma_{bc} < 1$  (resp.  $\bigcup_{i=1}^N E_{icc}^o = \mathbb{R}^2$  and  $\gamma_{bcc} < 1$ ), switch to the corresponding best clockwise (resp. counterclockwise) subsystem in each region for any initial state, as shown in Fig. 4.5(b).

The above two stabilization laws are similar to the ones in [82] for the two-mode case.

#### 4.4.3 Application of Theorem 4.1

**Example 4.1.** Consider a switched linear system with three unstable second-order LTI subsystems as follows

$$A_1 = \begin{bmatrix} 0 & -5 \\ 30 & 0.3 \end{bmatrix}, A_2 = \begin{bmatrix} 0 & -5 \\ 26 & 1 \end{bmatrix}, A_3 = \begin{bmatrix} 6 & -27 \\ 150 & 1 \end{bmatrix}. \quad (4.10)$$

It is noted that all the three subsystems are of Type 1. According to the switching stabilizability conditions in [82], it is impossible to stabilize any two of them by switching.

Based on equations (2.42)-(2.44),  $D_i(k)$ ,  $D_j(k)$  and  $N_{ij}(k)$  for  $i, j \in \{1, 2, 3\}$ ,  $i < j$  can be calculated. With all the real roots of  $D_i(k) = 0$ ,  $D_j(k) = 0$ , and  $N_{ij}(k) = 0$ , the polar coordinates space can then be partitioned into seven regions, as listed in Table 4.1. Moreover, all the boundaries are Type (b) Boundaries and all the regions are Type (b) Regions. According to Lemma 4.7, we have  $\bigcup_{i=1}^N E_{icc}^o = \mathbb{R}^2$  and  $\bigcup_{i=1}^N E_{ic}^o = \emptyset$ . Therefore, the first two conditions are violated.

Based on equations (2.38)-(2.39), the signs of  $H_{ij}$  and  $H_{ji}$  in each region are determined and listed in Table 4.1. According to Remark 4.2, the best counter-

Table 4.1: Generalized regions of  $k$  for Example 4.1

$k$	$H_{12}$	$H_{21}$	$H_{13}$	$H_{31}$	$H_{23}$	$H_{32}$	BCCS
$(-\infty, -21.4777)$	+	-	-	+	-	+	$A_3$
$(-21.4777, -1.7048)$	+	-	+	-	-	+	$A_1$
$(-1.7048, 0)$	+	-	+	-	+	-	$A_1$
$(0, 2.7035)$	-	+	+	-	+	-	$A_2$
$(2.7035, 4.1594)$	-	+	-	+	+	-	$A_2$
$(4.1594, 5.7143)$	-	+	-	+	-	+	$A_3$
$(5.7143, \infty)$	+	-	-	+	-	+	$A_3$

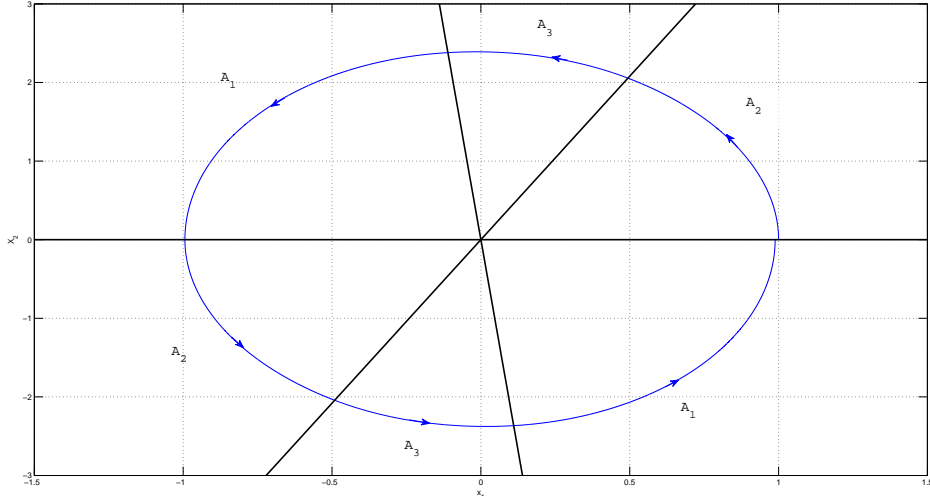


Figure 4.6: The best case trajectory of Example 4.1

clockwise subsystems (BCCS) for each region are also determined and listed in Table 4.1. From Table 4.1, we know that only three  $T_i$  need to be calculated. According to equation (4.7), we have  $T_2 = 0.0909\text{s}$ ,  $T_3 = 0.0100\text{s}$ ,  $T_1 = 0.1200\text{s}$ . Choosing an initial state  $x(t_0) = [1, 0]^T$ , we have

$$\gamma_{bcc} = \frac{\|e^{A_1 T_1} e^{A_3 T_3} e^{A_2 T_2} e^{A_1 T_1} e^{A_3 T_3} e^{A_2 T_2} x(t_0)\|}{\|x(t_0)\|} = 0.9884 < 1 \quad (4.11)$$

which means that the third condition in Theorem 4.1 is satisfied. Therefore, the switched system (4.10) is GAS. The best case trajectory is given in Fig. 4.6.

## 4.5 Extensions

In this section, the switching stabilizability condition for the switched system (4.1) of Category I with  $N \geq 2$  is extended to the switched systems (4.1) belonging to the other two categories.

### 4.5.1 Extension to the Switched System (4.1) of Category II with $N \geq 2$

**Theorem 4.2.** *The switched system (4.1) of Category II with  $N \geq 2$  is RAS subject to Assumptions 4.1-4.3 if and only if at least one of the following three conditions is satisfied.*

- 1) *There exists a stabilizable Type (a) Region;*
- 2)  $\bigcup_{i=1}^N E_{ic}^o = \mathbb{R}^2$ , and  $\gamma_{bc} < 1$ ;
- 3)  $\bigcup_{i=1}^N E_{icc}^o = \mathbb{R}^2$ , and  $\gamma_{bcc} < 1$ .

Theorem 4.2 is an extension of Theorem 4.1 by including subsystems of Type 2. The proof for Theorem 4.2 is very similar to that of Theorem 4.1, hence is omitted.

### 4.5.2 Extension to the Switched System (4.1) of Category III with $N \geq 2$

**Theorem 4.3.** *The switched system (4.1) of Category III with  $N \geq 2$  is always GAS subject to Assumptions 4.1-4.3.*

The proof for Theorem 4.3 is straightforward according to Theorem 3 and Remark 5 in [82].

## 4.6 Summary

Based on the results in Chapter 2, this chapter extended the best case switching signal (BCSS) criteria for second-order switched linear systems with two subsystems in [82] to the general case and derived three easily verifiable necessary and sufficient conditions for the switching stabilizability of second-order switched linear systems with any finite number of subsystems. Based on the derived conditions, two switching laws were proposed for the switching stabilization of second-order switched linear systems with any finite number of subsystems.

## Part II

# Controller Synthesis of Switched Systems



## Chapter 5

# Identification of Nonlinear Systems using Multiple Models

### 5.1 Introduction

As mentioned in Chapter 1, switched systems provide a switching control method for nonlinear dynamical systems based on the divide-and-conquer strategy. It is noted that a good multiple model architecture, which can provide accurate approximations of nonlinear systems, plays an important role in achieving a satisfactory control performance. While the PWA models have drawn most of the attention in approximating nonlinear systems in recent years, they encounter the “curse of dimensionality” problem when the dimension of the regressor space is high. To resolve this problem, we propose a novel multiple model architecture for the identification of nonlinear systems in this chapter. Instead of engaging all

dimensions of the regressor space into partitioning, the key idea of the proposed multiple model architecture is to partition only the range of the control input  $u(k)$  into several intervals and obtain a local model that is linear in  $u(k)$  within each interval. Based on the Taylor's theorem, a theoretical upper bound for the estimation error of the proposed model architecture can also be obtained. For each interval, the local model can be approximated by any universal approximator, such as artificial neural networks (ANN), assuming abundant input-output data. Both simulation studies and experimental results show that accurate approximation can be obtained by the proposed multiple model architecture.

The contents of this chapter are organized as follows. Section 5.2 presents some mathematical preliminaries. In Section 5.3, the novel multiple model architecture is presented. The identification of the proposed multiple model using neural networks is detailed in Section 5.4. Simulation studies and experimental results are given in Section 5.5 and Section 5.6 to demonstrate the effectiveness of the proposed multiple model in approximating nonlinear systems. Finally, in Section 5.7, a summary is given.

## 5.2 Mathematical Preliminaries

Consider a nonlinear discrete-time dynamical system described by the state-space equations

$$\begin{aligned}x(k+1) &= f[x(k), u(k)] \\ y(k) &= h[x(k)]\end{aligned}\tag{5.1}$$

where the state  $x(k) \in \mathbb{R}^n$ , the input  $u(k) \in \mathbb{R}$ , and the output  $y(k) \in \mathbb{R}$  are discrete-time sequences,  $f : \mathbb{R}^n \times \mathbb{R} \rightarrow \mathbb{R}^n$  and  $h : \mathbb{R}^n \rightarrow \mathbb{R}$  are smooth maps. However, both  $f$  and  $h$  are unknown, and only the input  $u(k)$  and output  $y(k)$  are accessible. Therefore, system identification and control have to be carried out using only input-output data, which is called data-driven identification and control of nonlinear systems. Our primary object in this thesis is to suggest a novel multiple model approach which circumvents the curse of dimensionality problem and is computationally effective in dealing with control problems. In particular, the control task is to determine a bounded control input  $u(k)$  such that the output  $y(k)$  tracks a specified bounded reference output  $y^*(k)$ .

For practical control problems, due to the limitation of the actuators, the input signals always have an operating range such that

$$U_{\min} \leq u \leq U_{\max} \tag{5.2}$$

where  $U_{\min}$  and  $U_{\max}$  are the minimal and maximum values of the control input signals. This operating range is assumed to be known to the users. For the simplicity of theoretical analysis, we make the following assumption.

**Assumption 5.1.** For any input sequence  $u(k)$  within the operating range, the output sequence  $y(k)$  is always bounded.

*Remark 5.1.* This assumption plays a very important role in the identification process and the theoretical analysis of the estimation error. It is a general assumption for most data-driven identification and control algorithms in the literature. It essentially implies that the system is bound-input-bounded-output (BIBO) stable. It is necessary since identification algorithms can only deal with

bounded signals. If not satisfied, it is assumed that we have a controller to stabilize the system first to assure that the input and output signals are all bounded.

Since only the input-output data are available, it is of great importance to investigate the existence of input-output models of the nonlinear system (5.1).

### 5.2.1 The NARMA Model

Under certain conditions, a local input-output model for the nonlinear system (5.1) in the neighborhood of the equilibrium state was derived in [122] and [123] with the form of

$$y(k+1) = F_l[y(k), \dots, y(k-n+1), u(k), \dots, u(k-n+1)] \quad (5.3)$$

where  $F_l : \mathbb{R}^{2n} \rightarrow \mathbb{R}$  is smooth. Considering the relative degree  $d$  of the nonlinear system (5.1), which represents the delay from input  $u$  to output  $y$  [124], the model becomes

$$y(k+d) = F_l[y(k), \dots, y(k-n+1), u(k), \dots, u(k-n+1)]. \quad (5.4)$$

By taking more past observations of input and output into consideration, the local input-output model (5.4) was extended to a global input-output representation for almost all nonlinear systems in [125] with the form of

$$y(k+d) = F_g[y(k), \dots, y(k-2n), u(k), \dots, u(k-2n)] \quad (5.5)$$

where  $F_g : \mathbb{R}^{4n+2} \rightarrow \mathbb{R}$  is smooth.

Overall, we have the following assumption regarding the existence of an input-output model of the nonlinear system (5.1).

**Assumption 5.2.** The nonlinear system (5.1) can be described by the nonlinear autoregressive moving average (NARMA) model of the form

$$y(k+d) = F[\phi(k)] \quad (5.6)$$

where  $\phi(k)$  is the regression vector defined by

$$\phi(k) = [y(k), \dots, y(k-n_a), u(k), \dots, u(k-n_b)]^T \quad (5.7)$$

and  $F : \mathbb{R}^{n_a+n_b+2} \rightarrow \mathbb{R}$  is smooth. Moreover,  $n_a + 1$  and  $n_b + 1$  are the orders of output and input in the regression vector respectively.

*Remark 5.2.* This assumption only assures the existence of the NARMA model. The mathematical form of the map  $F$  is unknown. However, in the identification process, the time delay  $d$ , the orders of output and input in the regression vector,  $n_a + 1$  and  $n_b + 1$ , are assumed to be known. If they are unknown a priori, there are various techniques to estimate them. For instance, the simplest way is to try different values and choose the smallest ones with satisfactory identification performance.

Under the existence assumption of  $F[\cdot]$ , a multilayer perceptron (MLP) or a radial basis function network (RBFN) can be used to identify it [126, 127]. Denoting the network mapping by  $N_0[\cdot]$ , the identification model has the form

$$\hat{y}(k+d) = N_0[\phi(k)] \quad (5.8)$$

where  $\hat{y}(k+d)$  is the estimate of  $y(k+d)$ .

*Remark 5.3.* Based on (5.8), the NARMA model can be approximated as accurate as desired. However, the NARMA model is not convenient for controller design since  $u(k)$  occurs nonlinearly in it.

### 5.2.2 The NARMA-L2 Model

In order to solve the control problem for the NARMA model mentioned in Remark 5.3, an approximation of the NARMA model in the neighborhood of the equilibrium state, called the NARMA-L2 model, was proposed in [128] of the form

$$y(k+d) \approx f_0[\varphi(k)] + g_0[\varphi(k)]u(k) \quad (5.9)$$

where the degraded regression vector  $\varphi(k)$  is the original regression vector  $\phi(k)$  without  $u(k)$ ,

$$\varphi(k) = [y(k), \dots, y(k-n_a), u(k-1), \dots, u(k-n_b)]^T \quad (5.10)$$

and  $f_0 : \mathbb{R}^{n_a+n_b+1} \rightarrow \mathbb{R}$ ,  $g_0 : \mathbb{R}^{n_a+n_b+1} \rightarrow \mathbb{R}$  are smooth.

The main feature of the NARMA-L2 model is that  $u(k)$  occurs linearly in the equation, which permits easy algebraic calculation of the control inputs. If  $g_0$  in (5.9) is sign definite in a neighborhood of the equilibrium state, the control input can be obtained by algebraic calculation as follows.

$$u(k) = \frac{y^*(k+d) - f_0[\varphi(k)]}{g_0[\varphi(k)]}. \quad (5.11)$$

Based on equation (5.9), a neural network comprising two subnetworks  $N_1[\cdot]$  and  $N_2[\cdot]$  can be constructed to identify the NARMA-L2 model. The identification model has the form

$$\hat{y}(k+d) = N_1[\varphi(k)] + N_2[\varphi(k)]u(k). \quad (5.12)$$

As mentioned in [128], the approximation can be made as accurate as desired by decreasing the amplitude of the input  $u$ . Therefore, the NARMA-L2 model only provides a local representation of the nonlinear system (5.1), which is its main drawback in approximating nonlinear systems with large operating range.

### 5.3 Multiple NARMA-L2 Models

Inspired by the NARMA-L2 model and the multiple model strategy, a novel multiple model architecture is proposed in this section.

Different from the PWA models where all dimensions of the regressor space are engaged in the partitioning, the key idea of the novel multiple model architecture is to partition only the range of the control input  $u(k)$  with length  $L$  into a suitable choice of intervals, say  $N$ , in the following form

$$[U_0, U_1], [U_1, U_2], \dots, [U_{N-1}, U_N] \quad (5.13)$$

where  $U_0 = U_{\min}$  and  $U_N = U_{\max}$ , and  $U_N - U_0 = L$ .

To make it simple, the partition is made with equal length, which means

$$U_1 - U_0 = U_2 - U_1 = \dots = U_N - U_{N-1} = \frac{L}{N}. \quad (5.14)$$

Express  $F[\phi(k)] = G[\varphi(k), u(k)]$  and denote  $\bar{U}_i = \frac{U_{i-1} + U_i}{2}$  as the middle point of the  $i^{\text{th}}$  ( $i = 1, \dots, N$ ) interval where  $u(k) \in [U_{i-1}, U_i]$ . In the  $i^{\text{th}}$  interval, the Taylor expansion of  $G[\varphi(k), u(k)]$  around the middle point  $\bar{U}_i$  can be expressed as

$$y(k+d) = G[\varphi(k), u(k)] = G[\varphi(k), \bar{U}_i] + \left. \frac{\partial G}{\partial u(k)} \right|_{(\varphi(k), \bar{U}_i)} (u(k) - \bar{U}_i) + R_i \quad (5.15)$$

where the second-order remainder  $R_i$  in Lagrange form is

$$R_i = \frac{1}{2} \left. \frac{\partial^2 G}{\partial u(k)^2} \right|_{(\varphi(k), \xi_i)} (u(k) - \bar{U}_i)^2 \quad (5.16)$$

where  $\xi_i$  lies between  $\bar{U}_i$  and  $u(k)$ . Since  $u(k) \in [U_{i-1}, U_i]$ , we have  $\xi_i \in [U_{i-1}, U_i]$ .

Since  $G$  is a smooth map,  $\frac{\partial^2 G}{\partial u(k)^2}$  is a continuous function. Note that  $\varphi(k)$  is bounded and  $\xi_i \in [U_{i-1}, U_i]$ . According to the Weierstrass extreme value theorem,  $\frac{\partial^2 G}{\partial u(k)^2}$  attains a maximum and a minimum in the compact set. Therefore, we have

$$\left| \left. \frac{\partial^2 G}{\partial u(k)^2} \right|_{(\varphi(k), \xi_i)} \right| \leq M_i \quad (5.17)$$

where  $M_i$  is the bounded maximum value of  $\left| \left. \frac{\partial^2 G}{\partial u(k)^2} \right|_{(\varphi(k), \xi_i)} \right|$ .

Then, we have

$$|R_i| \leq \frac{M_i L^2}{8N^2}. \quad (5.18)$$

In this case, the first-order Taylor polynomial of (5.15) can be used as an approximation of the NARMA model in the  $i^{\text{th}}$  interval where  $u(k) \in [U_{i-1}, U_i]$ ,



which can be written as

$$y(k+d) \approx f_i[\varphi(k)] + g_i[\varphi(k)]u(k), \quad u(k) \in [U_{i-1}, U_i] \quad (5.19)$$

which is in the NARMA-L2 form.

By combining all the submodels together, we have the multiple NARMA-L2 model of the form

$$y(k+d) \approx f_{\sigma(k)}[\varphi(k)] + g_{\sigma(k)}[\varphi(k)]u(k) \quad (5.20)$$

where

$$\sigma(k) = \begin{cases} \lceil N \cdot \frac{u(k)-U_0}{L} \rceil & \text{if } u(k) \neq U_0 \\ 1 & \text{if } u(k) = U_0 \end{cases} \quad (5.21)$$

is the switching signal that determines the active submodel at time  $k$ , and  $\lceil x \rceil$  is the ceiling function that returns the smallest integer not less than  $x$ .

Based on (5.18), the approximation error for the multiple NARMA-L2 model is bounded by

$$|e(k+d)| = |y(k+d) - f_{\sigma(k)}[\varphi(k)] - g_{\sigma(k)}[\varphi(k)]u(k)| \leq \frac{ML^2}{8N^2} \quad (5.22)$$

where  $M = \max\{M_1, M_2, \dots, M_N\}$ .

*Remark 5.4.* Different from the NARMA-L2 model, which is only valid in a small range of  $u(k)$ , the multiple NARMA-L2 model provides a representation of the nonlinear system (5.1) in the whole operating range  $[U_{\min}, U_{\max}]$ . Equation (5.22) indicates that the approximation can be made as accurate as desired by increasing the number of submodels, given the exact forms of  $f_i[\varphi(k)]$  and

$g_i[\varphi(k)]$ .

## 5.4 Identification of Multiple NARMA-L2 Models using Neural Networks

Since  $F[\phi(k)]$  is unknown, the mathematical forms of  $f_i[\varphi(k)]$  and  $g_i[\varphi(k)]$  cannot be obtained directly. However, they can be approximated by any universal approximator if we have sufficient input-output data. Based on equation (5.19), a neural network with two subnetworks  $N_{i1}[\cdot]$  and  $N_{i2}[\cdot]$  can be constructed to identify the  $i^{\text{th}}$  submodel of the multiple NARMA-L2 model with the form of

$$\hat{y}(k+d) = N_{i1}[\varphi(k)] + N_{i2}[\varphi(k)]u(k), \quad u(k) \in [U_{i-1}, U_i]. \quad (5.23)$$

Then, we have the multiple NARMA-L2 identification model in the following form

$$\hat{y}(k+d) = N_{\sigma(k)1}[\varphi(k)] + N_{\sigma(k)2}[\varphi(k)]u(k) \quad (5.24)$$

where

$$\sigma(k) = \begin{cases} \lceil N \cdot \frac{u(k)-U_0}{L} \rceil & \text{if } u(k) \neq U_0 \\ 1 & \text{if } u(k) = U_0 \end{cases}. \quad (5.25)$$

Given a set of input-output data of the nonlinear system (5.1), a training set can be constructed. Based on equation (5.25), we can classify the training data into  $N$  groups and train the corresponding neural networks.

*Remark 5.5.* In the identification of PWA models, the data assignment is a challenging task, which is coupled with parameter estimation and region estimation. However, in the identification of multiple NARMA-L2 models, the data assign-

ment becomes trivial due to the predefined data assignment rule (5.25).

*Remark 5.6.* The number of submodels in the multiple NARMA-L2 model,  $N$ , is a tuning parameter in the identification process. As mentioned in Remark 5.4, the theoretical upper bound for the estimation error becomes smaller as  $N$  increases. However, for a specific set of data in practice, as  $N$  increases, the number of data within each interval decreases, which will affect the neural networks approximation. Therefore,  $N$  should be chosen neither too large nor too small from the identification point of view.

*Remark 5.7.* The fundamental rule to choose an appropriate neural network structure is: the more complicated the nonlinear system is, the more complex neural networks we need. For a specific example, we need to first find an appropriate neural network structure for the NARMA model. Then, the neural network structures for each NARMA-L2 submodel should be simpler than that for the NARMA model.

## 5.5 Simulation Studies

In this section, simulation studies are carried out to demonstrate the effectiveness of the multiple NARMA-L2 models in approximating nonlinear systems. For comparison purposes, the identification results based on the NARMA model and the NARMA-L2 model are also included.

To evaluate the fit between the predicted output  $\hat{y}$  and the measured output  $y$ , we use the standard “Fit”-value, which is defined as

$$\text{Fit} = \left( 1 - \sqrt{\frac{\sum_k (y(k) - \hat{y}(k))^2}{\sum_k (y(k) - \bar{y})^2}} \right) \times 100\% \quad (5.26)$$

where  $\bar{y}$  is the arithmetic mean of  $y(k)$ .

### 5.5.1 Nonlinear Example 1

Consider the following nonlinear system

$$y(k+1) = \frac{y(k)}{1+y^2(k)} + u^3(k) \quad (5.27)$$

which was also used in [126, 107]. Note that this system is already in the NARMA form.

The training set consists of 4000 samples, which were generated by simulation using a uniformly distributed random input  $u(k) \in [-2, 2]$ . To test the quality of different models in approximating the original nonlinear system, the output of the original nonlinear system is compared with the output of different models when the test input is

$$u(k) = \sin \frac{2\pi k}{10} + \sin \frac{2\pi k}{25}, \quad k = 1, \dots, 200. \quad (5.28)$$

The three models used to identify the nonlinear system (5.27) are

$$\begin{aligned} \hat{y}_1(k+1) &= N_0[y(k), u(k)] \\ \hat{y}_2(k+1) &= N_1[y(k)] + N_2[y(k)]u(k) \\ \hat{y}_3(k+1) &= N_{\sigma(k)1}[y(k)] + N_{\sigma(k)2}[y(k)]u(k) \end{aligned} \quad (5.29)$$

where  $\hat{y}_1$ ,  $\hat{y}_2$ , and  $\hat{y}_3$  are the outputs predicted by the NARMA, NARMA-L2, and multiple NARMA-L2 models, respectively. In the simulation studies,  $N_0$  is an MLP chosen from the class  $N_{2,10,1}^2$  (i.e., two-layer networks with two inputs,

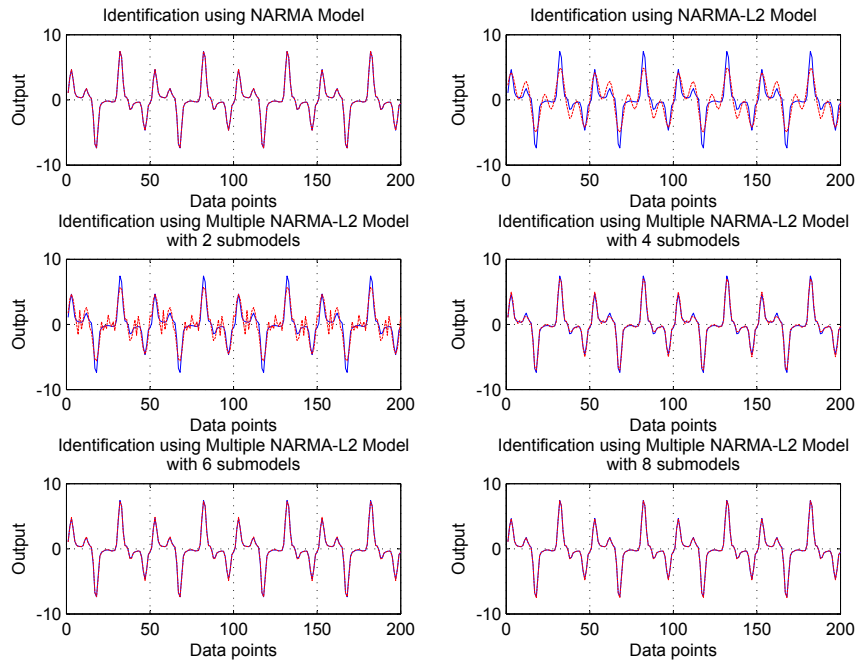


Figure 5.1: Identification results for the test set of nonlinear system 1 with different models. Solid: Real output, dashed: Estimation output

Table 5.1: Fit values for the test set of nonlinear system 1 with different models

Model Structure	NARMA	NARMA-L2	$N = 2$	$N = 4$	$N = 6$	$N = 8$
Fit Value	99.88%	58.59%	64.69%	90.31%	95.95%	97.43%

10 hidden neurons in the hidden layer, and one output node). Similarly,  $N_1$ ,  $N_2$ ,  $N_{i1}$  and  $N_{i2}$  are chosen to belong to  $N_{1,10,1}^2$ .

The simulation results for the test data of nonlinear system 1 using different models are shown in Fig. 5.1 and the corresponding Fit values are shown in Table 5.1. Note that  $N = 2$  in Table 5.1 stands for the multiple NARMA-L2 model with 2 submodels. As can be seen from Fig. 5.1 and Table 5.1, the fitting becomes better as the number of submodels increases. In particular, the identification performance based on the multiple NARMA-L2 model with 8 submodels is close to that using the NARMA model.

### 5.5.2 Nonlinear Example 2

Consider the following nonlinear system

$$y(k+1) = \frac{1.5y(k)y(k-1)}{1+y^2(k)+y^2(k-1)} + \sin[y(k)+y(k-1)] + u(k) + 0.8u(k-1) \quad (5.30)$$

which can be found in [108]. Note that this system is already in the NARMA-L2 form.

The training set consists of 4000 samples, which were generated by simulation using a uniformly distributed random input  $u(k) \in [-2.2, 2.2]$ . The test input signal is

$$u(k) = \sin \frac{2\pi k}{10} + \sin \frac{2\pi k}{25}, \quad k = 1, \dots, 200. \quad (5.31)$$

The three models used to identify the nonlinear system (5.30) are

$$\begin{aligned} \hat{y}_1(k+1) &= N_0[\phi(k)] \\ \hat{y}_2(k+1) &= N_1[\varphi(k)] + N_2[\varphi(k)]u(k) \\ \hat{y}_3(k+1) &= N_{\sigma(k)1}[\varphi(k)] + N_{\sigma(k)2}[\varphi(k)]u(k) \end{aligned} \quad (5.32)$$

where

$$\begin{aligned} \phi(k) &= [y(k), y(k-1), u(k), u(k-1)] \\ \varphi(k) &= [y(k), y(k-1), u(k-1)] \end{aligned} \quad (5.33)$$

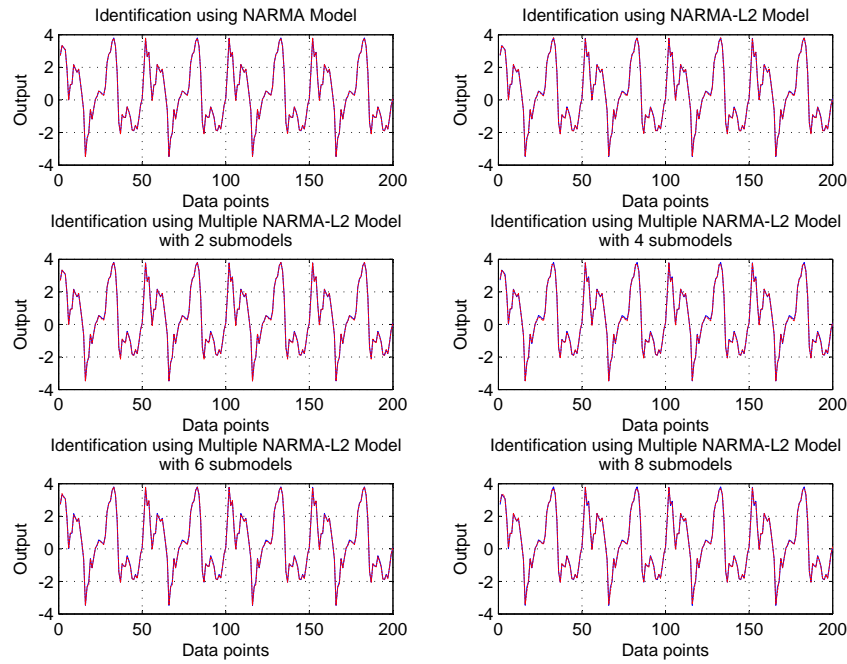


Figure 5.2: Identification results for the test set of nonlinear system 2 with different models. Solid: Real output, dashed: Estimation output

Table 5.2: Fit values for the test set of nonlinear system 2 with different models

Model Structure	NARMA	NARMA-L2	$N = 2$	$N = 4$	$N = 6$	$N = 8$
Fit Value	99.17%	98.38%	98.15%	97.22%	97.15%	96.42%

and  $\hat{y}_1$ ,  $\hat{y}_2$ , and  $\hat{y}_3$  are the outputs predicted by the NARMA, NARMA-L2, and multiple NARMA-L2 models, respectively. In the simulation studies,  $N_0$  is an MLP chosen from the class  $N_{4,20,1}^2$ , while  $N_1$ ,  $N_2$ ,  $N_{i1}$  and  $N_{i2}$  are chosen from the class  $N_{3,10,1}^2$ .

The simulation results for the test data of nonlinear system 2 using different models are shown in Fig. 5.2 and the corresponding Fit values are shown in Table 5.2. As can be seen from Fig. 5.2 and Table 5.2, there is no significant difference for the fitting using the NARMA, NARMA-L2 and multiple NARMA-L2 models, which is due to the NARMA-L2 form of the original nonlinear system.

### 5.5.3 Nonlinear Example 3

Consider a nonlinear system described by the state-space form

$$\begin{aligned}
 x_1(k+1) &= 0.1x_1(k) + 2\frac{u(k) + x_2(k)}{1 + [u(k) + x_2(k)]^2} \\
 x_2(k+1) &= 0.1x_2(k) + \frac{u^3(k) + x_1^2(k)}{1 + x_1^2(k) + x_2^2(k)} \\
 y(k) &= x_1(k) + x_2(k)
 \end{aligned} \tag{5.34}$$

The training set consists of 10000 samples, which were generated by simulation using a uniformly distributed random input  $u(k) \in [-2, 2]$ . The test input signal is

$$u(k) = \sin \frac{2\pi k}{10} + \sin \frac{2\pi k}{25}, \quad k = 1, \dots, 200. \tag{5.35}$$

Since this example is in the state-space form, appropriate  $n_a$  and  $n_b$  need to be chosen in the identification process. For different values of  $n_a$  and  $n_b$ , it was found that the Fit values of the NARMA model are almost the same when  $n_a = n_b \geq 2$ . For simplicity,  $n_a = n_b = 2$  is chosen. Therefore, the three models used to identify the nonlinear system (5.34) are

$$\begin{aligned}
 \hat{y}_1(k+1) &= N_0[\phi(k)] \\
 \hat{y}_2(k+1) &= N_1[\varphi(k)] + N_2[\varphi(k)]u(k) \\
 \hat{y}_3(k+1) &= N_{\sigma(k)1}[\varphi(k)] + N_{\sigma(k)2}[\varphi(k)]u(k)
 \end{aligned} \tag{5.36}$$



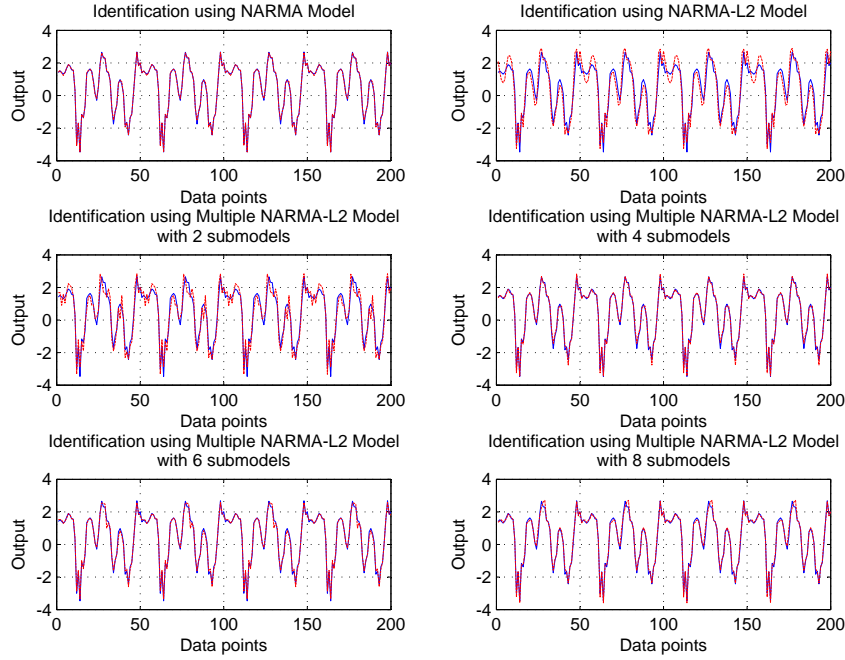


Figure 5.3: Identification results for the test set of nonlinear system 3 with different models. Solid: Real output, dashed: Estimated output

where

$$\begin{aligned}\phi(k) &= [y(k), y(k-1), y(k-2), u(k), u(k-1), u(k-2)] \\ \varphi(k) &= [y(k), y(k-1), y(k-2), u(k-1), u(k-2)]\end{aligned}\quad (5.37)$$

and  $\hat{y}_1$ ,  $\hat{y}_2$ , and  $\hat{y}_3$  are the outputs predicted by the NARMA, NARMA-L2, and multiple NARMA-L2 models, respectively. In the simulation studies,  $N_0 \in N_{6,20,10,1}^3$  while  $N_1$ ,  $N_2$ ,  $N_{i1}$  and  $N_{i2}$  are chosen from the class  $N_{5,20,1}^2$ .

The simulation results for the test data of nonlinear system 3 using different models are shown in Fig. 5.3 and the corresponding Fit values are shown in Table 5.3. As can be seen from Fig. 5.3 and Table 5.3, the fitting becomes better as the number of submodels increases from 1 to 4. In particular, the identification

Table 5.3: Fit values for the test set of nonlinear system 3 with different models

Model Structure	NARMA	NARMA-L2	$N = 2$	$N = 4$	$N = 6$	$N = 8$
Fit Value	96.14%	69.70%	73.43%	92.16%	91.45%	90.14%

performance based on the multiple NARMA-L2 model with 4 submodels is close to that using the NARMA model. However, from  $N = 4$  to  $N = 8$ , there is no increase but small decrease in the Fit value, which shows that bigger  $N$  does not guarantee better identification performance in the multiple NARMA-L2 model architecture.

#### 5.5.4 Nonlinear Example 4

Consider a nonlinear benchmark system described in the state-space form

$$\begin{aligned}
 x_1(k+1) &= \left( \frac{x_1(k)}{1+x_1^2(k)} + 1 \right) \sin[x_2(k)] \\
 x_2(k+1) &= x_2(k) \cos[x_2(k)] + x_1(k) \exp\left[-\frac{x_1^2(k) + x_2^2(k)}{8}\right] \\
 &\quad + \frac{u^3(k)}{1+u^2(k) + 0.5 \cos(x_1(k) + x_2(k))} \\
 y(k) &= \frac{x_1(k)}{1+0.5 \sin[x_2(k)]} + \frac{x_2(k)}{1+0.5 \sin[x_1(k)]}. \tag{5.38}
 \end{aligned}$$

This plant, taken from [129], does not correspond to any real physical system and is deliberately chosen to be complex and distinctly nonlinear so that conventional identification and control methods do not give satisfactory performance.

The training set consists of 50000 samples, which were generated by simulation using a uniformly distributed random input  $u(k) \in [-2.5, 2.5]$ . The test input signal is

$$u(k) = \sin \frac{2\pi k}{10} + \sin \frac{2\pi k}{25}, \quad k = 1, \dots, 200. \tag{5.39}$$

Similar to nonlinear example 3, appropriate  $n_a$  and  $n_b$  need to be chosen in the identification process. To keep consistent with other works [130, 131, 132, 133, 107], which also used this model,  $n_a = n_b = 2$  is chosen. Therefore, the three models used to identify the nonlinear system (5.38) are

$$\begin{aligned}\hat{y}_1(k+1) &= N_0[\phi(k)] \\ \hat{y}_2(k+1) &= N_1[\varphi(k)] + N_2[\varphi(k)]u(k) \\ \hat{y}_3(k+1) &= N_{\sigma(k)1}[\varphi(k)] + N_{\sigma(k)2}[\varphi(k)]u(k)\end{aligned}\quad (5.40)$$

where

$$\begin{aligned}\phi(k) &= [y(k), y(k-1), y(k-2), u(k), u(k-1), u(k-2)] \\ \varphi(k) &= [y(k), y(k-1), y(k-2), u(k-1), u(k-2)]\end{aligned}\quad (5.41)$$

and  $\hat{y}_1$ ,  $\hat{y}_2$ , and  $\hat{y}_3$  are the outputs predicted by the NARMA, NARMA-L2, and multiple NARMA-L2 models, respectively. In the simulation studies,  $N_0 \in N_{6,50,20,1}^3$  while  $N_1$ ,  $N_2$ ,  $N_{i1}$  and  $N_{i2}$  are chosen from the class  $N_{5,30,20,1}^3$ .

The simulation results for the test data of nonlinear system 4 using different models are shown in Fig. 5.4 and the corresponding Fit values are shown in Table 5.4. As can be seen from Fig. 5.4 and Table 5.4, the identification performance becomes better as the number of submodels increases. In particular, the identification result based on the multiple NARMA-L2 model with 4 submodels is close to that using the NARMA model.

*Remark 5.8.* Nonlinear system 4 is a benchmark example to evaluate the identification and control methods and has been extensively used in the literature

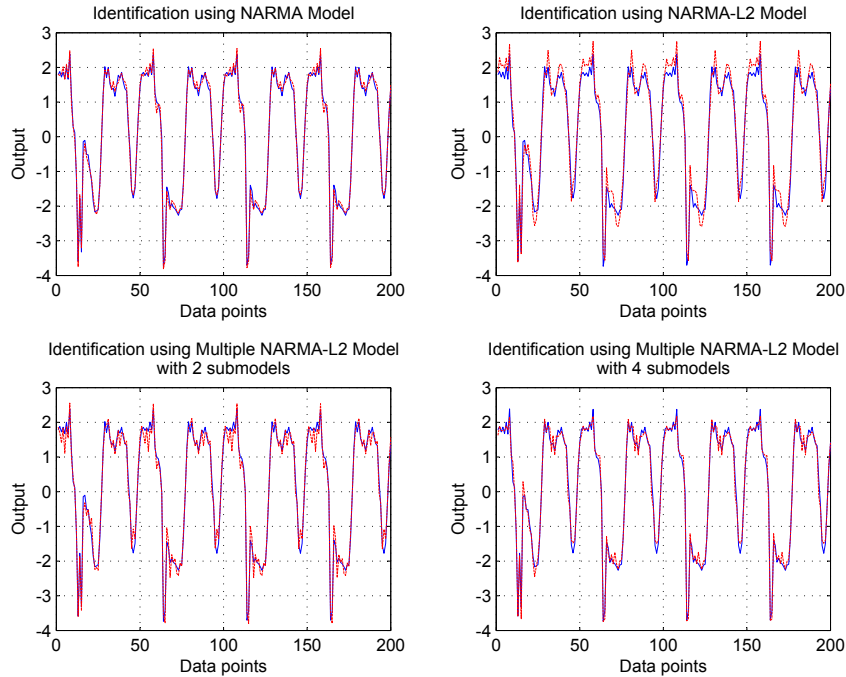


Figure 5.4: Identification results for the test set of nonlinear system 4 with different models. Solid: Real output, dashed: Estimated output

Table 5.4: Fit values for the test set of nonlinear system 4 with different models

Model Structure	NARMA	NARMA-L2	$N = 2$	$N = 4$
Fit Value	92.19%	82.95%	87.12%	89.97%

[130, 131, 132, 133, 107]. While our model architecture needs more sample data to train the neural networks, its identification results are indeed superior to others. In addition, our model can also facilitate the controller design problem, which is challenging for most of them. Although the PWA models in [107] can also deal with the controller design of this nonlinear system, its identification performance is not as good as ours.

## 5.6 Experimental Studies

In this section, we apply the proposed multiple model structure to the identification of a real-world system to show its effectiveness. Specifically, we utilize

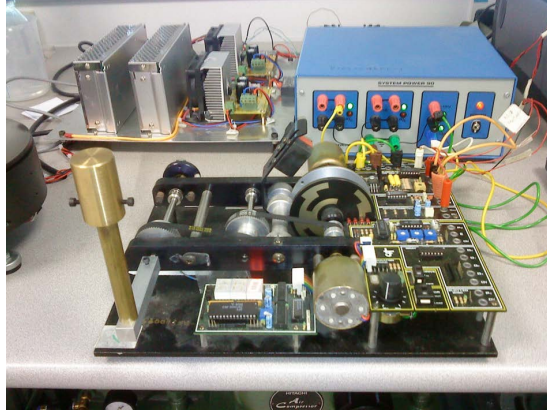


Figure 5.5: Original hardware setup

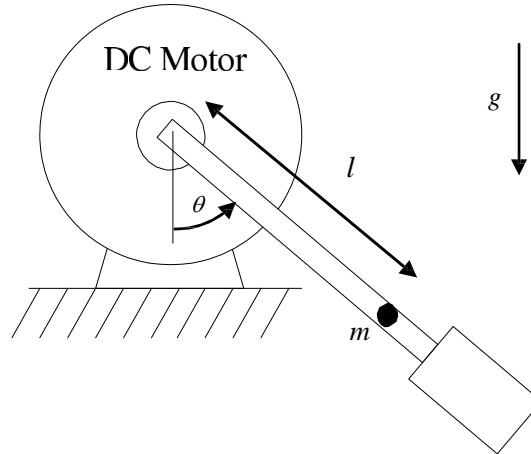


Figure 5.6: Schematics diagram of the original setup

the hardware setup used in [107], which is a modified version of an L.J. Electronics DC motor apparatus by replacing the original centric load by a brass rod with a heavy brass pendulum at the end, as shown in Fig. 5.5. Its schematics diagram is also given in Fig. 5.6.

The simplified continuous-time physical model of the system is

$$J\ddot{\theta} = -\beta\dot{\theta} - mgl\sin(\theta) + Ku \quad (5.42)$$

where  $J$  is the overall moment of inertia of the system including the motor

shaft, the rod and the pendulum,  $m$  is the mass of the rod and the pendulum,  $l$  is the distance from the pivot of rotation to the center of gravity of the rod and pendulum,  $g$  is the gravitational constant,  $\beta$  is the damping coefficient,  $\theta$  is the angle of rotation, and  $u$  is the input voltage.

In [107], the angular position  $\theta$  was treated as the output and PWA models were used to approximate the original nonlinear system. However, it was found that good identification performance can be obtained with even a single affine model (the Fit value is higher than 96%). Moreover, it is noted that the original system is already in the NARMA-L2 form (linear in  $u(k)$ ). Therefore, we cannot expect a significant improvement for the identification using multiple NARMA-L2 models.

In order to demonstrate the effectiveness of the multiple NARMA-L2 model, we make another modification by adding a cubic term to the input channel of the original setup and treat the angular velocity  $\dot{\theta}$  as the system output. Let  $x_1 = \theta$ ,  $x_2 = \dot{\theta}$ , the modified system can be represented by

$$\begin{aligned} \dot{x}_1 &= x_2 \\ \dot{x}_2 &= -\frac{mgl}{J} \sin x_1 - \frac{\beta}{J} x_2 + \frac{K}{J} u^3 \\ y &= x_2 \end{aligned} \tag{5.43}$$

In the data acquisition process, the MATLAB/Simulink and a dSPACE D-S1104 rapid control prototyping system is used to generate the physical control signal  $v(k)$  to the modified DC motor, based on the numerical value of the control signal  $u(k)$  in Matlab. In addition, the sensor reading of the angle velocity  $s(k)$  is sent into the computer via the dSPACE system and interpreted as numerical

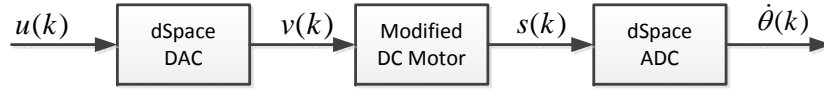


Figure 5.7: Working diagram for the identification process of the modified DC motor

values  $\dot{\theta}(k)$ . The working diagram for the identification process is shown in Fig. 5.7. For this experiment, the sampling period is chosen to be 0.05s.

The training set, which consists of 4000 data points, was obtained by setting the input signal  $u(k)$  to be the combination of a square wave (with magnitude of 0.7 and period of 2s) and a uniformly distributed random signal (with magnitude of 1). The test set, with 400 data points, was obtained by setting the input signal  $u(k)$  to be

$$u(k) = \sin \frac{2\pi k}{20} + \sin\left(\frac{2\pi k}{25} + \frac{\pi}{3}\right), \quad k = 1, \dots, 400. \quad (5.44)$$

For this experiment, we choose  $n_a = n_b = 1$ . Therefore, the three models used to identify the modified DC motor (5.43) are

$$\begin{aligned} \hat{y}_1(k+1) &= N_0[\phi(k)] \\ \hat{y}_2(k+1) &= N_1[\varphi(k)] + N_2[\varphi(k)]u(k) \\ \hat{y}_3(k+1) &= N_{\sigma(k)1}[\varphi(k)] + N_{\sigma(k)2}[\varphi(k)]u(k) \end{aligned} \quad (5.45)$$

where

$$\begin{aligned} \phi(k) &= [y(k), y(k-1), u(k), u(k-1)] \\ \varphi(k) &= [y(k), y(k-1), u(k-1)] \end{aligned} \quad (5.46)$$

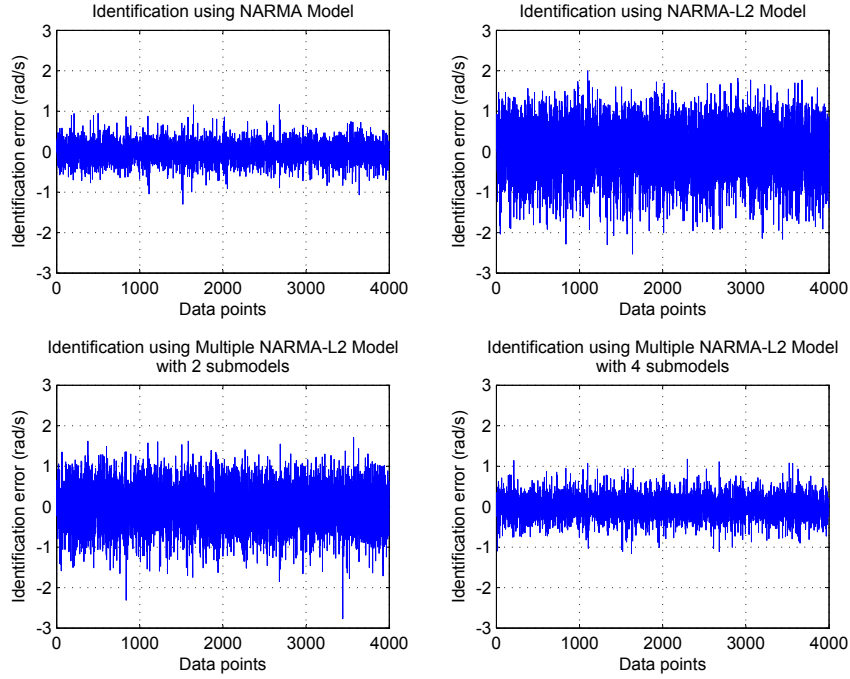


Figure 5.8: Identification errors for the training set of the modified DC motor with different models

Table 5.5: Fit values for the modified DC motor with different models

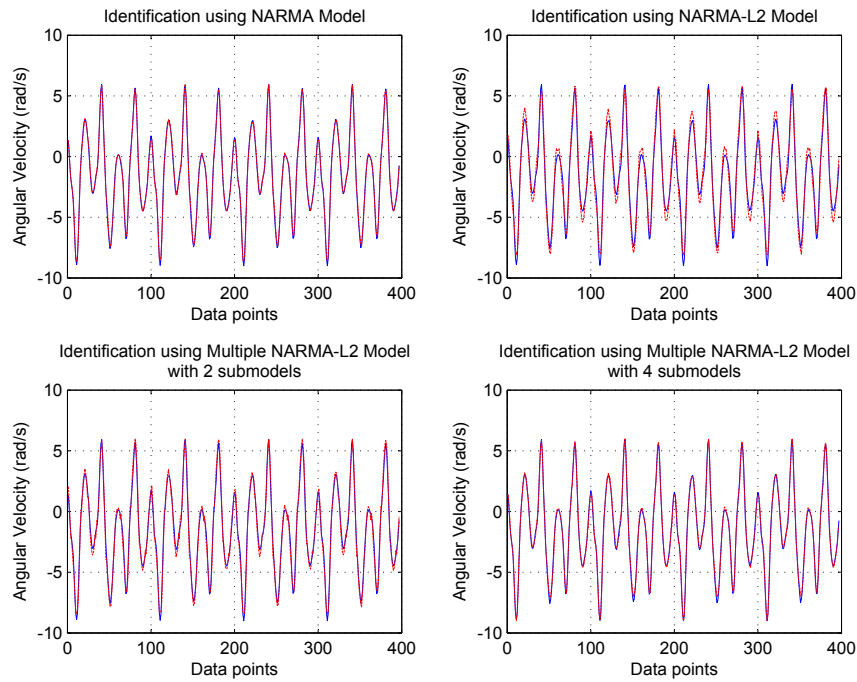
Model structure	NARMA	NARMA-L2	$N = 2$	$N = 4$
Training set	92.37%	77.81%	82.20%	91.36%
Test set	94.65%	82.69%	87.85%	93.33%

and  $\hat{y}_1$ ,  $\hat{y}_2$ , and  $\hat{y}_3$  are the outputs predicted by the NARMA, NARMA-L2, and multiple NARMA-L2 models, respectively. In the experiment,  $N_0 \in N_{4,20,10,1}^3$  while  $N_1$ ,  $N_2$ ,  $N_{i1}$  and  $N_{i2}$  are chosen from the class  $N_{3,10,1}^2$ .

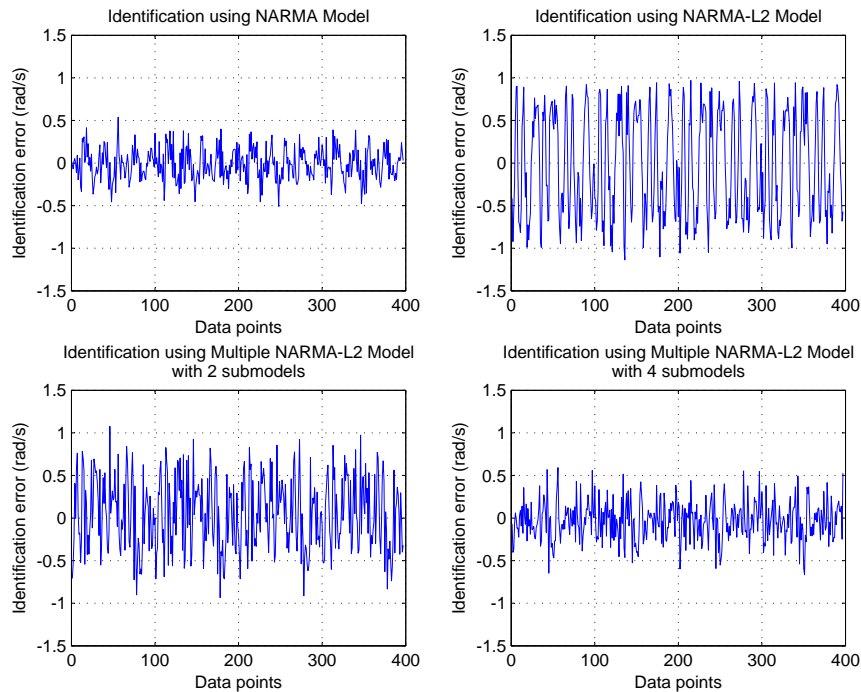
The identification errors for the training set with different models are shown in Fig. 5.8. It is observed that the identification error decreases as the number of submodels increases and the identification performance using the multiple NARMA-L2 model with 4 submodels is close to that using the NARMA model, which can also be concluded from the Fit values shown in Table 5.5.

On the other hand, the identification results for the test set are shown in





(a) Identification output. Solid: Real output, dashed: Estimated output



(b) Identification error

Figure 5.9: Identification results for the test set of the modified DC motor with different models

Fig. 5.9, and the corresponding Fit values are also listed in Table 5.5. As can be seen, the fitting becomes better as the number of submodels increases and the identification performance using the multiple NARMA-L2 model with 4 submodels is close to that using the NARMA model. This shows that the identified multiple NARMA-L2 model can generalize well to the test set.

## 5.7 Summary

In this chapter, a novel multiple model architecture was proposed to circumvent the curse of dimensionality problem for the identification of nonlinear systems. The key idea of this model structure is to partition only the range of the control input  $u(k)$  into several intervals and identify a local model that is linear in  $u(k)$  in each interval. A theoretical upper bound for the estimation error was obtained based on the Taylor's theorem. This methodology was applied to nonlinear systems using artificial neural networks (ANN). Both simulation studies and experimental results have demonstrated the effectiveness of the proposed multiple model architecture in approximating nonlinear systems.

## Chapter 6

# Control of Nonlinear Systems using Multiple Models and Switching

### 6.1 Introduction

In this chapter, we proceed to design a switching controller for nonlinear systems based on the multiple NARMA-L2 models proposed in Chapter 5. As mentioned in Chapter 1, there are two steps for the switching control algorithm: the design of sub-controllers and the determination of the switching mechanism.

In the first step, we utilize the weighted one-step-ahead predictive control technique [134, 135, 136]. Different from the sub-controllers design based on PWA models in [107] where a couple of quadratic optimization problems with complex nonlinear constraints need to be solved, we only need to solve several quadratic optimization problems with linear constraints due to the special

structure of the proposed multiple NARMA-L2 model architecture. This change greatly reduces the computational load and makes it possible to be used in real-time applications. In the second step, the active sub-controller at every time instant is determined by substituting the control signals for each submodel into the corresponding cost function and choosing the one with the smallest cost value. This control algorithm is applied to the numerical examples and experiment used in Chapter 5 to verify its effectiveness.

The contents of this chapter are organized as follows. Section 6.2 designs the sub-controllers based on the weighted one-step-ahead predictive control law and constrained optimization techniques. Section 6.3 provides the strategy to determine the switching mechanism at any time instant. Simulation studies and experimental results are presented in Section 6.4 and Section 6.5 to show the effectiveness of the proposed switching control algorithm. Finally, in Section 6.6, a summary is given.

## 6.2 Sub-controllers Design

The multiple NARMA-L2 model of the nonlinear system (5.1) in the form

$$y(k+d) \approx f_{\sigma(k)}[\varphi(k)] + g_{\sigma(k)}[\varphi(k)]u(k) \quad (6.1)$$

where

$$\sigma(k) = \begin{cases} \lceil N \cdot \frac{u(k)-U_0}{L} \rceil & \text{if } u(k) \neq U_0 \\ 1 & \text{if } u(k) = U_0 \end{cases} \quad (6.2)$$

was identified using neural networks in Section 5.4 with the form of

$$\hat{y}(k+d) = N_{\sigma(k)1}[\varphi(k)] + N_{\sigma(k)2}[\varphi(k)]u(k) \quad (6.3)$$

where

$$\sigma(k) = \begin{cases} \lceil N \cdot \frac{u(k)-U_0}{L} \rceil & \text{if } u(k) \neq U_0 \\ 1 & \text{if } u(k) = U_0 \end{cases} . \quad (6.4)$$

After  $N_{i1}[\varphi(k)]$  and  $N_{i2}[\varphi(k)]$  are obtained,  $f_i[\varphi(k)]$  and  $g_i[\varphi(k)]$  are assumed to be known although they are approximated by neural networks. Then, we can design the sub-controller for the  $i^{\text{th}}$  submodel (5.19), which is repeated here for the readers' convenience.

$$y_i(k+d) \approx f_i[\varphi(k)] + g_i[\varphi(k)]u(k), \quad u(k) \in [U_{i-1}, U_i]. \quad (6.5)$$

To design the sub-controller for the  $i^{\text{th}}$  submodel, we use the the weighted one-step-ahead predictive control method, which is considered as the result of a direct constrained optimization problem as follows

$$\begin{aligned} \min_{u_i(k)} J_i(k) &= \frac{1}{2} [f_i[\varphi(k)] + g_i[\varphi(k)]u(k) - y^*(k+d)]^2 + \frac{\rho}{2} (u_i(k) - u(k-1))^2 \\ \text{s.t.} \quad &U_{i-1} \leq u_i(k) \leq U_i \end{aligned} \quad (6.6)$$

where  $u_i(k)$  is the control input computed from the  $i$ th submodel, and  $\rho > 0$  is the control effort weighting factor, which is to achieve a compromise between perfect one-step-ahead control and the variation in the amount of control effort.

*Remark 6.1.* Theoretically, a smaller  $\rho$  is preferred so as to put more emphasize on the tracking error. However, a bigger  $\rho$  will result in a smoother control input signal, which is easier to be implemented in practice. Therefore, the basic strategy is to try different values for  $\rho$  from zero to one (equally weighted) and choose the biggest one with satisfactory tracking performance.

It is noted that (6.6) is only a one-dimensional quadratic optimization problem with linear constraints. Based on constrained optimization techniques, we can first obtain the optimal solution without constraints as

$$\tilde{u}_i(k) = \frac{g_i[\varphi(k)](y^*(k+d) - f_i[\varphi(k)]) + \rho u(k-1)}{g_i^2[\varphi(k)] + \rho}. \quad (6.7)$$

Then, the constrained optimal solution is

$$u_i(k) = \begin{cases} \tilde{u}_i(k) & \text{if } U_{i-1} \leq \tilde{u}_i(k) \leq U_i \\ U_{i-1} & \text{if } \tilde{u}_i(k) < U_{i-1} \\ U_i & \text{if } \tilde{u}_i(k) > U_i \end{cases}. \quad (6.8)$$

*Remark 6.2.* Equations (6.7)-(6.8) provide a very simple way to calculate the control signals for each submodel, which is due to the special structure of the proposed multiple model structure. The computational load is very small and therefore can be used in real-time applications.

### 6.3 Switching Mechanism

With the control signal  $u_i(k)$  for each submodel at time  $k$ , the submodel corresponding to the minimum  $J_i(k)$  ( $i = 1, 2, \dots, N$ ) is activated. In other

words, the control input  $u(k)$  is chosen as  $u_l(k)$  if

$$J_l(k) = \min_i J_i(k). \quad (6.9)$$

*Remark 6.3.* The probability that  $\tilde{u}_i(k)$  falls outside the  $i^{\text{th}}$  interval becomes higher as  $N$  increases, which may result in non-smooth control performance. Therefore, from the control point of view, the number of submodels,  $N$ , cannot be too large.

*Remark 6.4.* The stability analysis for the control of nonlinear systems using multiple models is extremely complicated. It is well known that even when each sub-controller can stabilize its corresponding region of the nonlinear system, the stability of the overall system still cannot be guaranteed after switching happens [4]. Moreover, the fact that the submodels in our scheme are not accurate makes the problem even more challenging. These issues are possible directions for our future work.

## 6.4 Simulation Studies

In this section, simulation studies are carried out to demonstrate the effectiveness of the switching control algorithm in controlling nonlinear systems based on the identification results in Chapter 5. Due to the complexity of the controller design based on the NARMA model, we only include the control performance based on the NARMA-L2 model for comparison purposes.

### 6.4.1 Nonlinear Example 1

Consider the following nonlinear system

$$y(k+1) = \frac{y(k)}{1+y^2(k)} + u^3(k) \quad (6.10)$$

which was identified in section 5.5.1.

With the identified NARMA-L2 model and multiple NARMA-L2 models of nonlinear system 1, we proceed to control it using the control algorithm in (6.7)-(6.9). For nonlinear system 1, the desired output is

$$y^*(k) = 4 \sin \frac{2\pi k}{10} + 4 \sin \frac{2\pi k}{25}, \quad k = 1, \dots, 100. \quad (6.11)$$

The simulation results for the tracking performance of nonlinear system 1 using different models are shown in Fig. 6.1. It is noted that the parameter  $\rho$  is chosen to be 0.01. As can be seen from Fig. 6.1, the tracking performance becomes better as the number of submodels increases. Moreover, perfect tracking can almost be achieved based on the multiple NARMA-L2 model with 8 submodels.

### 6.4.2 Nonlinear Example 2

Consider the following nonlinear system

$$\begin{aligned} y(k+1) = & \frac{1.5y(k)y(k-1)}{1+y^2(k)+y^2(k-1)} \\ & + \sin[y(k)+y(k-1)] + u(k) + 0.8u(k-1) \end{aligned} \quad (6.12)$$



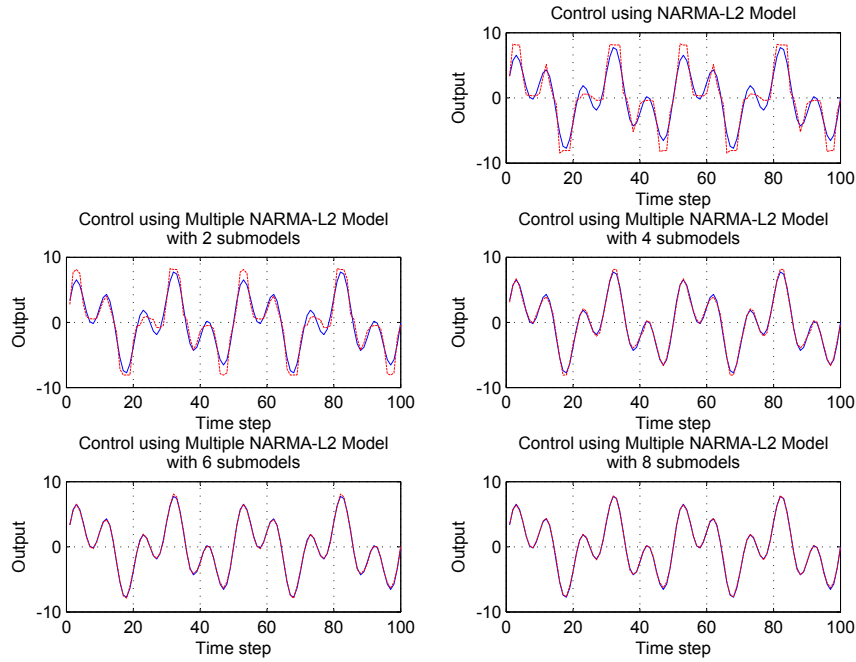


Figure 6.1: Control results of nonlinear system 1 with different models. Solid: Reference, dashed: System output

which was identified in section 5.5.2.

With the identified NARMA-L2 model and multiple NARMA-L2 models of nonlinear system 2, we proceed to control it using the control algorithm in (6.7)-(6.9). For nonlinear system 2, the desired output is

$$y^*(k) = \sin \frac{2\pi k}{10} + \sin \frac{2\pi k}{50}, \quad k = 1, \dots, 200. \quad (6.13)$$

The simulation results for the tracking performance of nonlinear system 2 are shown in Fig. 6.2. It is noted that the parameter  $\rho$  is chosen to be 0.01. As can be seen from Fig. 6.2, there is no significant difference for the tracking performance using NARMA-L2 model and multiple NARMA-L2 models, which is consistent with the identification results.

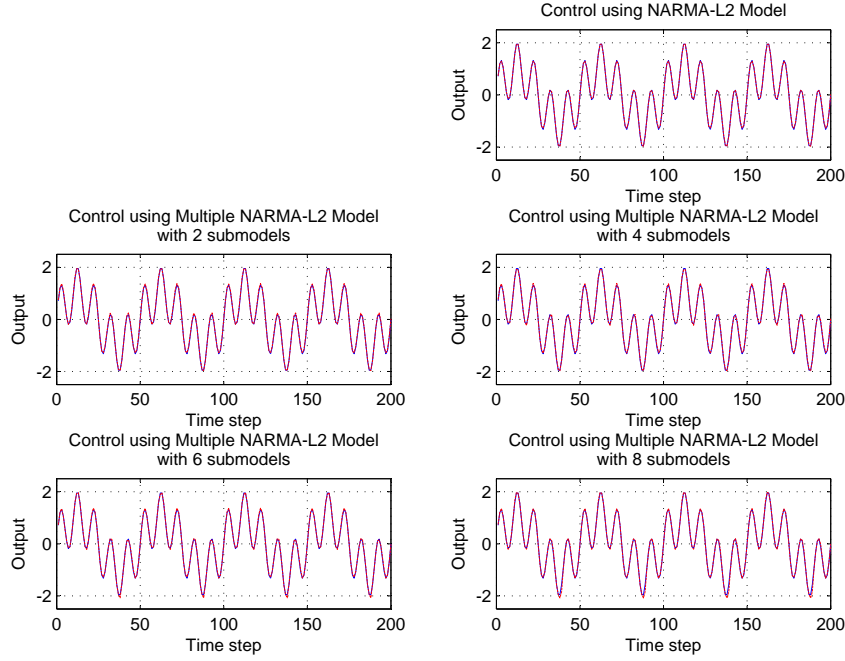


Figure 6.2: Control results of nonlinear system 2 with different models. Solid: Reference, dashed: System output

### 6.4.3 Nonlinear Example 3

Consider nonlinear system 3 that was previously identified in section 5.5.3.

$$\begin{aligned}
 x_1(k+1) &= 0.1x_1(k) + 2 \frac{u(k) + x_2(k)}{1 + [u(k) + x_2(k)]^2} \\
 x_2(k+1) &= 0.1x_2(k) + \frac{u^3(k) + x_1^2(k)}{1 + x_1^2(k) + x_2^2(k)} \\
 y(k) &= x_1(k) + x_2(k)
 \end{aligned} \tag{6.14}$$

With the identified NARMA-L2 model and multiple NARMA-L2 models of nonlinear system 3, we proceed to control it using the control algorithm in (6.7)-(6.9). For nonlinear system 3, the desired output is

$$y^*(k) = \sin \frac{2\pi k}{20} + \sin \frac{2\pi k}{100}, \quad k = 1, \dots, 200. \tag{6.15}$$

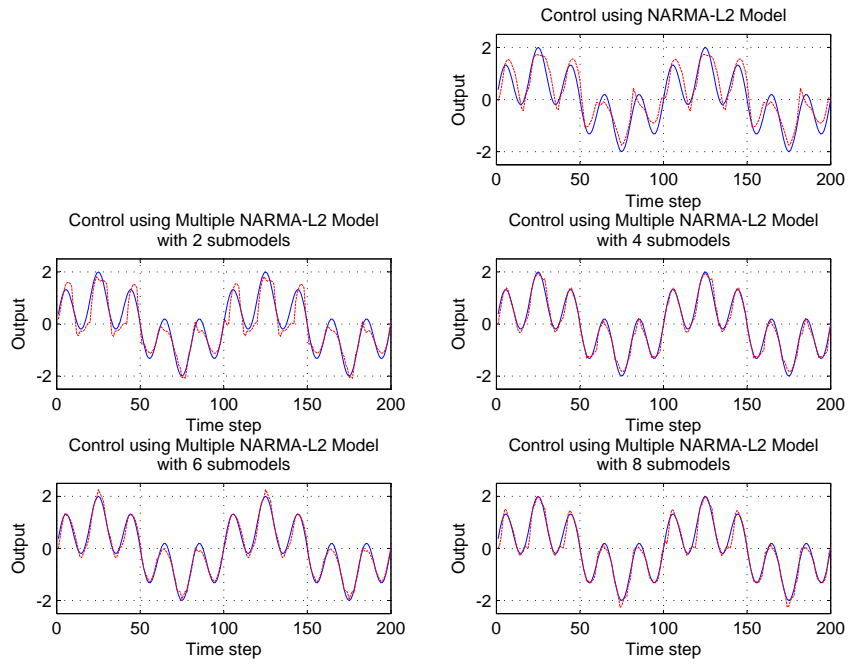


Figure 6.3: Control results of nonlinear system 3 with different models. Solid: Reference, dashed: System output

The simulation results for the tracking performance of nonlinear system 3 are shown in Fig. 6.3. It is noted that the parameter  $\rho$  is chosen to be 0.1. As can be seen from Figure 6.3, the tracking performance is satisfactory when the number of submodels is 4 or 6.

#### 6.4.4 Nonlinear Example 4

Consider again the nonlinear benchmark system that was identified in section 5.5.4.

$$\begin{aligned}
 x_1(k+1) &= \left( \frac{x_1(k)}{1+x_1^2(k)} + 1 \right) \sin[x_2(k)] \\
 x_2(k+1) &= x_2(k) \cos[x_2(k)] + x_1(k) \exp\left[-\frac{x_1^2(k) + x_2^2(k)}{8}\right] \\
 &\quad + \frac{u^3(k)}{1+u^2(k) + 0.5 \cos(x_1(k) + x_2(k))} \\
 y(k) &= \frac{x_1(k)}{1+0.5 \sin[x_2(k)]} + \frac{x_2(k)}{1+0.5 \sin[x_1(k)]}. \tag{6.16}
 \end{aligned}$$

With the identified NARMA-L2 model and multiple NARMA-L2 models of nonlinear system 4, we proceed to control it using the control algorithm in (6.7)-(6.9). For nonlinear system 4, the desired output is

$$y^*(k) = \sin \frac{2\pi k}{20} + \sin \frac{2\pi k}{100}, \quad k = 1, \dots, 200. \tag{6.17}$$

The simulation results for the tracking performance of nonlinear system 4 are shown in Fig. 6.4. It is noted that the parameter  $\rho$  is chosen to be 0.001. As can be seen from Figure 6.4, compared to the NARMA-L2 model, better tracking performance can be achieved by using the multiple NARMA-L2 model with 2 or 4 submodels.

## 6.5 Experimental Studies

Consider again the modified DC motor which was identified in section 5.6. Based on the obtained NARMA-L2 model and multiple NARMA-L2 models, we

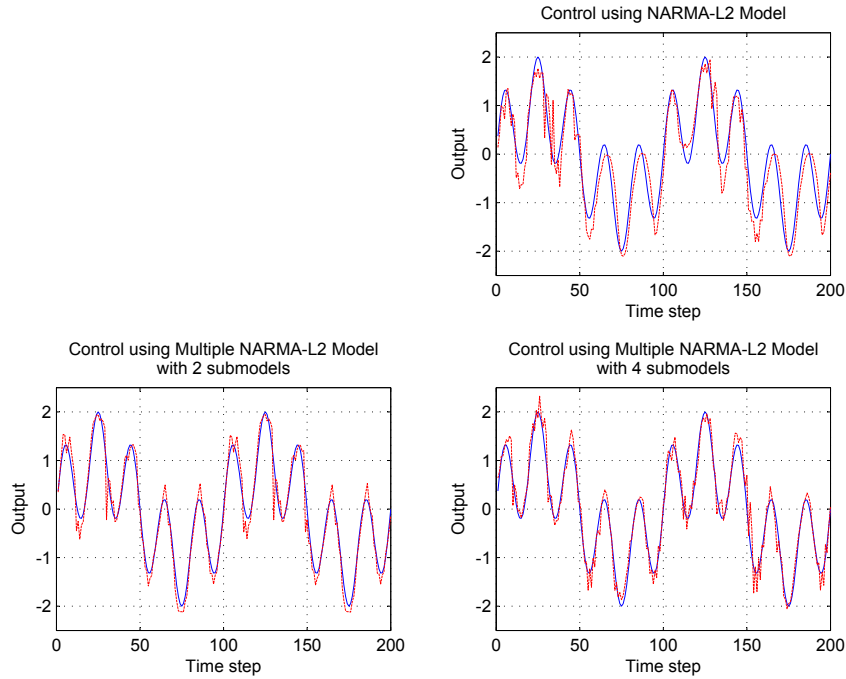


Figure 6.4: Control results of nonlinear system 4 with different models. Solid: Reference, dashed: System output

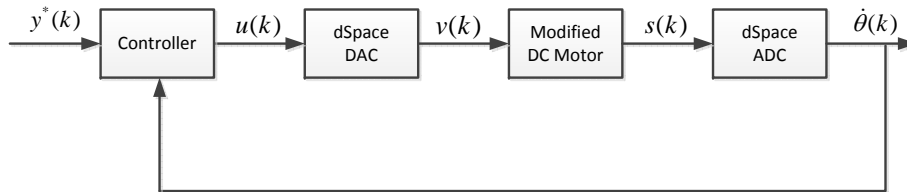


Figure 6.5: Working diagram for the control procedure of the modified DC motor

proceed to control the modified DC motor for angular velocity tracking. The working diagram of the control procedure is shown in Fig. 6.5.

For this plant, three reference signals are defined as follows

$$\begin{aligned}
 y_1^*(k) &= 8 \sin \frac{2\pi k}{200}, \quad k = 1, \dots, 1000 \\
 y_2^*(k) &= 4 \sin \frac{2\pi k}{400} + 4 \sin\left(\frac{2\pi k}{100} + \frac{\pi}{3}\right), \quad k = 1, \dots, 1000 \\
 y_3^*(k) &= 4 \sin \frac{2\pi k}{200} + 4 \sin\left(\frac{2\pi k}{40} + \frac{\pi}{6}\right), \quad k = 1, \dots, 1000. \quad (6.18)
 \end{aligned}$$

Table 6.1: Variance of tracking errors for the modified DC motor with different models

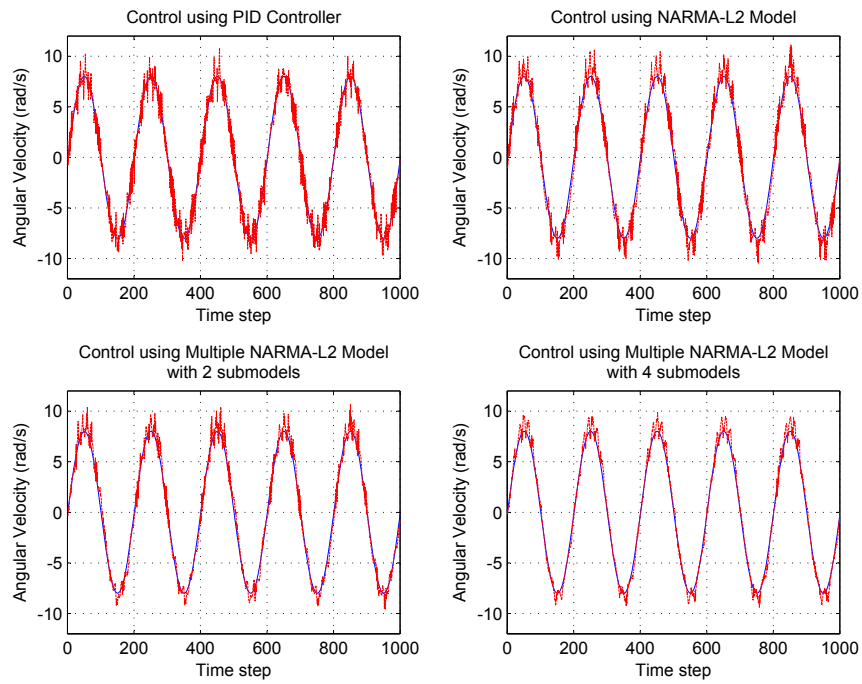
Reference	PID	NARMA-L2	$N = 2$	$N = 4$
$y_1^*$	0.8180	0.8911	0.4963	0.3870
$y_2^*$	0.8458	0.7321	0.4167	0.2424
$y_3^*$	0.9011	0.8140	0.4545	0.2454

The tracking performance for these three reference signals are shown in Fig. 6.6, Fig. 6.7 and Fig. 6.8, respectively. It is noted that the parameter  $\rho$  is chosen to be 0.003. Moreover, a PID controller with properly tuned parameters is also designed for comparison purposes.

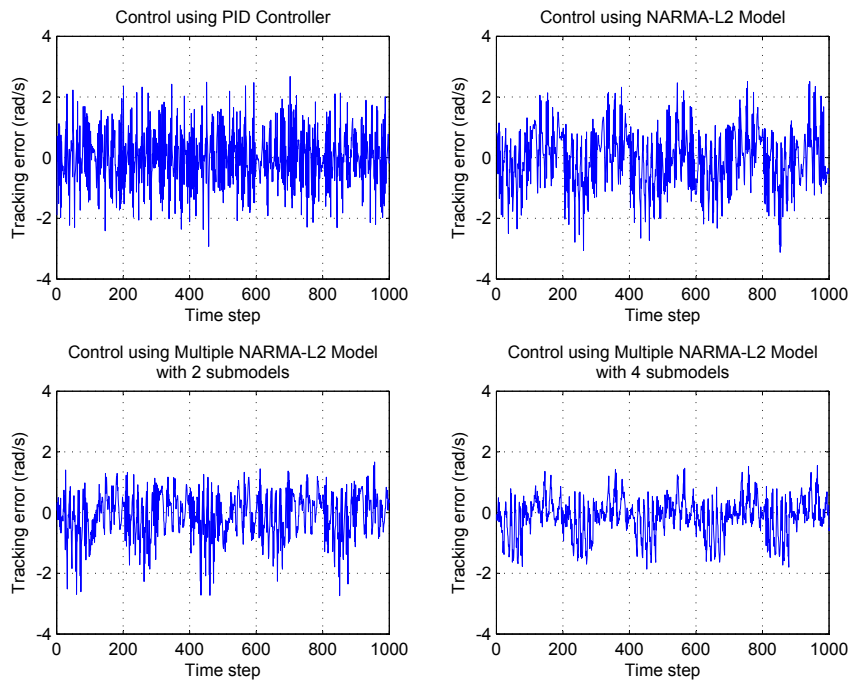
As can be seen from the three figures, the tracking performance using multiple NARMA-L2 models becomes better as the number of submodels increases, which can also be seen from the variance of errors in Table 6.1. Moreover, the tracking performance using multiple NARMA-L2 models is superior to that using the PID controller (the sampling period is 0.05s).

## 6.6 Summary

In this chapter, a switching controller was designed for nonlinear systems based on multiple NARMA-L2 models. By using the weighted one-step-ahead control method, the sub-controllers design problem was transformed into several easily solvable quadratic optimization problems with linear constraints. With the control signals computed from each submodel at time  $k$ , the active controller at that time corresponds to the one with the smallest cost value. While stability analysis of the designed control algorithm is still lacking, simulation studies and experimental results showed its effectiveness.

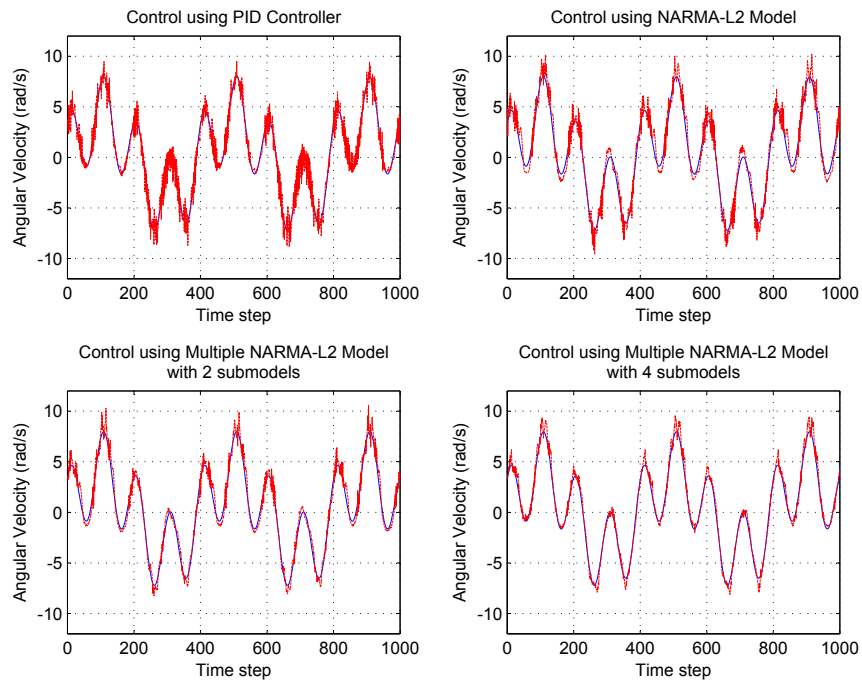


(a) System output vs Reference. Solid: Reference, dashed: System output

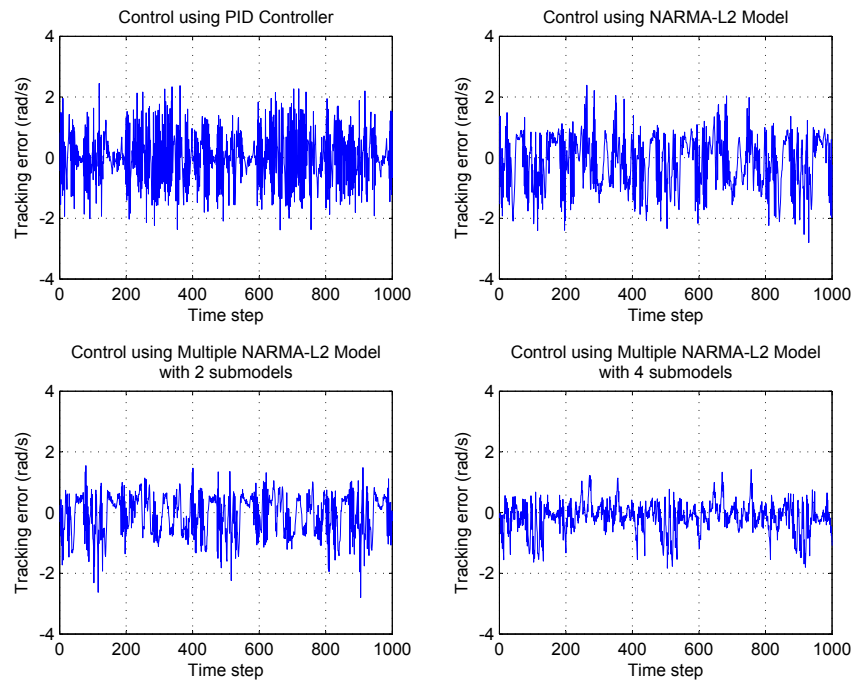


(b) Tracking error

Figure 6.6: Control results of the modified DC motor for reference signal 1 with different models



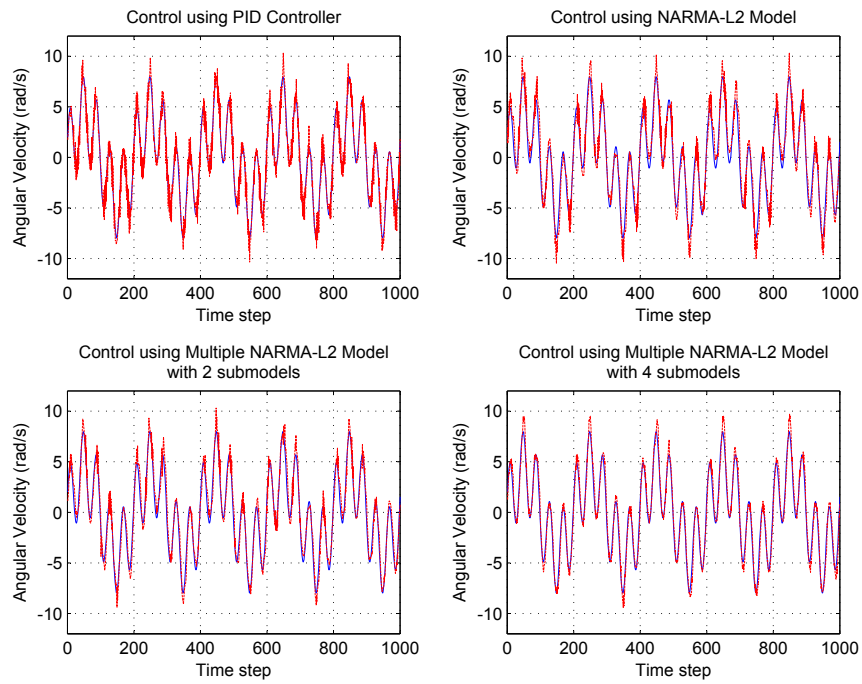
(a) System output vs Reference. Solid: Reference, dashed: System output



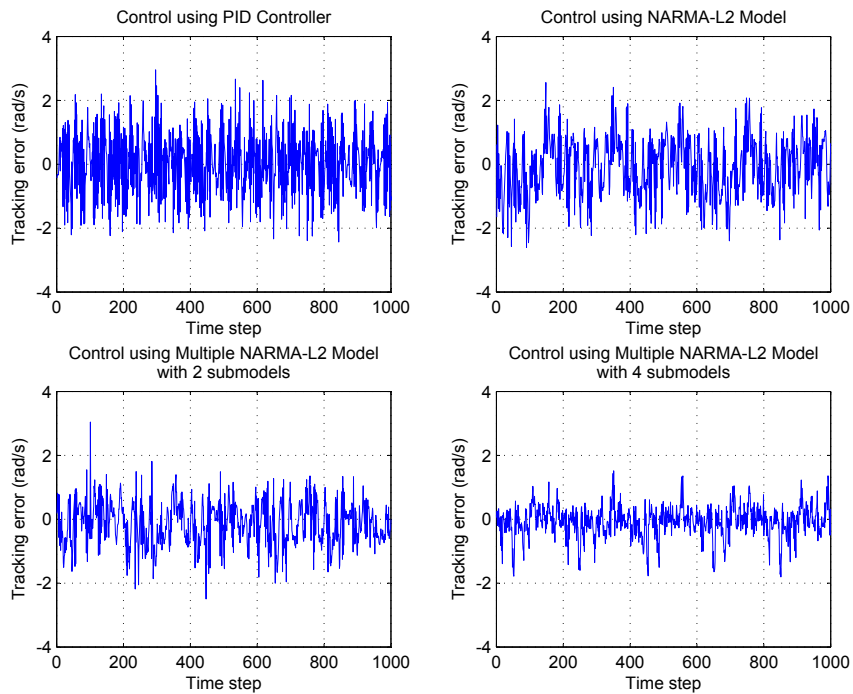
(b) Tracking error

Figure 6.7: Control results of the modified DC motor for reference signal 2 with different models





(a) System output vs Reference. Solid: Reference, dashed: System output



(b) Tracking error

Figure 6.8: Control results of the modified DC motor for reference signal 3 with different models

## Chapter 7

# Conclusions

Switched systems are dynamical systems that consist of a number of subsystems and a switching rule governing the switching among these subsystems. Due to their importance in theory and great potential in application, the last two decades have witnessed numerous research activities in this field. Among the various topics, we focused on the stability analysis and controller synthesis of switched systems in this dissertation.

On the one hand, the stability analysis of switched systems, even with LTI subsystems, is very challenging due to the existence of switching. While many valuable results have been obtained regarding their stability issues, there are still several open problems that need further investigation. In this thesis, some novel and easily verifiable stability and stabilizability conditions were derived for second-order switched linear systems with any finite number of subsystems. On the other hand, switched systems provide a powerful approach for the identification and control of nonlinear systems based on the divide-and-conquer strategy. While the PWA models have drawn most of the attention in recent years, there

are two major issues for the PWA model based identification and control: the curse of dimensionality and the computational complexity. To resolve these two issues, a novel multiple approach, which includes a multiple model structure and a switching control algorithm, was proposed for the identification and control of nonlinear systems in this thesis.

## 7.1 Main Contributions

In Chapter 3, we investigated the stability of second-order switched linear systems under arbitrary switching based on the worst case analysis approach. Different from most of the existing results, which are only applicable to the special case with two subsystems, we considered the general case with any finite number of subsystems. First, for second-order switched linear systems with more than two subsystems, the polar coordinates space can be partitioned into several regions by considering all the subsystems pairwise. Then, the worst case analysis among all the subsystems in the interior of a region can be reduced to the worst case analysis between two subsystems in the interior of that region, which was achieved by dividing all the subsystems in that region into two groups based on their trajectory directions and determining the “most unstable” subsystem for each group. Based on this idea, we extended the worst case switching signal (WCSS) criteria for the two-mode case to the general case, and derived an easily verifiable necessary and sufficient condition for the stability of second-order switched linear systems with any finite number of subsystems under arbitrary switching.

In Chapter 4, the switching stabilizability for second-order switched linear

systems was studied based on the best case analysis approach. Similar to the stability under arbitrary switching problem, most of the existing switching stabilizability results are restricted to second-order switched linear systems with two subsystems. Based on a similar strategy described in Chapter 3, we extended the best case switching signal (BCSS) criteria for the two-mode case to the general case and derived several easily verifiable necessary and sufficient switching stabilizability conditions for second-order switched linear systems with any finite number of subsystems.

To resolve the curse of dimensionality problem for the PWA models in approximating nonlinear systems, a novel multiple model architecture called the multiple NARMA-L2 model was proposed in Chapter 5. In contrast to the PWA models where all dimensions of the regressor space were engaged in the partitioning, the key idea of the proposed model structure is to partition only the range of the control input  $u(k)$  at time  $k$  (the instant of interest in the control problem) into several intervals and identify a local model that is linear in  $u(k)$  within each interval. Based on the Taylor's theorem, a theoretical upper bound for the estimation error was also obtained. Finally, artificial neural networks (ANN) such as MLP or RBFN were utilized to apply the proposed methodology to nonlinear systems. Extensive simulation studies and experimental results showed that satisfactory identification performance can be obtained by the proposed multiple model architecture.

In Chapter 6, a switching control algorithm for the multiple NARMA-L2 model was designed based on the weighted one-step-ahead predictive control method and constrained optimization techniques. In particular, the sub-controllers

design problem was converted into several easily solvable quadratic optimization problems with linear constraints. Moreover, the switching mechanism was determined by evaluating the cost functions for each sub-controller and choosing the one with the smallest cost value. Both simulation studies and experimental results demonstrated the effectiveness of the proposed control algorithm.

## 7.2 Suggestions for Future Work

Based on the prior research, the following questions deserve further consideration and investigation.

1. As mentioned in Chapter 1, most of the easily verifiable conditions for the stability under arbitrary switching problem are restricted to second-order switched linear systems with two subsystems. While we made some progress in establishing an easily verifiable necessary and sufficient condition for second-order switched linear systems with more than two subsystems in Chapter 3, it is challenging to adopt the worst case analysis approach to higher-order switched linear systems since the direction of trajectories for a higher-order LTI system may have infinite possibilities while there are only two choices for the second-order case (clockwise and counterclockwise). As a starting point, it is a possible direction to derive an easily verifiable sufficient condition for the stability of third-order switched linear systems with two subsystems under arbitrary switching.

2. In Chapter 4, easily verifiable necessary and sufficient switching stabilizability conditions were proposed for second-order switched linear systems with any finite number of subsystems based on the best case analysis approach. Simi-

lar to the worst case analysis approach, it is difficult to adopt the best case analysis approach to higher-order switched systems. Therefore, it is desirable to derive an easily verifiable sufficient condition for the switching stabilizability of third-order switched linear systems with two subsystems as a starting point. Moreover, for non-autonomous switched linear systems, it is also a possible direction to study the combination of feedback stabilization and switching stabilization.

3. Even though the switching controller in Chapter 6 showed good tracking performance in simulation studies and experimental results, the stability of the closed-loop system was not established mathematically. As discussed in Chapter 1, the stability analysis of switched systems is extremely complicated even for autonomous switched systems (i.e. without control input) with second-order LTI subsystems. Moreover, the fact that the submodels in our scheme are not accurate makes the problem even more challenging. Although complicated, it is still a possible direction to study the closed-loop stability for some special cases based on certain assumptions.

4. Some fundamental issues related to the multiple NARMA-L2 model, such as how to determine the optimal number of submodels and how to fix the control coefficient in the weighted one-step-ahead predictive control law, also need to be investigated.

In conclusion, the study of switched systems is very important since they have been employed as useful mathematical models for many practical systems. On the one hand, easily verifiable conditions are greatly needed to verify the stability and stabilizability of switched systems. On the other hand, a systematic framework is needed to apply switched systems to the identification and control

of nonlinear systems. This dissertation represents a further step in both these directions.

# Bibliography

- [1] R. W. Brockett. Hybrid models for motion control systems. In H. Trentelman and J. C. Willems, editors, *Essays on Control: Perspectives in the Theory and Its Applications*, pages 29–53. Birkhäuser, Boston, 1993.
- [2] T. I. Seidman. Optimal control for switching systems. In *Proc. 21st Annual Conf. Information Sciences and Systems*, pages 485–489, 1987.
- [3] D. J. Hidde, J. L. Gouzé, C. Hernandez, M. Page, T. Sari, and J. Geiselman. Qualitative simulation of genetic regulatory networks using piecewise-linear models. *Bulletin of Mathematical Biology*, 66(2):301–340, 2004.
- [4] D. Liberzon and A. S. Morse. Basic problems in stability and design of switched systems. *IEEE Control Systems Magazine*, 19(5):59–70, 1999.
- [5] H. Lin and P. J. Antsaklis. Stability and stabilizability of switched linear systems: A survey of recent results. *IEEE Trans. Automat. Control*, 54(2):308–322, 2009.
- [6] D. Liberzon. *Switching in Systems and Control*. Birkhäuser, Boston, 2003.
- [7] M. Johansson. *Piecewise Linear Control Systems—A Computational Approach*. Springer-Verlag, New York, 2003.
- [8] Z. Sun and S. S. Ge. *Switched Linear Systems: Control and Design*. Springer-Verlag, New York, 2005.
- [9] R. W. Brockett. Asymptotic stability and feedback stabilization. In R. W. Brockett, R. S. Millman, and H. J. Sussmann, editors, *Differential Geometric Control Theory*, pages 181–191. Birkhäuser, Boston, 1983.
- [10] G. Xie, D. Zheng, and L. Wang. Controllability of switched linear systems. *IEEE Trans. Automat. Control*, 47(8):1401–1405, 2002.
- [11] Z. Sun, S. S. Ge, and T. H. Lee. Controllability and reachability criteria for switched linear systems. *Automatica*, 38(5):775–786, 2002.
- [12] D. Cheng. Controllability of switched bilinear systems. *IEEE Trans. Automat. Control*, 50(4):511–515, 2005.
- [13] D. Cheng, Y. Lin, and Y. Wang. Accessibility of switched linear systems. *IEEE Trans. Automat. Control*, 51(9):1486, 2006.



- 
- [14] A. Bemporad, G. Ferrari-Trecate, and M. Morari. Observability and controllability of piecewise affine and hybrid systems. *IEEE Trans. Automat. Control*, 45(10):1864–1876, 2000.
- [15] J. P. Hespanha, D. Liberzon, D. Angeli, and E. D. Sontag. Nonlinear norm-observability notions and stability of switched systems. *IEEE Trans. Automat. Control*, 50(2):154–168, 2005.
- [16] A. N. Michel. Recent trends in the stability analysis of hybrid dynamical systems. *IEEE Trans. Circuits Syst. I*, 46(1):120–134, 1999.
- [17] R. A. DeCarlo, M. S. Branicky, S. Pettersson, and B. Lennartson. Perspectives and results on the stability and stabilizability of hybrid systems. *Proceedings of the IEEE*, 88(7):1069–1082, 2000.
- [18] R. Shorten, F. Wirth, O. Mason, K. Wulff, and C. King. Stability criteria for switched and hybrid systems. *SIAM Review*, 49(4):545–592, 2007.
- [19] A. Bemporad and M. Morari. Control of systems integrating logic, dynamics, and constraints. *Automatica*, 35(3):407–427, 1999.
- [20] J. P. Hespanha and A. S. Morse. Switching between stabilizing controllers. *Automatica*, 38(11):1905–1917, 2002.
- [21] Z. Sun and S. S. Ge. Analysis and synthesis of switched linear control systems. *Automatica*, 41(2):181–195, 2005.
- [22] D. Liberzon, J. P. Hespanha, and A. S. Morse. Stability of switched systems: A Lie-algebraic condition. *Systems Control Lett.*, 37(3):117–122, 1999.
- [23] J. P. Hespanha and A. S. Morse. Stability of switched systems with average dwell-time. In *Proc. 38th IEEE Conf. on Decision and Control*, pages 2655–2660, 1999.
- [24] D. Mignone, G. Ferrari-Trecate, and M. Morari. Stability and stabilization of piecewise affine and hybrid systems: An LMI approach. In *Proc. 39th IEEE Conf. on Decision and Control*, pages 504–509, 2000.
- [25] M. S. Branicky. Multiple Lyapunov functions and other analysis tools for switched and hybrid systems. *IEEE Trans. Automat. Control*, 43(4):475–482, 1998.
- [26] J. Daafouz, P. Riedinger, and C. Iung. Stability analysis and control synthesis for switched systems: A switched Lyapunov function approach. *IEEE Trans. Automat. Control*, 47(11):1883–1887, 2002.
- [27] L. Fang, H. Lin, and P. J. Antsaklis. Stabilization and performance analysis for a class of switched systems. In *Proc. 43rd IEEE Conf. on Decision and Control*, pages 3265–3270, 2004.
- [28] D. Cheng, L. Guo, Y. Lin, and Y. Wang. Stabilization of switched linear systems. *IEEE Trans. Automat. Control*, 50(5):661–666, 2005.

- [29] L. Rodrigues and S. Boyd. Piecewise-affine state feedback for piecewise-affine slab systems using convex optimization. *Systems Control Lett.*, 54(9):835–853, 2005.
- [30] A. Arapostathis and M. E. Broucke. Stability and controllability of planar, conewise linear systems. *Syst. Control Lett.*, 56(2):150–158, 2007.
- [31] A. M. Lyapunov. The general problem of the stability of motion. *Int. J. Control*, 55(3):531–534, 1992.
- [32] V. M. Popov. On the absolute stability of nonlinear control systems. *Automatic Remote Control*, 22(8):961–979, 1961.
- [33] A. P. Molchanov and Y. S. Pyatnitskiy. Criteria of asymptotic stability of differential and difference inclusions encountered in control theory. *Systems Control Lett.*, 13(1):59–64, 1989.
- [34] W. P. Dayawansa and C. F. Martin. A converse Lyapunov theorem for a class of dynamical systems which undergo switching. *IEEE Trans. Automat. Control*, 44(4):751–760, 1999.
- [35] N. Cohen and I. Lewkowicz. A necessary and sufficient criterion for the stability of a convex set of matrices. *IEEE Trans. Automat. Control*, 38(4):611–615, 1993.
- [36] S. Boyd, L. El Ghaoui, E. Feron, and V. Balakrishnan. *Linear Matrix Inequalities in System and Control Theory*. Philadelphia, PA: SIAM, 1994.
- [37] K. S. Narendra and J. Balakrishnan. A common Lyapunov function for stable LTI systems with commuting A-matrices. *IEEE Trans. Automat. Control*, 39(12):2469–2471, 1994.
- [38] R. Shorten and K. S. Narendra. Necessary and sufficient conditions for the existence of a common quadratic Lyapunov function for two stable second order linear time-invariant systems. In *Proc. 1999 American Control Conf.*, pages 1410–1414, 1999.
- [39] R. Shorten and K. S. Narendra. Necessary and sufficient conditions for the existence of a common quadratic Lyapunov function for a finite number of stable second order linear time-invariant systems. *Int. J. Adaptive Control Signal Processing*, 16(10):709–728, 2002.
- [40] C. King and R. Shorten. A singularity test for the existence of common quadratic Lyapunov functions for pairs of stable LTI systems. In *Proc. 2004 American Control Conf.*, pages 3881–3884, 2004.
- [41] C. King and R. Shorten. Singularity conditions for the non-existence of a common quadratic Lyapunov function for pairs of third order linear time invariant dynamic systems. *Linear algebra and its applications*, 413(1):24–35, 2006.
- [42] R. Shorten, K. S. Narendra, and O. Mason. A result on common quadratic Lyapunov functions. *IEEE Trans. Automat. Control*, 48(1):110–113, 2003.

- 
- [43] R. Shorten, O. Mason, F. O’Cairbre, and P. Curran. A unifying framework for the SISO circle criterion and other quadratic stability criteria. *Int. J. Control*, 77(1):1–8, 2004.
- [44] R. Shorten and K. S. Narendra. On common quadratic Lyapunov functions for pairs of stable LTI systems whose system matrices are in companion form. *IEEE Trans. Automat. Control*, 48(4):618–621, 2003.
- [45] C. King and M. Nathanson. On the existence of a common quadratic Lyapunov function for a rank one difference. *Linear algebra and its applications*, 419(2):400–416, 2006.
- [46] L. Gurvits, R. Shorten, and O. Mason. On the stability of switched positive linear systems. *IEEE Trans. Automat. Control*, 52(6):1099–1103, 2007.
- [47] D. Cheng, L. Guo, and J. Huang. On quadratic Lyapunov functions. *IEEE Trans. Automat. Control*, 48(5):885–890, 2003.
- [48] A. A. Agrachev and D. Liberzon. Lie-algebraic stability criteria for switched systems. *SIAM J. Control Optim.*, 40(1):253–269, 2001.
- [49] M. Margaliot and D. Liberzon. Lie-algebraic stability conditions for nonlinear switched systems and differential inclusions. *Systems Control Lett.*, 55(1):8–16, 2006.
- [50] G. Zhai and H. Lin. Controller failure time analysis for symmetric control systems. *Int. J. Control*, 77(6):598–605, 2004.
- [51] G. Zhai, X. Xu, H. Lin, and A. N. Michel. Analysis and design of switched normal systems. *Nonlinear Anal., Theory, Methods Appl.*, 65(12):2248–2259, 2006.
- [52] R. Shorten and K. S. Narendra. On the stability and existence of common Lyapunov functions for stable linear switching systems. In *Proc. 37th IEEE Conf. on Decision and Control*, pages 3723–3724, 1998.
- [53] Y. Mori, T. Mori, and Y. Kuroe. A solution to the common Lyapunov function problem for continuous-time systems. In *Proc. 36th IEEE Conf. on Decision and Control*, pages 3530–3531, 1997.
- [54] J. L. Mancilla-Aguilar and R. A. Garcia. A converse Lyapunov theorem for nonlinear switched systems. *Systems Control Lett.*, 41(1):67–71, 2000.
- [55] F. Blanchini. Nonquadratic Lyapunov functions for robust control. *Automatica*, 31(3):451–461, 1995.
- [56] R. K. Brayton and C. H. Tong. Constructive stability and asymptotic stability of dynamical systems. *IEEE Trans. Circuits Syst.*, 27(11):1121–1130, 1980.
- [57] A. Polański. On absolute stability analysis by polyhedral Lyapunov functions. *Automatica*, 36(4):573–578, 2000.

- [58] C. A. Yfoulis and R. Shorten. A numerical technique for the stability analysis of linear switched systems. *Int. J. Control*, 77(11):1019–1039, 2004.
- [59] E. S. Pyatnits. Absolute stability of nonstationary nonlinear systems. *Automation and Remote Control*, (1):1, 1970.
- [60] E. S. Pyatnitskiy and L. B. Rapoport. Criteria of asymptotic stability of differential inclusions and periodic motions of time-varying nonlinear control systems. *IEEE Trans. Circuits Syst. I*, 43(3):219–229, 1996.
- [61] M. Margaliot and G. Langholz. Necessary and sufficient conditions for absolute stability: The case of second-order systems. *IEEE Trans. Circuits Syst. I*, 50(2):227–234, 2003.
- [62] M. Margaliot and R. Gitzadeh. The problem of absolute stability: A dynamic programming approach. *Automatica*, 40(7):1247–1252, 2004.
- [63] M. Margaliot and C. Yfoulis. Absolute stability of third-order systems: A numerical algorithm. *Automatica*, 42(10):1705–1711, 2006.
- [64] M. Margaliot. Stability analysis of switched systems using variational principles: An introduction. *Automatica*, 42(12):2059–2077, 2006.
- [65] U. Boscain. Stability of planar switched systems: The linear single input case. *SIAM J. Control Optim.*, 41(1):89–112, 2002.
- [66] M. Balde and U. Boscain. Stability of planar switched systems: The nondiagonalizable case. *Communications on Pure and Applied Analysis*, 7(1):1–21, 2008.
- [67] M. Balde, U. Boscain, and P. Mason. A note on stability conditions for planar switched systems. *Int. J. Control*, 82(10):1882–1888, 2009.
- [68] Z. Huang, C. Xiang, H. Lin, and T. H. Lee. A stability criterion for arbitrarily switched second order LTI systems. In *Proc. 6th IEEE Conf. Control Automat.*, pages 951–956, 2007.
- [69] Z. Huang. *Stability Analysis of Switched Systems*. PhD thesis, National University of Singapore, 2010.
- [70] M. A. Wicks, P. Peleties, and R. A. DeCarlo. Construction of piecewise Lyapunov functions for stabilizing switched systems. In *Proc. 33rd IEEE Conf. on Decision and Control*, pages 3492–3497, 1994.
- [71] E. Feron. Quadratic stabilizability of switched systems via state and output feedback. Technical report, CICS-p-468, MIT, 1996.
- [72] M. A. Wicks, P. Peleties, and R. A. DeCarlo. Switched controller synthesis for the quadratic stabilisation of a pair of unstable linear systems. *Eur. J. Control*, 4(2):140–147, 1998.
- [73] S. Pettersson and B. Lennartson. Stabilization of hybrid systems using a min-projection strategy. In *Proc. 2001 American Control Conf.*, pages 223–228, 2001.

- 
- [74] E. Skafidas, R. J. Evans, A. V. Savkin, and I. R. Petersen. Stability results for switched controller systems. *Automatica*, 35(4):553–564, 1999.
- [75] M. A. Wicks and R. A. DeCarlo. Solution of coupled Lyapunov equations for the stabilization of multimodal linear systems. In *Proc. 1997 American Control Conf.*, pages 1709–1713, 1997.
- [76] S. Pettersson. Synthesis of switched linear systems. In *Proc. 42nd IEEE Conf. on Decision and Control*, pages 5283–5288, 2003.
- [77] H. Ishii, T. Basar, and R. Tempo. Synthesis of switching rules for switched linear systems through randomized algorithms. In *Proc. 42nd IEEE Conf. on Decision and Control*, pages 4788–4793, 2003.
- [78] D. Corona, A. Giua, and C. Seatzu. Stabilization of switched systems via optimal control. In *Proc. 16th IFAC World Congress*, 2005.
- [79] X. Xu and P. J. Antsaklis. Stabilization of second-order LTI switched systems. *Int. J. Control*, 73(14):1261–1279, 2000.
- [80] L. Zhang, Y. Chen, and P. Cui. Stabilization for a class of second-order switched systems. *Nonlinear Anal., Theory, Methods Appl.*, 62(8):1527–1535, 2005.
- [81] A. Bacciotti and F. Ceragioli. Closed loop stabilization of planar bilinear switched systems. *Int. J. Control*, 79(1):14–23, 2006.
- [82] Z. Huang, C. Xiang, H. Lin, and T. H. Lee. Necessary and sufficient conditions for regional stabilisability of generic switched linear systems with a pair of planar subsystems. *Int. J. Control*, 83(4):694–715, 2010.
- [83] G. Stein, G. L. Hartmann, and R. Hendrick. Adaptive control laws for F-8 flight test. *IEEE Trans. Automat. Control*, 22(5):758–767, 1977.
- [84] C. G. Källström, K. J. Åström, N. E. Thorell, J. Eriksson, and L. Sten. Adaptive autopilots for tankers. *Automatica*, 15(3):241–254, 1979.
- [85] D. J. Leith and W. E. Leithead. Survey of gain-scheduling analysis and design. *Int. J. Control*, 73(11):1001–1025, 2000.
- [86] W. J. Rugh and J. S. Shamma. Research on gain scheduling. *Automatica*, 36(10):1401–1425, 2000.
- [87] A. S. Morse. Supervisory control of families of linear set-point controllers—Part 1: Exact matching. *IEEE Trans. Automat. Control*, 41(10):1413–1431, 1996.
- [88] A. S. Morse. Supervisory control of families of linear set-point controllers—Part 2: Robustness. *IEEE Trans. Automat. Control*, 42(11):1500–1515, 1997.
- [89] K. S. Narendra and J. Balakrishnan. Improving transient response of adaptive control systems using multiple models and switching. *IEEE Trans. Automat. Control*, 39(9):1861–1866, 1994.

- [90] K. S. Narendra and J. Balakrishnan. Adaptive control using multiple models. *IEEE Trans. Automat. Control*, 42(2):171–187, 1997.
- [91] K. S. Narendra and C. Xiang. Adaptive control of discrete-time systems using multiple models. *IEEE Trans. Automat. Control*, 45(9):1669–1686, 2000.
- [92] K. S. Narendra, J. Balakrishnan, and M. K. Ciliz. Adaptation and learning using multiple models, switching, and tuning. *IEEE Control Systems Magazine*, 15(3):37–51, 1995.
- [93] E. D. Sontag. Nonlinear regulation: The piecewise linear approach. *IEEE Trans. Automat. Control*, 26(2):346–358, 1981.
- [94] S. A. Billings and W. S. F. Voon. Piecewise linear identification of nonlinear systems. *Int. J. Control*, 46(1):215–235, 1987.
- [95] A. Bemporad, G. Ferrari-Trecate, and M. Morari. Observability and controllability of piecewise affine and hybrid systems. *IEEE Trans. Automat. Control*, 45(10):1864–1876, 2000.
- [96] W. P. M. H. Heemels, B. De Schutter, and A. Bemporad. Equivalence of hybrid dynamical models. *Automatica*, 37(7):1085–1091, 2001.
- [97] J. N. Lin and R. Unbehauen. Canonical piecewise-linear approximations. *IEEE Trans. Circuits Syst. I*, 39(8):697–699, 1992.
- [98] L. Breiman. Hinging hyperplanes for regression, classification, and function approximation. *IEEE Trans. Information Theory*, 39(3):999–1013, 1993.
- [99] G. Ferrari-Trecate, M. Muselli, D. Liberati, and M. Morari. A clustering technique for the identification of piecewise affine systems. *Automatica*, 39(2):205–217, 2003.
- [100] R. Vidal, S. Soatto, Y. Ma, and S. Sastry. An algebraic geometric approach to the identification of a class of linear hybrid systems. In *Proc. 42nd IEEE Conf. on Decision and Control*, pages 167–172, 2003.
- [101] J. Roll, A. Bemporad, and L. Ljung. Identification of piecewise affine systems via mixed-integer programming. *Automatica*, 40(1):37–50, 2004.
- [102] A. L. Juloski, S. Weiland, and W. P. M. H. Heemels. A bayesian approach to identification of hybrid systems. *IEEE Trans. Automat. Control*, 50(10):1520–1533, 2005.
- [103] A. Bemporad, A. Garulli, S. Paoletti, and A. Vicino. A bounded-error approach to piecewise affine system identification. *IEEE Trans. Automat. Control*, 50(10):1567–1580, 2005.
- [104] H. Nakada, K. Takaba, and T. Katayama. Identification of piecewise affine systems based on statistical clustering technique. *Automatica*, 41(5):905–913, 2005.

- 
- [105] A. L. Juloski, W. P. M. H. Heemels, G. Ferrari-Trecate, R. Vidal, S. Paoletti, and J. H. G. Niessen. Comparison of four procedures for the identification of hybrid systems. In *Hybrid Systems: Computation and Control*, pages 354–369. 2005.
- [106] S. Paoletti, A. L. Juloski, G. Ferrari-Trecate, and R. Vidal. Identification of hybrid systems: A tutorial. *Eur. J. Control*, 13(2):242–260, 2007.
- [107] C. Y. Lai, C. Xiang, and T. H. Lee. Data-based identification and control of nonlinear systems via piecewise affine approximation. *IEEE Trans. Neural Networks*, 22(12):2189–2200, 2011.
- [108] C. Y. Lai. *Identification and Control of Nonlinear Systems using Multiple Models*. PhD thesis, National University of Singapore, 2011.
- [109] A. Bemporad, F. Borrelli, and M. Morari. Piecewise linear optimal controllers for hybrid systems. In *Proc. 2000 American Control Conf.*, volume 2, pages 1190–1194, 2000.
- [110] L. Özkan, M. V. Kothare, and C. Georgakis. Model predictive control of nonlinear systems using piecewise linear models. *Computers & Chemical Engineering*, 24(2):793–799, 2000.
- [111] B. De Schutter and T.J.J van den Boom. MPC for continuous piecewise-affine systems. *Systems Control Lett.*, 52(3):179–192, 2004.
- [112] F. Borrelli, M. Baotić, A. Bemporad, and M. Morari. Dynamic programming for constrained optimal control of discrete-time linear hybrid systems. *Automatica*, 41(10):1709–1721, 2005.
- [113] L. Özkan and M. V. Kothare. Stability analysis of a multi-model predictive control algorithm with application to control of chemical reactors. *Journal of Process Control*, 16(2):81–90, 2006.
- [114] N. N. Nandola and S. Bhartiya. A multiple model approach for predictive control of nonlinear hybrid systems. *Journal of Process Control*, 18(2):131–148, 2008.
- [115] Q. Chen, L. Gao, R. A. Dougal, and S. Quan. Multiple model predictive control for a hybrid proton exchange membrane fuel cell system. *Journal of Power Sources*, 191(2):473–482, 2009.
- [116] B. Pregelj and S. Gerškšič. Hybrid explicit model predictive control of a nonlinear process approximated with a piecewise affine model. *Journal of Process Control*, 20(7):832–839, 2010.
- [117] E. F. Camacho, D. R. Ramirez, D. Limon, D. Muñoz de la Peña, and T. Alamo. Model predictive control techniques for hybrid systems. *Annual Reviews in Control*, 34(1):21–31, 2010.
- [118] M. Morari and M. Barić. Recent developments in the control of constrained hybrid systems. *Computers & Chemical Engineering*, 30(10):1619–1631, 2006.

- [119] A. Kordon, P. S. Dhurjati, Y. O. Fuentes, and B. A. Ogunnaike. An intelligent parallel control system structure for plants with multiple operating regimes. *Journal of Process Control*, 9(5):453–460, 1999.
- [120] R. Shorten and K. S. Narendra. A sufficient condition for the existence of a common Lyapunov function for two second order linear systems. In *Proc. 1997 American Control Conf.*, pages 3521–3522, 1997.
- [121] T. V. Nguyen, Y. Mori, T. Mori, and Y. Kuroe. QE approach to common Lyapunov function problem. *Journal of Japan Society for Symbolic and Algebraic Computation*, 10(1):52–62, 2003.
- [122] I. J. Leontaritis and S. A. Billings. Input-output parametric models for non-linear systems Part I: Deterministic non-linear systems. *Int. J. Control*, 41(2):303–328, 1985.
- [123] A. U. Levin and K. S. Narendra. Control of nonlinear dynamical systems using neural networks—Part II: Observability, identification, and control. *IEEE Trans. Neural Networks*, 7(1):30–42, 1996.
- [124] N. Nijmeijer and A. J. Van der Schaft. *Nonlinear Dynamic Control Systems*. Springer-Verlag, New York, 1990.
- [125] C. Xiang. Existence of global input-output model for nonlinear systems. In *Proc. 5th IEEE Conf. Control Automat.*, pages 125–130, 2005.
- [126] K. S. Narendra and K. Parthasarathy. Identification and control of dynamical systems using neural networks. *IEEE Trans. Neural Networks*, 1(1):4–27, 1990.
- [127] S. Chen, S. A. Billings, and P. M. Grant. Non-linear system identification using neural networks. *Int. J. Control*, 51(6):1191–1214, 1990.
- [128] K. S. Narendra and S. Mukhopadhyay. Adaptive control using neural networks and approximate models. *IEEE Trans. Neural Networks*, 8(3):475–485, 1997.
- [129] K. S. Narendra and S. M. Li. Neural networks in control systems. In P. Smolensky, M. C. Mozer, and D. E. Rumelhart, editors, *Mathematical perspectives on neural networks*. Mahwah, NJ: Lawrence Erlbaum Associates, 1996.
- [130] J. Roll, A. Nazin, and L. Ljung. Nonlinear system identification via direct weight optimization. *Automatica*, 41(3):475–490, 2005.
- [131] E. W. Bai and Y. Liu. Recursive direct weight optimization in nonlinear system identification: A minimal probability approach. *IEEE Trans. Automat. Control*, 52(7):1218–1231, 2007.
- [132] C. Wen, S. Wang, X. Jin, and X. Ma. Identification of dynamic systems using piecewise-affine basis function models. *Automatica*, 43(10):1824–1831, 2007.



- [133] J. Xu, X. Huang, and S. Wang. Adaptive hinging hyperplanes and its applications in dynamic system identification. *Automatica*, 45(10):2325–2332, 2009.
- [134] G. C. Goodwin and K. S. Sin. *Adaptive Filtering, Prediction, and Control*. Prentice Hall, Englewood Cliffs, New Jersey, 1984.
- [135] Y. Tan and A. Van Cauwenberghe. Nonlinear one-step-ahead control using neural networks: Control strategy and stability design. *Automatica*, 32(12):1701–1706, 1996.
- [136] C. Kambhampati, J. D. Mason, and K. Warwick. A stable one-step-ahead predictive control of non-linear systems. *Automatica*, 36(4):485–495, 2000.

# Appendix: Publication List

## Journal Papers

Y. Yang, C. Xiang and T. H. Lee, “Data-based identification and control of nonlinear systems using multiple NARMA-L2 models”, submitted to *Automatica* for publication, 2014.

Y. Yang, C. Xiang and T. H. Lee, “Necessary and sufficient conditions for regional stabilizability of second-order switched linear systems with a finite number of subsystems”, *Automatica*, vol. 50, no. 3, pp. 931-939, Mar 2014.

Y. Yang, C. Xiang and T. H. Lee, “Sufficient and necessary conditions for the stability of second-order switched linear systems under arbitrary switching”, *International Journal of Control*, vol. 85, no. 12, pp. 1977-1995, Dec 2012.

## Conference Papers

Y. Yang, C. Xiang and T. H. Lee, “Identification and control of nonlinear systems using neural networks and multiple models”, in *Proc. 11th IEEE International Conference on Control and Automation (ICCA)*, pp. 1298-1303, 2014.

Y. Yang, C. Xiang and T. H. Lee, “Robust identification of piecewise affine systems from noisy data”, in *Proc. 10th IEEE International Conference on*

*Control and Automation (ICCA)*, pp. 646-651, 2013.

Y. Yang, C. Xiang and T. H. Lee, "Feedback stabilization for planar switched linear systems with two subsystems under arbitrary switching", in *Proc. 9th IEEE International Conference on Control and Automation (ICCA)*, pp. 738-743, 2011.